

Contents of issue 3–4 vol. LVII

- 127 P. MARAZIOTI, P. KOUTMOS, *Simulations of combustion roar in turbulent attached and lifted turbulent methane jet flames*
- 145 K. KOWALCZYK – GAJEWSKA, J. OSTROWSKA – MACIEJEWSKA, *Review on spectral decomposition of Hooke's tensor for all symmetry groups of linear elastic material*
- 185 W. BURZYŃSKI, *Study on Material Effort Hypotheses (selected passages from doctoral dissertation)*

SIMULATIONS OF COMBUSTION ROAR IN TURBULENT ATTACHED AND LIFTED TURBULENT METHANE JET FLAMES

P. Marazioti^{1,2)}, P. Koutmos²⁾

¹⁾ **Technological Education Institute (TEI)**
Department of Energy Technology

Athens, Greece

²⁾ **University of Patras**
Department of Mechanical and Aeronautics Engineering

Greece 26 500

The present work presents sample results of preliminary computations of the turbulent aerothermodynamic flow field and of the noise generated by the flame front, due to turbulent fluctuations in the flame (combustion roar), in lifted and attached jet diffusion flames of methane. The two-dimensional (2D) time-dependent numerical model was built based on Reynolds-averaged Navier–Stokes (N-S) equations, equipped with the standard k - ϵ turbulence models to calculate the reacting jet flows. A reactedness – mixture fraction two-scalar exponential PDF model, based on non-premixed flame arguments, was combined with a local Damkohler number extinction criterion to delineate between the reacting and non-reacting regions. Although the inclusion of the effects of premixed flame propagation could help to improve the model, initial comparisons with experimental results suggest adequate qualitative agreement between the computations and reported data. The reasonable agreement obtained for the aerothermodynamic flame characteristics permitted a meaningful computation of the combustion noise (roar) characteristics of the studied flames, in order to address the coupled effects of heat release by the flame and turbulent interactions on the autonomous flame noise generation.

Key words: combustion roar, lifted flame, sound spectrum, turbulent combustion modeling.

NOTATIONS

| | |
|---------------------|---|
| ν_t | turbulent eddy viscosity, |
| L_t | turbulent length scale, |
| k | turbulent kinetic energy, |
| ϵ | eddy dissipation rate, |
| f | mixture fraction, |
| u | instantaneous velocity, |
| $\langle u \rangle$ | phase-averaged (or resolved) velocity, |
| \bar{u} | time-mean component, |
| u'' | large-scale (resolved) fluctuating component, |

| | |
|---|--|
| u' | stochastic (subgrid) turbulent fluctuation, |
| $\langle u'_i u'_j \rangle$ | Reynolds stresses, |
| Δ | mesh size, |
| J | Jacobian of the transformation, |
| Y | mass fraction, |
| τ_k | Kolmogorov time scale, |
| Da_l | local Damkohler number, |
| τ_λ | turbulent time scale, |
| τ_{ch} | chemical time scale, |
| τ_{id} | mixing-dependent chemical ignition delay time, |
| $\overline{u'_j f'}, \overline{u'_j Y'_{CO_2}}$ | turbulent fluxes, |
| C_0 | speed of sound, |
| S | area of combustor nozzle, |
| D | laminar diffusion coefficient, |
| x | scalar dissipation, |
| E_{1D} | one-dimensional turbulence spectrum of the assumed shape, |
| $\theta_{f\nu}$ | thickness of the mixing layer between fuel and air = $1/\sqrt{(\nabla^2 f_\nu)}$, |
| A | $A = [T_{\text{flame}} - T_0]/[T_{\text{flame}} f_{st} (1 - f_{st})]$, |
| f_ν | frequency, |
| SPL | sound pressure level. |

1. INTRODUCTION

Renewed interest has emerged in recent years in the study of interaction between the combustion process and the acoustics of the reacting environment [1]. Combustion roar is related to the noise generated directly by the flame due to turbulent fluctuations, independently or in combination with acoustic resonance of the reacting environment and usually involves a broadly distributed spectrum [2, 3]. The topic is of interest for practical combustor designs since it is interrelated with combustor acoustic/pressure oscillations or resonance, acoustic pollution of the environment diagnosis of operational variations and faults, and ultimately active or hybrid combustor operation control techniques [4, 5]. Practical examples which are interesting from the point of view of research on combustion roar are the combustion chambers of aircraft jet engines, flares and hot-air balloons, where minimization of flame noise is desirable.

In the present work, modeling of the autonomous noise generation by the turbulence/chemistry fluctuations in the flame front vicinity of jet diffusion flames is investigated. To describe the acoustic performance of the jet flame as an autonomous source of sound, an integral expression is employed that provides the (acoustically one-dimensional) noise spectrum of the flame, in terms of an assumed shape turbulence spectrum at the flame front, closely following the formulation put forward and derived in closed form by KLEIN [5].

As a first step towards understanding of the phenomenon, the turbulent non-premixed jet flames attached and lifted from the burner rim are studied as model problems. A diffusion flame attached to the burner nozzle lifts above the jet exit rim or blows out abruptly, when the fuel jet velocity steadily increases and exceeds the critical value. Apart from their relevance in the design and safe operation of industrial systems, such jet flame stability phenomena provide a useful research tool for experimental and numerical studies of turbulent reacting flow characteristics and related phenomena such as those presently addressed. A recent review by PITTS [6] and non-intrusive measurements by SCHEFER *et al.* [7] suggest that individual theories such as turbulent premixed flame propagation, laminar flameless quenching, large or small scale mixing, are all plausible theoretical viewpoints to describe the coupled aero-thermochemical phenomena of lift-off and blow-out.

In the described work, a 2D time-dependent phase-averaged Navier–Stokes flow simulation method [8] capable of calculating the mean and turbulent properties of the momentum and thermo-chemical fields, is employed to study the behavior of axisymmetric co-flowing methane-air jet diffusion flame configurations. Both the laminar and turbulent (lifted-off) operational conditions have been investigated to test and develop the model over a range of conditions with increasing complexity. A modular post-processor is then employed for the prediction of turbulent combustion noise, exploiting the time-mean and fluctuating thermo-chemical quantities obtained from the basic reacting flow field predictions.

2. NUMERICAL METHOD

2.1. Aerodynamic model

The reacting flows were calculated with the 2D time-dependent N-S equations governing the temporal and spatial variation of the velocities and pressures, e.g. $u = \langle u \rangle + u'$ with $\langle u \rangle = \bar{u} + u''$ where u and $\langle u \rangle$ are the instantaneous and phase-averaged (or resolved) velocities, \bar{u} and u'' are the time-mean and large-scale (resolved) fluctuating components and u' is the stochastic (subgrid) turbulent fluctuation. The model description given below closely follows the formulations adopted in [8]. For the reacting flows, density-weighted values are used i.e. $\langle \tilde{f} \rangle = \frac{\rho \langle f \rangle}{\bar{\rho}}$. The equation set may be written as follows:

$$(2.1) \quad \begin{aligned} \frac{\partial \bar{p}}{\partial t} + \frac{\partial \langle \tilde{u}_i \rangle}{\partial x_i} &= 0, \\ \frac{\partial \langle \tilde{u}_i \rangle}{\partial t} + \langle \tilde{u}_i \rangle \frac{\partial \langle \tilde{u}_i \rangle}{\partial x_j} &= -\frac{1}{\rho} \frac{\partial \bar{p}}{\partial x_i} + \frac{\partial}{\partial x_j} \left[\nu \frac{\partial \langle \tilde{u}_i \rangle}{\partial x_j} - \langle u'_i u'_j \rangle \right] + (\bar{p} - \rho_\infty) g_i, \end{aligned}$$

with the Reynolds stresses obtained from the standard eddy-viscosity formula:

$$(2.2) \quad -\langle \overline{u'_i u'_j} \rangle = \langle \nu_t \rangle \left(\frac{\partial \langle \tilde{u}_i \rangle}{\partial x_j} + \frac{\partial \langle \tilde{u}_j \rangle}{\partial x_i} \right) - \frac{2}{3} \left[\langle \tilde{\nu}_t \rangle \frac{\partial \langle \tilde{u}_i \rangle}{\partial x_i} + \langle \tilde{k} \rangle \right] \delta_{ij}.$$

In the conventional $k - \varepsilon$ model, $\langle \tilde{\nu}_t \rangle$ is related to the turbulence energy $\langle \tilde{k} \rangle$ and its dissipation rate $\langle \varepsilon \rangle$ as $\langle \tilde{\nu}_t \rangle = C_\mu \langle \tilde{k} \rangle^2 / \langle \varepsilon \rangle$, where $\langle \tilde{k} \rangle$ and $\langle \varepsilon \rangle$ are obtained from the standard transport equations:

$$(2.3) \quad \frac{\partial}{\partial x_j} (U_j k) = \frac{\partial}{\partial x_j} \left(\frac{\nu_t}{\sigma_k} \frac{\partial k}{\partial x_j} \right) - \overline{u_i u_j} \frac{\partial U_i}{\partial x_j} - \varepsilon,$$

$$(2.4) \quad \frac{\partial}{\partial x_j} (U_j \varepsilon) = \frac{\partial}{\partial x_j} \left(\frac{\nu_t}{\sigma_\varepsilon} \frac{\partial \varepsilon}{\partial x_j} \right) - C_{\varepsilon 1} \frac{\varepsilon}{k} \overline{u_i u_j} \frac{\partial U_i}{\partial x_j} - C_{\varepsilon 2} \frac{\varepsilon^2}{k},$$

where $C_\mu = 0.009$, $C_{\varepsilon 1} = 1.44$, $C_{\varepsilon 2} = 1.92$, $\sigma_k = 1.0$, $\sigma_\varepsilon = 1.3$.

The standard $k - \varepsilon$ model has been formulated and tested within the steady-state calculation procedures, against a range of plane shear flows with no distinct peaks in their energy spectrum. When a 2D time-dependent calculation is used, part of the energy spectrum is directly resolved by this type of calculation. There is clearly a certain ambiguity as to whether the standard model is capable of partitioning the total stress into its stochastic and periodic contributions [8].

In the present time-dependent calculations, the spatial filtering due to the employed mesh is also accounted for in an effort to distinguish the directly computed (albeit 2D) turbulent motions, which are resolved by the mesh of size $\Delta = (\Delta x \Delta y)^{1/2}$, from the turbulence already modeled by the $k - \varepsilon$ model. $\langle \tilde{\nu}_t \rangle$ is therefore evaluated here by borrowing the Smagorinsky mixing length model from the large-eddy simulation (LES) formalism and the hybrid turbulence model is:

$$(2.5) \quad \langle \tilde{\nu}_t \rangle = (C_s \Delta)^2 \left(2 \langle \tilde{S}_{ij} \rangle \langle \tilde{S}_{ij} \rangle \right)^{1/2} \quad \text{if} \quad L_t = \frac{\langle \tilde{k} \rangle^{3/2}}{\langle \tilde{\varepsilon} \rangle} > \Delta \quad \text{and}$$

$$\langle \tilde{\nu}_t \rangle = C_\mu \langle \tilde{k} \rangle^2 / \langle \tilde{\varepsilon} \rangle \quad \text{if} \quad L_t < \Delta.$$

C_s is taken as 0.1. The resulting $\tilde{\nu}_t$ is fed back into the production of $\langle \tilde{k} \rangle$ in the $k - \varepsilon$ equations, thereby producing a continuous distribution of ν_t . The implicit scheme used here is therefore well suited for this hybrid formulation. Calculations with the standard $k - \varepsilon$ model have been proven clearly to be inferior to the recent hybrid method predictions, both for cold and reacting bluff-body flows, what has been demonstrated in KOUTMOS *et al.* [8].

2.2. Combustion model

2.2.1. *Basic turbulence/chemistry interaction model.* A partial equilibrium scheme corresponding to a two-scalar description employing the mixture fraction, f , and the CO_2 concentration, Y_{CO_2} , were used. The reaction $\text{CO} + \text{OH} \leftrightarrow \text{CO}_2 + \text{H}$ was introduced to allow for non-equilibrium effects, and CO_2 formation from CO is assumed to proceed as:

$$\dot{r}_{\text{CO}_2} = k_f Y_{\text{CO}} Y_{\text{OH}} - \left(\frac{k_f}{k_\varepsilon} \right) Y_{\text{CO}_2} Y_{\text{H}}, \quad k_f = 6.76 \cdot 10^{11} \exp \left(\frac{T}{1102} \right)$$

and k_ε is taken from the JANAF (Tables).

Additionally, when the mixture strength exceeds the rich flammability limit, the composition is taken as that of equilibrium at this limit diluted with pure fuel. The final composition is calculated from the NASA equilibrium code for given f and Y_{CO_2} values by defining Y_{CO_2} as an ‘element’. The passive, f , and the reactive, Y_{CO_2} , variables, are calculated from the equations

$$(2.6) \quad \frac{\partial (\bar{\rho} \langle \tilde{f} \rangle)}{\partial t} + \frac{\partial}{\partial \chi_j} (\bar{\rho} \langle \tilde{u}_j \rangle \langle \tilde{f} \rangle) = \frac{\partial}{\partial \chi_j} \left[\left(\bar{\rho} D + \frac{\mu_t}{Sc_t} \right) \frac{\partial \langle \tilde{f} \rangle}{\partial \chi_j} \right],$$

$$(2.7) \quad \frac{\partial (\bar{\rho} \langle \tilde{Y}_{\text{CO}_2} \rangle)}{\partial t} + \frac{\partial}{\partial \chi_j} (\bar{\rho} \langle \tilde{u}_j \rangle \langle \tilde{Y}_{\text{CO}_2} \rangle) = \frac{\partial}{\partial \chi_j} \left[\left(\bar{\rho} D + \frac{\mu_t}{Sc_t} \right) \frac{\partial \langle \tilde{Y}_{\text{CO}_2} \rangle}{\partial \chi_j} \right] + \bar{\rho} \tilde{r}_{\text{CO}_2},$$

with gradient transport assumptions for the turbulent fluxes $\overline{u'_j f'}$ and $\overline{u'_j Y'_{\text{CO}_2}}$.

An exponential joint PDF is constructed from the normalized mixture fraction and CO_2 concentration values, f^* and $Y_{\text{CO}_2}^*$, which are used to transform the physically allowable space of f and Y_{CO_2} into a normalized square area suitable for integration. The relationships established by this transformation are:

$$(2.8) \quad f^* = f + Y_{\text{CO}_2} / Y_{\text{CO}_2, \text{air}}, \quad Y_{\text{CO}_2}^* = Y_{\text{CO}_2} / (f Y_{\text{CO}_2, \text{fuel}}),$$

where

$$Y_{\text{CO}_2, \text{fuel}} = n M_{\text{CO}_2} / M_{\text{C}_N \text{H}_M},$$

$$Y_{\text{CO}_2, \text{air}} = M_{\text{CO}_2} / (M_{\text{O}_2} + M_{\text{N}_2} / 0.259).$$

The local PDF is of the form:

$$(2.9) \quad P(f^*, Y_{\text{CO}_2}^*) = \exp[a_1 + a_2 f^* + a_3 Y_{\text{CO}_2}^* + a_4 f^{*2} + a_5 Y_{\text{CO}_2}^* + a_6 f^* Y_{\text{CO}_2}^*],$$

where f^* and $Y_{\text{CO}_2}^*$ are appropriately transformed variables, and it is calculated through the coefficients $(a_1 \dots a_6)$ which depend on the local moments $\overline{f'^2}$, $\overline{Y_{\text{CO}_2}'^2}$, $\overline{f'Y_{\text{CO}_2}'}$, which are obtained by assuming equilibrium between the turbulent production and destruction of these moments in their transport equation:

$$(2.10) \quad \frac{\partial (\overline{\rho X'Z'})}{\partial t} + \frac{\partial (\overline{\rho \tilde{u}_j X'Z'})}{\partial x_j} = \frac{\partial}{\partial x_j} \left[\left(\overline{\rho D} + \frac{\mu_t}{Sc_t} \right) \frac{\partial \overline{X'Z'}}{\partial x_j} \right] \\ + 2 \frac{\mu_t}{Sc_t} \left[\frac{\partial \tilde{X}}{\partial x_i} \frac{\partial \tilde{Z}}{\partial x_i} \right] - C_\Phi \overline{\rho} \frac{1}{\tau_t} \overline{X'Z'} + \overline{X'S_Z} + \overline{Z'S_X}.$$

The moments are then obtained from the following expression:

$$(2.11) \quad \overline{X'Z'} = \frac{1}{2.0\overline{\rho}} \left[\frac{2\mu_t}{Sc_t} \frac{\partial \tilde{X}}{\partial x_i} \frac{\partial \tilde{Z}}{\partial x_i} + \overline{X'S_Z} + \overline{Z'S_X} \right] \tau_t,$$

$$\overline{X} = \langle \tilde{f} \rangle \quad \text{or} \quad \langle \tilde{Y}_{\text{CO}_2} \rangle \quad \text{and} \quad \overline{Z} = \langle \tilde{f} \rangle \quad \text{or} \quad \langle \tilde{Y}_{\text{CO}_2} \rangle, \quad C_\Phi = 2.0.$$

Mean quantities and correlations are evaluated by using the PDF information, e.g.

$$(2.12) \quad \tilde{r}_{\text{CO}_2} = \frac{1}{\overline{\rho}} \iint \tilde{r}_{\text{CO}_2} J \rho P(f^* \tilde{Y}_{\text{CO}_2}^*) df^* dY_{\text{CO}_2}^*,$$

where J is the Jacobian of the transformation, τ_t is evaluated as follows in line with the hybrid model formulation: if $L_t > \Delta$ then $\tau_t = \Delta / \sqrt{\langle \tilde{k} \rangle}$, and if $L_t < \Delta$ then $\tau_t = \langle \tilde{k} \rangle / \langle \tilde{\varepsilon} \rangle$.

2.2.2. Extinction/reignition model. The modeling of finite-rate chemistry effects such as partial extinctions and reignitions encountered in the lifted flames follows the approach of KOUTMOS [9]. Local extinction is predicted when the local Damkohler number, Da_l , defined as the ratio of the turbulent time scale $\tau_\lambda = 3.88\tau_k$ (τ_k is the Kolmogorov time scale) to the chemical time scale, τ_{ch} , is below the local critical ‘limit’ Da_{cr} being a function of position and local conditions. The criterion for local quenching reads then:

$$(2.13) \quad \lambda = \frac{Da_l}{Da_{cr}} = \frac{[\tau_\lambda / \tau_{ch}]}{\left[\frac{\Sigma_f}{\sqrt{2}\Delta f_R} R_{et}^{1/4} \right]} \leq 1.$$

The mean gas state subsequent to extinction \tilde{Y}_Q is obtained by convoluting with the local exponential PDF involving the reactedness, B , and the mixture fraction:

$$(2.14) \quad \tilde{Y}_Q = (1/\tilde{\rho}) \iint Y_Q \rho P(\tilde{f}, \tilde{B}) df dB,$$

\tilde{B} is here calculated from the following model Lagrange-type transport equation [10]:

$$(2.15) \quad \frac{\partial (\rho \tilde{B})}{\partial t} + \frac{\partial (\tilde{\rho} u_j \tilde{B})}{\partial \chi_j} = S_B,$$

while its fluctuations, \tilde{B}^2 and $\tilde{f}\tilde{B}'$, are obtained by invoking a scale-similarity assumption [12]. Further details of the full model may be found in Refs. [8, 9, 12].

Reignition is allowed when a) the time-scale criterion, Eq. (2.13), is inoperative and b) the cumulative probability of finding a flammable mixture at this location, defined as

$$P_F = \int_{f_1}^{f_2} P(f^*) df^*,$$

is greater than 0.65. Then the source term in Eq. (2.15) is equal to

$$(B_0 - \tilde{B})/\tau_{id},$$

where τ_{id} is a mixing-dependent chemical ignition delay time [8–12].

2.3. Turbulent flame noise model

For evaluation of the autonomous sound radiation due to interaction of the turbulent fluctuations with the flame front, the model formulation of KLEIN [5] has been followed closely. Starting from the basic wave equation for low Mach number flows [1, 2], the one-dimensional sound generated by the fluctuating heat release from a turbulent non-premixed flame is evaluated [5] by deriving an integral expression, assuming that the instantaneous combustion zone is infinitely thin and that combustion is fast and determined by mixing of fuel and air. The sound spectrum can then be expressed [5] as a function of a one-dimensional turbulence spectrum (of assumed shape) of the mixture fraction at the flame front. The resulting expression for the sound spectrum for a non-premixed turbulent flame is then given in integral form as a function of frequency:

$$(2.16) \quad pp(f_\nu) = 2\pi \left(\frac{C_0}{S}\right)^2 \iint_{\mathbf{x}} \left[(\rho D B A)^2 \frac{L_{\text{cor}} \theta_{f_\nu}}{2U} E_{ID}^2 \left(\frac{2\pi f_\nu}{2U}\right) \right] dx dy,$$

where C_0 – speed of sound, S – area of combustor nozzle, D – laminar diffusion coefficient B ,

$$B = \frac{1}{2}x \left/ \frac{1}{\pi} D \int_0^{\infty} E_{ID}(k) dk, \right.$$

x – scalar dissipation = $2.0 \frac{\varepsilon}{k} \tilde{f}'_{\nu}{}^2$, E_{ID} – one-dimensional turbulence spectrum of assumed shape,

$$E_{ID} = \left\{ \begin{array}{ll} 1, & k_1 < k_{\varepsilon} \\ (k_1/k_2)^{-(5/3)}, & k_{\varepsilon} < k_1 < k_{\text{kol}} \\ 0, & k_1 > k_{\text{kol}} \end{array} \right\}$$

with $k_1 = 2\pi f_{\nu}/2U$, $k_{\varepsilon} = \pi/l_t$, $k_{\text{kol}} = (\varepsilon/\nu^3)^{1/4}$, $\theta_{f_{\nu}}$ – thickness of the mixing layer between fuel and air, equal to $1/\sqrt{(\nabla^2 f_{\nu})}$,

$$A = [T_{\text{flame}} - T_0]/[T_{\text{flame}} f_{st} (1 - f_{st})],$$

f_{ν} – frequency.

The parameter sound pressure level, SPL , expressed in dB, can also be evaluated as:

$$(2.17) \quad SPL(f_{\nu}) = 20 \log \left(\frac{\sqrt{pp(f_{\nu})}}{20 \cdot 10^{-6}} \right).$$

The time-averaged information about the turbulence sound spectrum and other parameters required in the above expression is derived from the basic reacting flow calculation, the computation of the sound spectrum being performed in a post-processing step.

2.4. Numerical details

The coflowing methane-air jet configuration and computational domain are shown in Fig. 1. The convective condition $\partial\phi/\partial t + U_0(\partial\phi/\partial x) = 0$, ($C = \bar{U}_0$) was used at the outlet. A mesh of 205×123 (x, y) grid points was used with an axial expansion ratio of 1.1. For inlet conditions, a fully developed flow was assumed.

The equations were solved using a finite-volume method based on a staggered mesh, a pressure correction method (SIMPLE) and the QUICK differencing scheme [8]. A second-order scheme was used for temporal integration. Time steps were of the order $10^{-4} - 10^{-5}$ sec, depending on the fuel Reynolds number. After an initial transient of about $30t_0$ ($t_0 = D/U_0$), the statistics were computed over approximately $100t_0$.

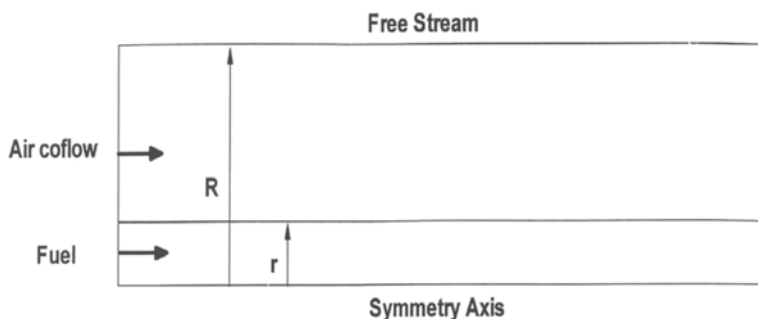


FIG. 1. Methane-air coflowing jet flame configuration Investigated $R = 27r$ and the length of computation Domain is $50r$.

3. RESULTS AND DISCUSSION

Computations were initially performed for a steady-state, laminar CH_4 -air diffusion flame for which experimental data by MITCHELL *et al.* [13] is available. Figures 1 and 2 show the flow configuration and sample results for undiluted CH_4 jet flow at 5 cm/sec through a 1.2 cm-diameter tube, with a coflow of air at 10 cm/sec, which are compared against the experimental data of reference [13]. Results are compared with the data at the final steady-state, which was reached after about 25,000 time-steps ($\Delta t = 0.06$ sec). Overall, the agreement is satisfactory in both the reactive scalar (temperature) and the momentum field (axial velocity), despite some experimental uncertainties concerning the rig exit conditions and these comparisons lend support for an extension of the basic model to more complex, turbulent lifted flames.

Figure 3 displays time-averaged temperature contours for the three jet velocities of 2, 20 and 40 m/sec investigated. The stoichiometric contour is also superimposed on the plot. By comparison to the reported non-dimensional lift-off heights, the present simulation seems to underestimate the stabilization position by about 7% and 12% for the two jet velocities respectively. An instantaneous isotherm snapshot of the reacting flow field is illustrated in Fig. 4. A variation of the lifted flame base with an up and down movement of about 12%, was observed in the time-dependent simulations. Due to their two-dimensional nature, the resulting spectra could not allow a reliable evaluation of the spectral behavior of this important lifted flame base region.

An overall qualitative picture of the velocity field is shown in the form of vector plots in Fig. 5. The mean velocity (Favre-averaged) due to expansion slows down approaching the flame front and accelerates as it flows past it. Any relevant local scaling is therefore expected to include the effects of expansion on local parameters, e.g. the flame front propagation speed in relation to the laminar flame speed.

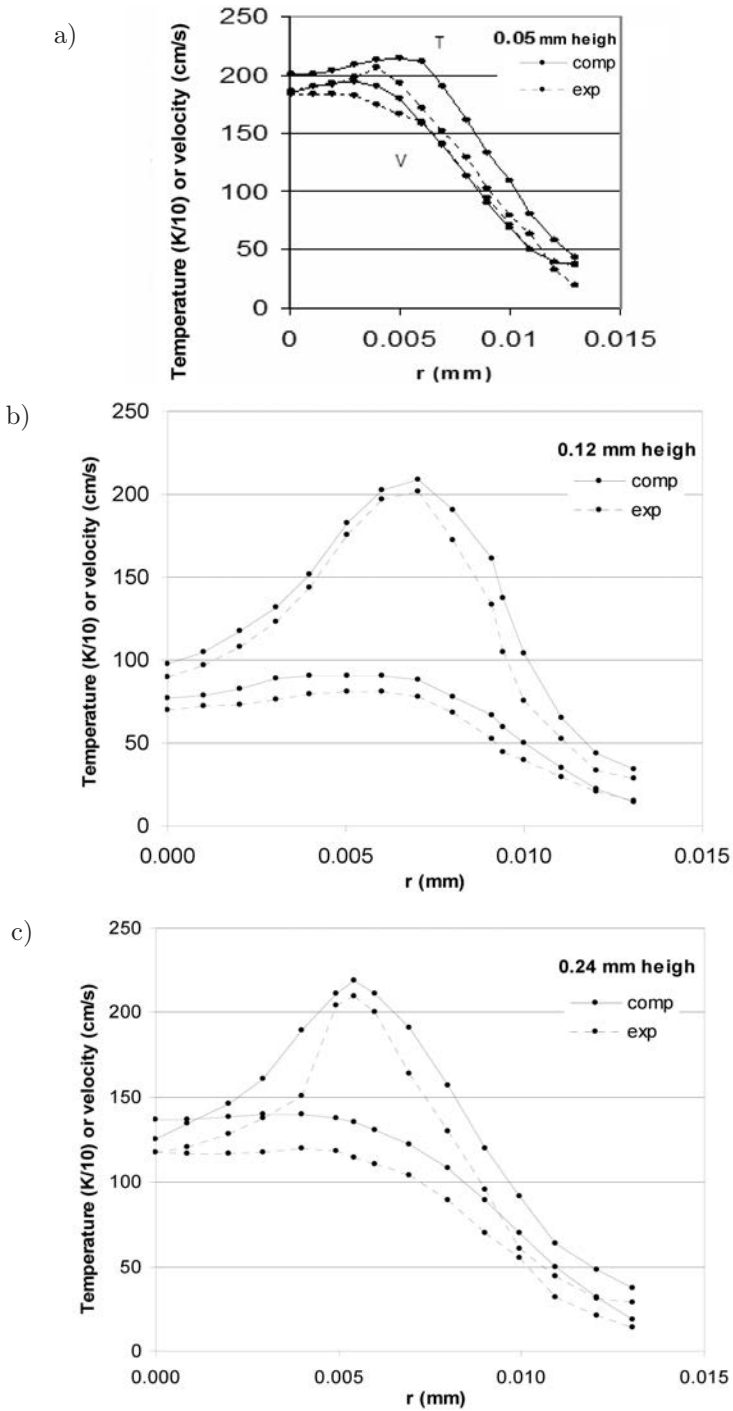


FIG. 2. Laminar CH₄ jet flame predictions for fuel jet velocity a) 2 m/s, b) 20 m/s, c) 40 m/s.

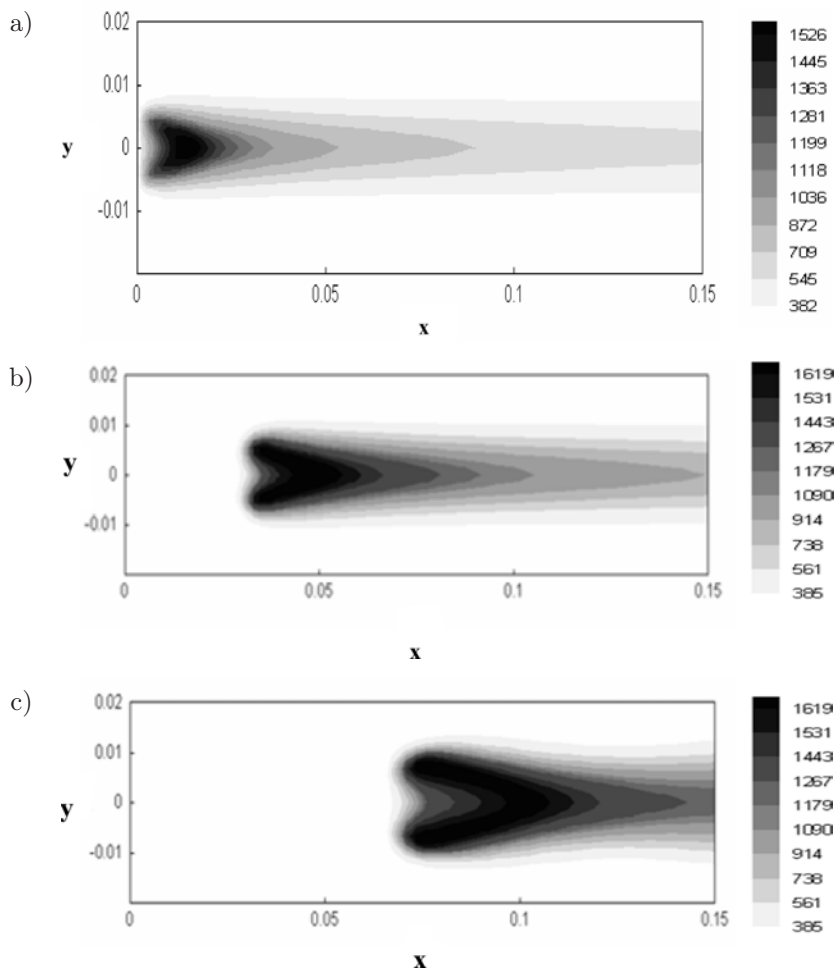
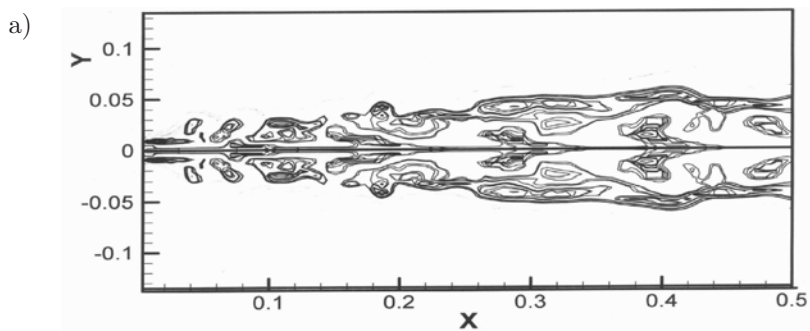


FIG. 3. Time-average temperature contours for fuel jet velocity a) 2 m/s, b) 20 m/s, c) 40 m/s.



[Fig. 4a]

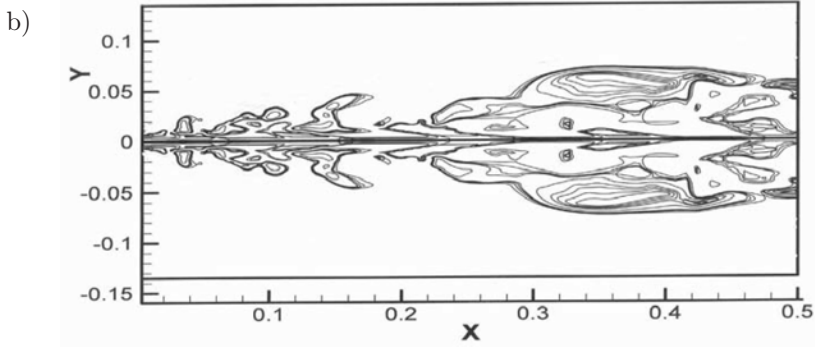
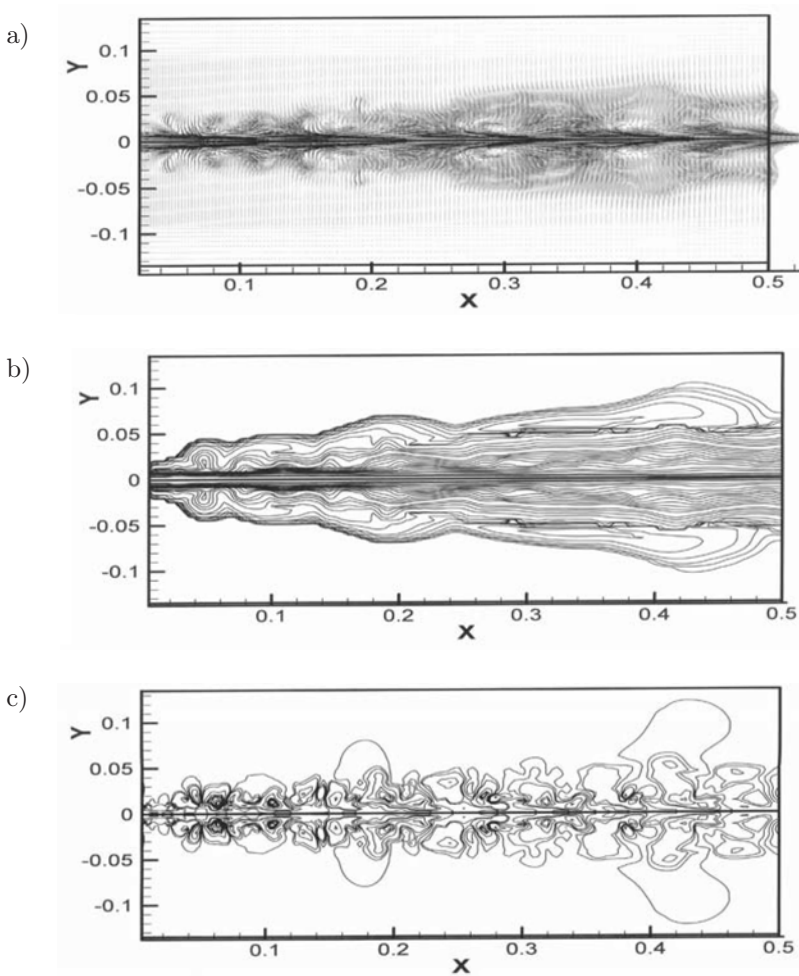


FIG. 4. Instantaneous temperature isotherms: a) $u_j = 20$ m/s, b) $u_j = 40$ m/s.



[Fig. 5a, b, c]

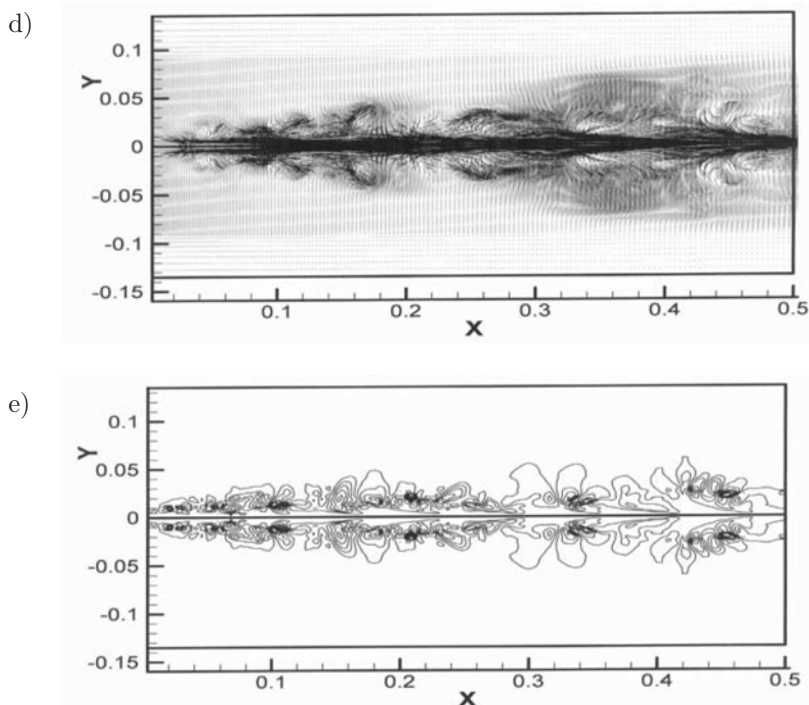


FIG. 5. a) Instantaneous plot of velocity vectors ($u_j = 20$ m/s); b) instantaneous plot of fuel fraction contours ($u_j = 20$ m/s); c) instantaneous plot of V contours ($u_j = 20$ m/s); d) instantaneous plot of velocity vectors ($u_j = 40$ m/s); e) instantaneous plot of V contours ($u_j = 40$ m/s).

Some preliminary joint statistics between temperature and mixture fraction, two important scaling parameters for the partially premixed regime [14], have been produced from the time-dependent calculation of the higher fuel jet velocity of 20 m/sec and they are shown in Fig. 6. The collected points lie close to the stoichiometric contour in the vicinity of the movement of the flame base. Methane is well-known for its bimodal approach to extinction from a wide range of the previously reported papers (e.g. [12]). The present plot implies a lower level of bimodality, with the scatter points located mostly above the mixing asymptote and below the partial equilibrium levels. The variance of mixture fraction spreads the points over an area slightly broader than the lean limit.

Experimental data of this nature would be very helpful in identifying the detailed nature and flow behavior of the near-stabilization region. The reduced bimodality with respect to customary diffusion flames [12, 14] may be attributed to the loss of resolution in the present simulation, to deficiencies in the reignition model which is formulated for pure diffusion flames, or to a lower variability of the chemical time-scale arising from omission of the effects of partially premixed

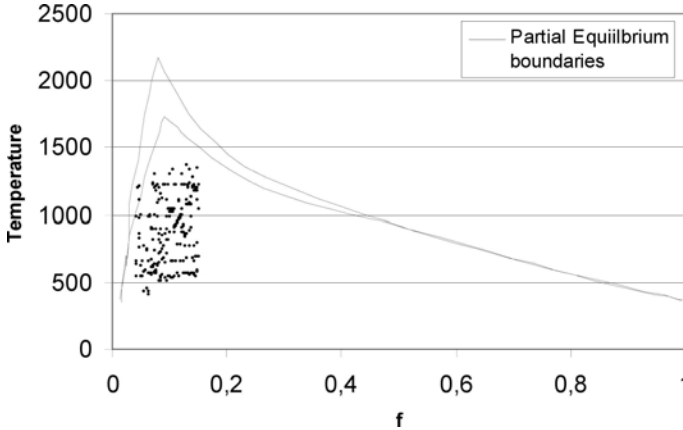


FIG. 6. Mixture fraction-Temperature scatter plot taken in the vicinity of the lifted flame base.

flame propagation. This aspect is not treated explicitly in the model other than through the inclusion of the relevant chemical time-scale.

Encouragingly, the present modeling formulation recovered two important, experimentally observed trends. Firstly, the linear relationship between the flame lift-off height and jet exit velocity, that has been extensively verified through global and detailed measurements, as well as the correct slope of this linear variation. Secondly, it reproduced adequately the increase in lift-off height for a given jet inflow velocity as the fuel flow is diluted, e.g. with N_2 , something expected since the residence time is now longer when the fuel stream is diluted.

The reasonable performance of the computational model of prediction of the experimentally observed aerothermodynamic parameter variations and trends, lends support to the extension of the method to include and apply the flame noise described previously, to enable a meaningful evaluation of the combustion noise radiated by the present flames. Flame noise calculations were performed for two selected flame configurations, the attached flame with exit fuel velocity of 2 m/s and the lifted-off flame configuration with exit fuel velocity of 20 m/s.

Equation (2.16) was discretized to be able to calculate it numerically and the integral is computed numerically at every grid cell. The part in square brackets in the expression of Eq. (2.16) can be considered as the strength of the local noise source and gives an indication of a spatial distribution of the local noise ‘intensity’ in the reacting flow field for each selected frequency. Integrating numerically Eq. (2.16) for all cell surface and over the full frequency range ($\Delta f_\nu = 1$ Hz, $P_{\text{ref}} = 20 \mu\text{Pa}$), we deduce the sound spectrum expressed in dB sound pressure level from Eq. (2.17). The turbulent aero-thermochemical data produced by the basic time-dependent computation are time-averaged and supply the required information necessary to evaluate the parameters involved in Eq. (2.16) for every

cell surface and frequency. Figures 7a, b display contours of the local noise intensity (the term between the square brackets in Eq. (2.16)) for a frequency of 100 Hz.

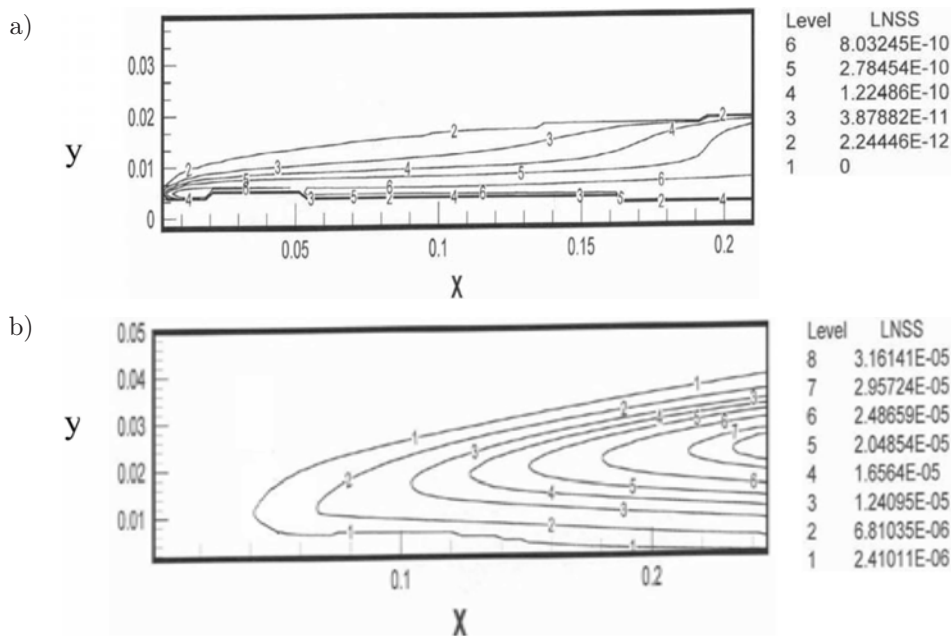


FIG. 7. The local noise source intensity distribution for fuel jet velocity: a) 2 m/s, b) 20 m/s.

It is seen that noise generation levels are predominant mainly in vicinity of the mixing interface between the fuel and the oxidizer. These attain maximum values downstream of the lift-off flame base for the lifted flame, while for the attached flame the peak noise strength region is again dislocated downstream of the burner rim. In both cases, the location of the maximum noise intensity coincides with the region of the peak temperatures levels. The lifted flame produces significantly increased maximum values of the local noise source strength with respect to the attached flame and this appears to be a reasonably predicted trend, since the lifted flame produces increased turbulence levels and temperature fluctuations downstream of its lifted base.

The calculated sound spectra for the above-discussed flames are plotted in Figs. 8a, b. The lifted flame gives elevated energy content in the sound spectrum by about 30% with respect to the attached case, particularly near the lower frequency range at about 80 Hz, thereafter falling off to nearly similar levels. This is evidently consistent with the previously discussed predictions of the local noise intensity levels. It should also be noted that the qualitative distribution of the spectral density also depends on the assumed turbulence spectrum used in Eq. (2.16).

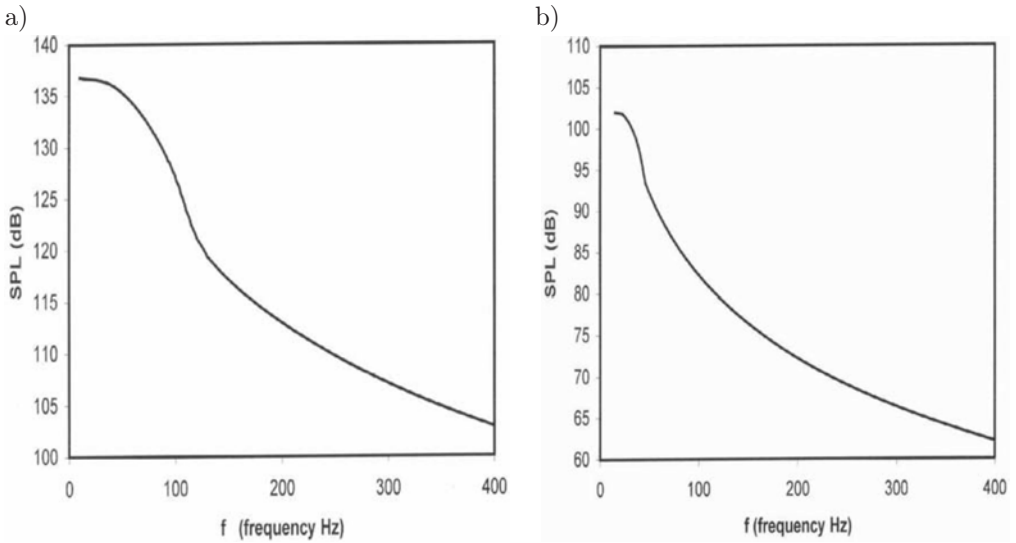


FIG. 8. The calculated sound spectra for: a) lifted and b) attached flame, plotted in SPL dB ($\Delta f = 1$ Hz).

An aspect that merits discussion is whether the assumption of fast chemistry can still be applied for the partially-premixed flame configuration with lift-off when using Eq. (2.15), and to what extent the expected discrepancies affect the validity of the present prediction. Experimental results would be quite helpful to identify the extent of disagreement in the sound pressure level predictions of this flame and this would help to improve the present modeling effort. Notwithstanding the above arguments, it is believed that the present procedure has captured the basic behaviors and trends in the aero-thermochemical and flame noise generation characteristics of the studied flames, although further tests and refinements would be required to enlarge the applicability of the method.

4. SUMMARY

A computational procedure of the time-dependent reactive Navier–Stokes equations has been employed to study the stabilization mechanism and the autonomous noise generation by the flame front, due to turbulent fluctuations in attached and lifted methane jet flames. Although the method exploited primarily the diffusion flame concepts with the effects of partial extinctions/reignitions embodied, it produced reasonable qualitative agreement with the reported data. Despite the fact that these exploratory and preliminary computations are based on axisymmetric configurations and hence the 3-D or the non-symmetric turbulent behavior is excluded, the present method captured many important trends

and behaviors and allows for evaluation and further development of the overall methodology. Further extensions along the line of addressing in a more clear-cut manner the impact of partial-premixing are also required.

The adequate accord between computations and experimental observation in the turbulent aerothermodynamic flow and flame parameters enabled a first attempt to evaluate the turbulent combustion noise (roar) characteristics of the complex flame configurations investigated here. The developed methodology provides a basis to address the coupled effects of turbulence interactions, heat release and chemistry, and the autonomous turbulent combustion noise generated at the flame front. These preliminary results suggest that the modeling procedure followed such complex behaviors as the variation of the flame lift-off height with fuel jet velocity and the accompanying increase of the radiated flame noise levels. Further detailed assessment and improvements of the described methodology may however be required to demonstrate its wider applicability.

ACKNOWLEDGMENT

The research was sponsored by the program “K. Karatheodori”, Epitropi Ereunon, University of Patras.

REFERENCES

1. J. M. TRUFFAUT, G. SEARBY and L. BOYER, *Sound emission by non-isomolar combustion at low Mach numbers*, Combustion Theory and Modeling, **2**, 423–428, 1998.
2. S. M. CANDEL, *Combustion instabilities coupled by pressure waves and their active control*, Proc. Combustion Institute, **24**, 1277–1296, 1992.
3. W. C. STRAHLE, C. CASCI and C. BRUNO, Recent Advances in the Aerospace Sciences, (New York: Plenum) 103–140, 1985
4. P. BOIENAU, Y. GERRAIS and V. MORICE, *An aerothermoacoustic model for computation of sound radiated by turbulent flames*, Internoise, **96**, 495–508, 1996.
5. S. A. KLEIN, *On the acoustics of turbulent non-premixed flames*, PhD thesis, University of Twente, Enschede, The Netherlands, 2000.
6. W. M. PITTS, *Assessment of the theories for the behaviour and blow-out of lifted turbulent jet diffusion flames*, 22nd Symposium (International) on Combustion, The Combustion Institute, Pittsburgh, 809–816, 1989.
7. R. W. SCHEFER, M. NAMAZIAN, E. E. J. FILTOPOULOS and J. KELLY, *Temporal evolution of turbulence/chemistry interactions in lifted turbulent-jet flames*, 25th Symposium (International) on Combustion, The Combustion Institute, Pittsburgh, 1223–1231, 1994.
8. P. KOUTMOS, C. MAVRIDIS and D. PAPAILIOU, *Time-dependent computation of turbulent bluff-body diffusion flames close to extinction*, International Journal of Numerical Methods for Heat and Fluid Flow, **9**, 39–59, 1999.

9. P. KOUTMOS, *Damkohler number description of local extinction in turbulent methane jet diffusion flames*, *Fuel*, **78**, 623–626, 1999.
10. R. BORGHİ, *Turbulent combustion modeling*, *Prog. in Energy and Combustion Science*, **14**, 245–292, 1988.
11. P. KOUTMOS and P. MARAZIOTI, *Identification of local extinction topology in axisymmetric bluff-body diffusion flames with a reactedness-mixture fraction presumed probability density function model*, *International Journal for Numerical Methods in Fluids*, **35**, 939–959, 2001.
12. D. PAPAILIOU, P. KOUTMOS, C. MAVRIDIS and A. BAKROZIS, *Simulations of local extinction phenomena in bluff-body stabilized diffusion flames with a Lagrangian reactedness model*, *Combustion Theory and Modelling*, **3**, 409–431, 1999.
13. R. E. MITCHELL, A. F. SAROFIN and L. A. CLOMBURG, *Experimental and numerical investigation of confined laminar diffusion flames*, *Combustion and Flame*, **37**, 227–244, 1980.
14. T. ECHEKKI and J. H. CHEN, *The effects of complex chemistry on triple flames*, NASA CTR manuscript, *Proceedings of the Summer School*, 217–233, 1996.

Received May 27, 2009.

REVIEW ON SPECTRAL DECOMPOSITION OF HOOKE'S TENSOR FOR ALL SYMMETRY GROUPS OF LINEAR ELASTIC MATERIAL

K. K o w a l c z y k – G a j e w s k a,
J. O s t r o w s k a – M a c i e j e w s k a

**Institute of Fundamental Technological Research
Polish Academy of Sciences**

Pawińskiego 5B, 02-106 Warszawa, Poland

The spectral decomposition of elasticity tensor for all symmetry groups of a linearly elastic material is reviewed. In the paper it has been derived in non-standard way by imposing the symmetry conditions upon the orthogonal projectors instead of the stiffness tensor itself. The numbers of independent Kelvin moduli and stiffness distributors are provided. The corresponding representation of the elasticity tensor is specified.

Key words: linear elasticity, anisotropy, symmetry group, spectral decomposition.

1. INTRODUCTION

This work is devoted to the review on the spectral decomposition of the elasticity tensor (Hooke's tensor). Possibility of application of the spectral theorem within this context was first noticed by Lord Kelvin (W. THOMPSON) in 1856 [10]. Then the idea was forgotten and rediscovered by RYCHLEWSKI in 1983 [22] and independently by MEHRABADI and COWIN in 1990 [7]. The consequences of the theorem have been thoroughly explored by the above researchers and their co-workers, leading to many inspiring results, i.e. the spectral form of elasticity tensor was derived for all elastic symmetry classes [2, 6, 25], the role of pure shears was analyzed [3], the extremum of elastic energy was found for the selected sets of stress states [19], the properties of biological materials were identified [7]. After that the idea has found numerous applications, especially when dealing with anisotropic materials. Now, this invariant decomposition of the elasticity tensors is widely known, though, still some aspects of it remain not fully understood. The main goal of this paper is to clarify the issue of invariance of the decomposition, mainly the crucial notion of orthogonal projector introduced by RYCHLEWSKI [22] with respect to the notion of an eigen-state which is preferably used in the papers by COWIN and co-workers, e.g. [6]. Furthermore the spectral theorem is applied for elastic material of each symmetry class. The novelty of

the present work is the derivation of the form of the stiffness tensor for the subsequent elastic symmetry groups by imposing the symmetry conditions upon the orthogonal projectors instead of the stiffness tensor itself. We think that the present paper will be useful for all who would like to apply the spectral theorem in their fields of research.

Linear elastic material (classical elastic body) is considered for which the small strain tensor $\boldsymbol{\varepsilon}$ depends on the stress tensor $\boldsymbol{\sigma}$ according to Hooke's law:

$$(1.1) \quad \boldsymbol{\varepsilon} = \mathbf{M} \cdot \boldsymbol{\sigma} \quad \text{or} \quad \boldsymbol{\sigma} = \mathbf{L} \cdot \boldsymbol{\varepsilon}, \quad \mathbf{M} \circ \mathbf{L} = \mathbb{I}^S,$$

$$\varepsilon_{ij} = M_{ijkl}\sigma_{kl} \quad \text{or} \quad \sigma_{ij} = L_{ijkl}\varepsilon_{kl}, \quad M_{ijmn}L_{mnkl} = \frac{1}{2}(\delta_{ik}\delta_{jl} + \delta_{il}\delta_{jk}),$$

where \mathbf{M} is a compliance tensor and \mathbf{L} is a stiffness tensor. The above law is valid for the stress states restricted by the limit Mises condition

$$\boldsymbol{\sigma} \cdot \mathbf{H} \cdot \boldsymbol{\sigma} \leq 1, \quad \sigma_{ij}H_{ijkl}\sigma_{kl} \leq 1,$$

where \mathbf{H} is the limit tensor. Theory of elasticity of anisotropic bodies is presented in detail e.g. in [9, 16]. In this paper we deal only with the properties of the stiffness tensor resulting from its spectral decomposition, without referring to any boundary value problem.

Hooke's tensors \mathbf{M} , \mathbf{L} are linear operators which project the space \mathcal{S} of symmetric II-nd order tensors into itself. Hooke's tensors are defined as positive-definite IV-th order Euclidean tensors with the following internal symmetries, namely

$$A_{ijkl} = A_{jikl} = A_{ijlk} = A_{klij} \quad (\mathbf{A} \rightarrow \mathbf{L}, \mathbf{M}).$$

Because of the above internal symmetries, in any Cartesian basis Hooke's tensor is, in general, specified by 21 independent components M_{ijkl} and $L_{mnr s}$. These components change when the basis in physical space is transformed, therefore they are not material constants. The compliance and stiffness tensors are also used in quadratic forms specifying the energy functional

$$(1.2) \quad 2\Phi = \boldsymbol{\sigma} \cdot \mathbf{M} \cdot \boldsymbol{\sigma} = \boldsymbol{\varepsilon} \cdot \mathbf{L} \cdot \boldsymbol{\varepsilon}.$$

Unfortunately, the complete set of the invariants for Hooke's tensor, which uniquely describe such tensor with an accuracy to the rigid rotation of the considered body, is not known. Because there are 21 independent components of Hooke's tensor, while the orientation of a sample with respect to the laboratory is specified by 3 parameters (i.e. Euler angles), an irreducible functional basis of orthogonal invariants for \mathbf{L} (\mathbf{M} , \mathbf{H}) consists of $21 - 3 = 18$ invariants. Conventional approach does not provide the form of such basis for the whole set of

elastic continua. However, some results can be derived when the material enjoys some external symmetries.

Note that for the tensor of even order, the following eigen-problem is well-posed. Using the general theory of linear operators one finds that the conditions

$$(1.3) \quad \mathbf{L} \cdot \boldsymbol{\omega} = \lambda \boldsymbol{\omega}, \quad \mathbf{M} \cdot \boldsymbol{\omega} = \frac{1}{\lambda} \boldsymbol{\omega}$$

specify eigenvalues and eigen-elements of these operators. Eigen-elements corresponding to different eigenvalues are always pairwise orthogonal. The condition (1.3) is also the necessary condition for the elastic energy (1.2) to reach an extremum value over the unit sphere (that is for $\boldsymbol{\sigma} \cdot \boldsymbol{\sigma} = 1$).

In general, the tensor \mathbf{L} has no more than six real different eigenvalues $\lambda_I, \lambda_{II}, \dots, \lambda_{VI}$ to which one can relate six mutually orthogonal unit eigen-elements $\boldsymbol{\omega}_I, \boldsymbol{\omega}_{II}, \dots, \boldsymbol{\omega}_{VI}$. These normalized eigen-elements are called *elastic eigen-states*. They are specified with accuracy to a sign and constitute an orthonormal basis in the space \mathcal{S} of the II-nd order tensors

$$(1.4) \quad \boldsymbol{\omega}_K \cdot \boldsymbol{\omega}_L = \delta_{KL}, \quad K, L = I, \dots, VI.$$

Eigenvalues $\lambda_I, \lambda_{II}, \dots, \lambda_{VI}$ specify the material stiffness in response to the deformations $\boldsymbol{\varepsilon} = e \boldsymbol{\omega}_K$ of direction of $\boldsymbol{\omega}_K$, where $\boldsymbol{\omega}_K$ are the elastic eigen-states. λ_K are called *stiffness moduli* or Kelvin moduli [22, 25], and they are non-negative. This is the only constraint imposed on elastic constants by thermodynamics. For any deformation $\boldsymbol{\varepsilon} = e \boldsymbol{\omega}$, where $\boldsymbol{\omega}$ is an eigen-state, Hooke's law takes the form of the proportionality rule

$$\boldsymbol{\sigma} = \lambda \boldsymbol{\varepsilon},$$

where λ is the Kelvin modulus corresponding to $\boldsymbol{\omega}$. The resulting form of the elastic energy for the elastic eigen-states has been specified already by Kelvin [10] as follows:

$$\boldsymbol{\varepsilon} \cdot \mathbf{S} \cdot \boldsymbol{\varepsilon} = \lambda_I e_I^2 + \lambda_{II} e_{II}^2 + \dots + \lambda_{VI} e_{VI}^2, \quad e_K = \boldsymbol{\varepsilon} \cdot \boldsymbol{\omega}_K$$

and

$$\boldsymbol{\varepsilon} = e_I \boldsymbol{\omega}_I + e_{II} \boldsymbol{\omega}_{II} + \dots + e_{VI} \boldsymbol{\omega}_{VI}.$$

Each sequence

$$(1.5) \quad (\lambda_I, \dots, \lambda_{VI}; \boldsymbol{\omega}_I, \dots, \boldsymbol{\omega}_{VI}),$$

consisting of six Kelvin moduli $\lambda_K \geq 0$ and six elastic eigen-states $\boldsymbol{\omega}_K$ specifies an elastic material which is theoretically admissible.

In order to derive 6 eigen-states $\boldsymbol{\omega}_K$ (symmetric second-order tensors) it is sufficient to specify 15 quantities. Conditions (1.4) of orthonormality of the eigen-states provide 21 additional conditions

$$\binom{6}{1} + \binom{6}{2} = 6 + 15 = 21,$$

which reduce the number of independent quantities from 36 (6×6) to 15 ($36 - 21 = 15$). Consequently, the variety of elastic continua is locally described in a continuous way by a set of $6 + 15 = 21$ parameters.

Out of the 15 parameters describing eigen-states one can separate three which are not invariants. They orient the stiffness tensor \mathbf{L} with respect to a reference frame (a laboratory). These three parameters can be defined as three Euler angles ϕ_1, ϕ_2, ϕ_3 . Remaining 12 parameters are dimensionless material constants – invariants and common invariants of eigen-states (eigen-tensors) \aleph_k [15]. They are common for the stiffness tensor \mathbf{L} and compliance tensor \mathbf{M} and they are called *stiffness distributors* as far as they characterize the distribution of stiffness between the material fibers and the material planes. Stiffness distributors specify the orthonormal basis of eigen-states $\boldsymbol{\omega}_K$ with accuracy to the rotation in a physical space [25].

In conclusion, parameters describing some elastic continua can be subdivided into three groups

$$(6 + 12) + 3 = 21.$$

1. The first group consists of 6 **Kelvin moduli** $\lambda_I, \dots, \lambda_{VI}$ which have a dimension of the stress tensor.
2. The second group consists of dimensionless 12 **stiffness distributors** $\aleph_1, \dots, \aleph_{12}$,
3. The third group consists of three **Euler angles** ϕ_1, ϕ_2, ϕ_3 .

Therefore, one has

$$(1.6) \quad \langle \lambda_I, \dots, \lambda_{VI}; \aleph_1, \dots, \aleph_{12}; \phi_1, \phi_2, \phi_3 \rangle.$$

Two elastic bodies are made of the same material if values of 18 invariants, that is $\lambda_I, \dots, \lambda_{VI}$ and $\aleph_1, \dots, \aleph_{12}$, are equal for both of them.

Knowing the Kelvin moduli λ_K and the corresponding elastic eigen-states $\boldsymbol{\omega}_K$, the tensors \mathbf{L} and \mathbf{M} can be represented in the form of their spectral decompositions [17, 22, 28]:

$$(1.7) \quad \mathbf{L} = \lambda_I \boldsymbol{\omega}_I \otimes \boldsymbol{\omega}_I + \dots + \lambda_{VI} \boldsymbol{\omega}_{VI} \otimes \boldsymbol{\omega}_{VI},$$

$$(1.8) \quad \mathbf{M} = \frac{1}{\lambda_I} \boldsymbol{\omega}_I \otimes \boldsymbol{\omega}_I + \dots + \frac{1}{\lambda_{VI}} \boldsymbol{\omega}_{VI} \otimes \boldsymbol{\omega}_{VI}.$$

Note that the following relations result from the above equations:

$$\begin{aligned}\mathrm{Tr}\mathbf{L} &= L_{ijij} = \lambda_I + \lambda_{II} + \dots + \lambda_{VI}, \\ \mathbf{L} \cdot \mathbf{L} &= L_{ijkl}L_{ijkl} = \lambda_I^2 + \lambda_{II}^2 + \dots + \lambda_{VI}^2,\end{aligned}$$

in view of which $1/6\mathrm{Tr}\mathbf{L}$ is the average stiffness modulus, while $\sqrt{\mathbf{L} \cdot \mathbf{L}}$ is the total stiffness (the norm of \mathbf{L}). Moreover, as for any other basis in \mathcal{S} , the identity tensor $\mathbb{I}^{\mathcal{S}}$ is

$$(1.9) \quad \mathbb{I}^{\mathcal{S}} = \boldsymbol{\omega}_I \otimes \boldsymbol{\omega}_I + \dots + \boldsymbol{\omega}_{VI} \otimes \boldsymbol{\omega}_{VI}.$$

As a consequence of the spectral theorem, the space of symmetric second-order tensors \mathcal{S} has been decomposed into the sum of six one-dimensional pairwise orthogonal subspaces \mathcal{P}_K of eigen-states

$$\mathcal{S} = \mathcal{P}_I \oplus \mathcal{P}_{II} \oplus \dots \oplus \mathcal{P}_{VI}.$$

Let us introduce the notion of *projector*. Projector is defined as a identity operator for the subspace \mathcal{P} of second-order tensors, that is, it is the IV-th order tensor \mathbf{P} which specifies the linear operation defined as follows:

$$\mathbf{P} \cdot \boldsymbol{\omega} = \begin{cases} \boldsymbol{\omega} & \text{if } \boldsymbol{\omega} \in \mathcal{P}, \\ \mathbf{0} & \text{if otherwise.} \end{cases}$$

Consider the identity operation for the subspace \mathcal{P}_K of eigen-states and find the corresponding projector \mathbf{P}_K , called now the eigen-projector. Using (1.9) we find (no summation over repeated indices!)

$$(1.10) \quad \begin{aligned}\mathbf{P}_K &= \mathbf{P}_K \circ \mathbb{I}^{\mathcal{S}} = \mathbf{P}_K \circ (\boldsymbol{\omega}_I \otimes \boldsymbol{\omega}_I + \dots + \boldsymbol{\omega}_{VI} \otimes \boldsymbol{\omega}_{VI}) \\ &= (\mathbf{P}_K \cdot \boldsymbol{\omega}_K) \otimes \boldsymbol{\omega}_K = \boldsymbol{\omega}_K \otimes \boldsymbol{\omega}_K.\end{aligned}$$

Accordingly for any II-nd order tensor $\boldsymbol{\omega} \in \mathcal{S}$ the following relation is true

$$\mathbf{P}_K \cdot \boldsymbol{\omega} = \alpha \boldsymbol{\omega}_K \in \mathcal{P}_K.$$

Projectors \mathbf{P}_K and \mathbf{P}_L corresponding to two eigen-subspaces are orthogonal, that is

$$\mathbf{P}_K \circ \mathbf{P}_L = \begin{cases} \mathbb{O} & \text{if } K \neq L, \\ \mathbf{P}_K & \text{if } K = L, \end{cases}$$

and

$$\mathbf{P}_I + \dots + \mathbf{P}_{VI} = \mathbb{I}^{\mathcal{S}}.$$

The above conditions of orthogonality of projectors result from the orthogonality of corresponding eigen-subspaces. Decompositions (1.7), (1.8) and orthogonal projectors \mathbf{P}_K (1.10) have the above diadic form if the corresponding Kelvin moduli are single, that is if $\lambda_K \neq \lambda_L$ for all $K \neq L$. Only in such a case the spectral decompositions (1.7), (1.8) are unique.

If the material enjoys some symmetry then the number of parameters describing this material decreases. The sequence of parameters (1.6) can be then presented as follows:

$$(1.11) \quad \langle \lambda_1, \dots, \lambda_\rho; \aleph_1, \dots, \aleph_t; \phi_1, \dots, \phi_n \rangle,$$

where $\rho \leq 6$, $t \leq 12$ and $n \leq 3$. Kelvin moduli can be then multiple and the spectral theorem takes the form

$$(1.12) \quad \mathbf{L} = \lambda_1 \mathbf{P}_1 + \dots + \lambda_\rho \mathbf{P}_\rho, \quad \rho \leq 6$$

and

$$\mathcal{S} = \mathcal{P}_1 \oplus \mathcal{P}_2 \oplus \dots \oplus \mathcal{P}_\rho, \quad \mathbb{I}^{\mathcal{S}} = \mathbf{P}_1 + \dots + \mathbf{P}_\rho.$$

The dimension of the subspace \mathcal{P}_k is equal to the multiplicity of the corresponding Kelvin modulus λ_k . The decomposition (1.12) is unique. In order to show how the orthogonal eigen-projector looks like in the case of multiple Kelvin moduli, let us assume that $\lambda_V = \lambda_{VI}$ in (1.7). In such a case, the subspace $\mathcal{P}_{V,VI}$ is two-dimensional and one can define in this subspace the basis $\{\boldsymbol{\omega}_V, \boldsymbol{\omega}_{VI}\}$. Using (1.9) we find

$$\begin{aligned} \mathbf{P}_{V,VI} &= \mathbf{P}_{V,VI} \circ \mathbb{I}^{\mathcal{S}} = \mathbf{P}_{V,VI} \circ (\boldsymbol{\omega}_I \otimes \boldsymbol{\omega}_I + \dots + \boldsymbol{\omega}_{VI} \otimes \boldsymbol{\omega}_{VI}) \\ &= (\mathbf{P}_{V,VI} \cdot \boldsymbol{\omega}_V) \otimes \boldsymbol{\omega}_V + (\mathbf{P}_{V,VI} \cdot \boldsymbol{\omega}_{VI}) \otimes \boldsymbol{\omega}_{VI} = \boldsymbol{\omega}_V \otimes \boldsymbol{\omega}_V + \boldsymbol{\omega}_{VI} \otimes \boldsymbol{\omega}_{VI}. \end{aligned}$$

It can be easily verified that the form of eigen-projector does not depend on the basis of eigen-states selected in the subspace $\mathcal{P}_{V,VI}$.

If one denotes the dimensions of eigen-subspaces $\mathcal{P}_1, \dots, \mathcal{P}_\rho$ by q_1, \dots, q_ρ , correspondingly then according to [22], the expression

$$(1.13) \quad \langle q_1 + q_2 + \dots + q_\rho \rangle, \quad q_1 + q_2 + \dots + q_\rho = 6$$

is called the **I-st structural index** of material, while the expression

$$(1.14) \quad [\rho + t + n]$$

is the **II-nd structural index**. These expressions are material characteristics.

It should be noted that the symmetry of the tensor \mathbf{L} , which is equivalent to the symmetry of a linear elastic continuum, results from the properties of the IV-th order symmetric Euclidean tensors or, to be more specific, from the linearity

of Hooke's law and the properties of 3-dimensional Euclidean space. Therefore, the classification of the linear elastic materials in view of their symmetry has, in general, nothing to do with the crystallography. Elastic anisotropy of crystals is classified in the same way as elastic anisotropy of other bodies without crystal structure. Consequently, some of the crystal structures have their counterparts within the elastic symmetry classes, while some of them have not [11]. An example of the latter case are crystals of hexagonal lattice symmetry. As far as they have a 6-fold axis of symmetry, in view of Hermann-German theorem [25], in order to account for all present symmetries, they must be described as elastically transversely isotropic.

2. KELVIN MODULI $\lambda_I, \dots, \lambda_{VI}$

The Kelvin moduli $\lambda_I, \dots, \lambda_{VI}$ are obtained as roots of characteristic polynomial, which has the form

$$(2.1) \quad \det(\mathbf{L} - \lambda \mathbb{I}^S) = \lambda^6 + a_1(\mathbf{L})\lambda^5 + \dots + a_5(\mathbf{L})\lambda + a_6(\mathbf{L}) = 0.$$

Determinant of a IV-th order tensor \mathbf{A} is defined as follows:

$$(2.2) \quad \det \mathbf{A} \equiv \det(A_{KL}) = \det(\mathbf{v}_K \cdot \mathbf{A} \cdot \mathbf{v}_L),$$

where \mathbf{v}_K , ($K = I, \dots, VI$) is any orthonormal basis in \mathcal{S} , while A_{KL} is the 6×6 matrix of representation of the tensor \mathbf{A} in this basis (see Appendix). The choice of a basis \mathbf{v}_K has no influence on the value of the coefficients $a_i(\mathbf{L})$ in the Eq. (2.1); therefore, they are the invariants of \mathbf{L} .

For the considered λ^* the corresponding eigen-state $\boldsymbol{\omega}^*$ is derived from the homogeneous system of 6 linear equations:

$$(2.3) \quad \mathbf{L} \cdot \boldsymbol{\omega}^* = \lambda^* \boldsymbol{\omega}^* \implies (\mathbf{L} - \lambda^* \mathbb{I}^S) \cdot \boldsymbol{\omega}^* = \mathbf{0}$$

with constraint $\boldsymbol{\omega}^* \cdot \boldsymbol{\omega}^* = \text{tr}(\boldsymbol{\omega}^* \boldsymbol{\omega}^*) = 1$. If the basis $\mathbf{v}_K = \boldsymbol{\omega}_K$, that is it coincides with the basis of eigen-states, then the matrix $L_{KL} = \boldsymbol{\omega}_K \cdot \mathbf{L} \cdot \boldsymbol{\omega}_L$ is diagonal.

3. ORTHOGONAL PROJECTORS $\mathbf{P}_1, \dots, \mathbf{P}_\rho$

Knowing Kelvin's moduli λ_K , number ρ of which is different, one can introduce some rule which orders them $\lambda_1, \dots, \lambda_\rho$. For example, one can number the moduli by increasing (decreasing) values. After unique numbering of moduli,

the corresponding orthogonal projectors \mathbf{P}_k can be derived using the following system of ρ tensorial equations of fourth-order [22]:

$$\begin{aligned}
 \mathbf{P}_1 + \mathbf{P}_2 + \dots + \mathbf{P}_\rho &= \mathbb{I}^S, \\
 \lambda_1 \mathbf{P}_1 + \lambda_2 \mathbf{P}_2 + \dots + \lambda_\rho \mathbf{P}_\rho &= \mathbf{L}, \\
 &\vdots \quad \ddots \quad \vdots \\
 \lambda_1^{\rho-1} \mathbf{P}_1 + \lambda_2^{\rho-1} \mathbf{P}_2 + \dots + \lambda_\rho^{\rho-1} \mathbf{P}_\rho &= \mathbf{L}^{\rho-1},
 \end{aligned}
 \tag{3.1}$$

where

$$\mathbf{L}^k = \underbrace{\mathbf{L} \circ \mathbf{L} \circ \dots \circ \mathbf{L}}_{k \text{ times}}.$$

Consequently, one obtains

$$\begin{bmatrix} \mathbf{P}_1 \\ \mathbf{P}_2 \\ \vdots \\ \mathbf{P}_\rho \end{bmatrix} = \begin{bmatrix} 1 & 1 & \dots & 1 \\ \lambda_1 & \lambda_2 & \dots & \lambda_\rho \\ \vdots & \vdots & \ddots & \vdots \\ \lambda_1^{\rho-1} & \lambda_2^{\rho-1} & \dots & \lambda_\rho^{\rho-1} \end{bmatrix}^{-1} \begin{bmatrix} \mathbb{I}^S \\ \mathbf{L} \\ \vdots \\ \mathbf{L}^{\rho-1} \end{bmatrix}.$$

Inversion of the above matrix exists because its determinant (the Vandermonde determinant) is equal to

$$\Delta = \prod_{\rho \geq k \neq l \geq 1} (\lambda_k - \lambda_l)$$

and by definition $\lambda_k \neq \lambda_l$. One finds

$$\mathbf{P}_k = \frac{(\mathbf{L} - \lambda_1 \mathbb{I}^S) \circ \dots \circ (\mathbf{L} - \lambda_{k-1} \mathbb{I}^S) \circ (\mathbf{L} - \lambda_{k+1} \mathbb{I}^S) \circ \dots \circ (\mathbf{L} - \lambda_\rho \mathbb{I}^S)}{(\lambda_k - \lambda_1) \dots (\lambda_k - \lambda_{k-1})(\lambda_k - \lambda_{k+1}) \dots (\lambda_k - \lambda_\rho)}.$$

Distributors $\aleph_1, \dots, \aleph_{12}$ are parameters which enable one to specify, in a unique way, the orthogonal projectors \mathbf{P}_k in the selected basis. The form of these functions, which would enable one to specify the projectors for all material symmetries, has not been proposed yet. Some proposal for orthotropic symmetry has been derived in [15]. To this end the harmonic decomposition discussed in [8, 26, 27] was utilized.

Using the relation (3.1)₁ it can be shown that the following identity is true:

$$\mathbf{1} \cdot \mathbf{P}_1 \cdot \mathbf{1} + \mathbf{1} \cdot \mathbf{P}_2 \cdot \mathbf{1} + \dots + \mathbf{1} \cdot \mathbf{P}_\rho \cdot \mathbf{1} = \mathbf{1} \cdot \mathbb{I}^S \cdot \mathbf{1} = 3.$$

The above identity provides the following relation between the traces of the eigen-states $\boldsymbol{\omega}_K$, if $\rho = 6$:

$$(\text{tr} \boldsymbol{\omega}_I)^2 + (\text{tr} \boldsymbol{\omega}_{II})^2 + \dots + (\text{tr} \boldsymbol{\omega}_{VI})^2 = 3.$$

4. SYMMETRIES OF AN ANISOTROPIC LINEAR ELASTIC MATERIAL

4.1. Notation and symmetry conditions

In what follows, the following notation is used:

- \mathcal{Q} – orthogonal group in 3-dimensional Euclidean space E^3 , the set of all orthogonal tensors,
- \mathcal{Q}^+ – the group of rotations in E^3 , the set of all orthogonal tensors for which $\det \mathbf{Q} = 1$, where $\mathcal{Q}^+ \subset \mathcal{Q}$,
- \mathbf{R}_a^ϕ – the orthogonal tensor describing the right-hand rotation around the axis of direction \mathbf{a} about the angle ϕ . For the rotation presented in Fig. 1 one obtains the following representation of \mathbf{R}_a^ϕ in the basis $\{\mathbf{e}_i\}$

$$\mathbf{R}_a^\phi \sim \begin{bmatrix} 1 & 0 & 0 \\ 0 & \cos \phi & -\sin \phi \\ 0 & \sin \phi & \cos \phi \end{bmatrix},$$

while the corresponding orthogonal tensor in 6-dimensional space has the following representation in poly-basis $\{\mathbf{a}_K\}$ (see Appendix):

$$\mathbf{R}_a^\phi \sim \begin{bmatrix} 1 & 0 & 0 & 0 & 0 & 0 \\ 0 & \cos \phi^2 & \sin \phi^2 & -\sqrt{2} \sin \phi \cos \phi & 0 & 0 \\ 0 & \sin \phi^2 & \cos \phi^2 & \sqrt{2} \sin \phi \cos \phi & 0 & 0 \\ 0 & \sqrt{2} \sin \phi \cos \phi & -\sqrt{2} \sin \phi \cos \phi & \cos 2\phi & 0 & 0 \\ 0 & 0 & 0 & 0 & \cos \phi & \sin \phi \\ 0 & 0 & 0 & 0 & -\sin \phi & \cos \phi \end{bmatrix}.$$

Hooke's tensors are of even order, therefore one can restrict analysis only to the rotation tensors because symmetry resulting from the mirror reflection will be equivalent to the symmetry resulting from the rotation around the appropriate axis through the angle π . Note that the representation of the orthogonal tensor in six-dimensional space loses the information about the determinant of the corresponding 3×3 orthogonal matrix.

- \mathbf{I}_a – the orthogonal tensor which describes the mirror reflection with respect to the plane with the unit normal $\mathbf{a} = \mathbf{e}_1$. For the mirror reflection presented in Fig. 1 one obtains the following representation of \mathbf{I}_a in $\{\mathbf{e}_i\}$:

$$\mathbf{I}_a \sim \begin{bmatrix} -1 & 0 & 0 \\ 0 & 1 & 0 \\ 0 & 0 & 1 \end{bmatrix},$$

and the corresponding representation in 6-dimensional space is the same as that for the rotation through the angle π around $\mathbf{a} = \mathbf{e}_1$:

$$\mathbb{I}_{\mathbf{a}} \sim \begin{bmatrix} 1 & 0 & 0 & 0 & 0 & 0 \\ 0 & 1 & 0 & 0 & 0 & 0 \\ 0 & 0 & 1 & 0 & 0 & 0 \\ 0 & 0 & 0 & 1 & 0 & 0 \\ 0 & 0 & 0 & 0 & -1 & 0 \\ 0 & 0 & 0 & 0 & 0 & -1 \end{bmatrix}.$$

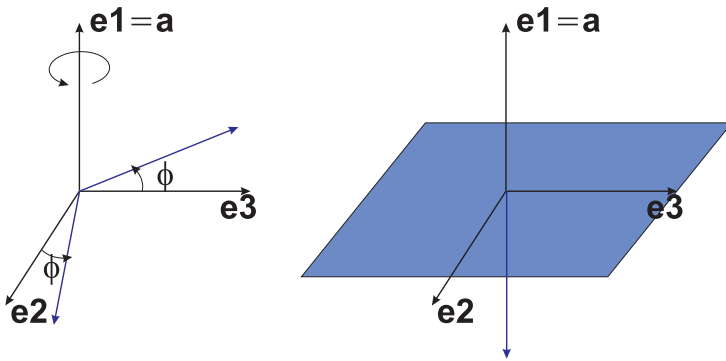


FIG. 1. Rotation and mirror reflection specified by the direction \mathbf{a} .

Below, we explain the relation between the spectral decomposition of stiffness (compliance) tensor and the well-known classification of linear elastic bodies according to their material symmetry. As it was already discussed, if the material enjoys some symmetry properties then the number of Kelvin moduli and stiffness distributors decreases. The symmetry group $\mathcal{Q}_{\mathbf{L}}$ of a stiffness tensor \mathbf{L} (a compliance tensor \mathbf{M}) is defined as follows:

$$(4.1) \quad \mathcal{Q}_{\mathbf{L}} = \mathcal{Q}_{\mathbf{M}} = \{\mathbf{Q} \in \mathcal{Q}; \mathbf{Q} \star \mathbf{L} = \mathbf{L}\},$$

where \mathbf{Q} is the orthogonal II-nd order tensor in 3-dimensional physical space. It should be recalled that one has for \mathbf{Q}

$$(4.2) \quad \mathbf{Q}\mathbf{Q}^T = \mathbf{Q}^T\mathbf{Q} = \mathbf{1}.$$

Symbol \star denotes the rotation operation for the IV-th order tensor defined in the following way. Let $\{\mathbf{e}_i\}$ be the selected orthonormal basis in E^3 , consequently

$$\mathbf{L} = L_{ijkl}\mathbf{e}_i \otimes \mathbf{e}_j \otimes \mathbf{e}_k \otimes \mathbf{e}_l$$

and then

$$\begin{aligned} \mathbf{Q} \star \mathbf{L} &= L_{ijkl}(\mathbf{Q}\mathbf{e}_i) \otimes (\mathbf{Q}\mathbf{e}_j) \otimes (\mathbf{Q}\mathbf{e}_k) \otimes (\mathbf{Q}\mathbf{e}_l) \\ &= L_{mnpq}Q_{im}Q_{jn}Q_{kp}Q_{lq}\mathbf{e}_i \otimes \mathbf{e}_j \otimes \mathbf{e}_k \otimes \mathbf{e}_l \end{aligned}$$

where

$$\mathbf{Q} = Q_{ij}\mathbf{e}_i \otimes \mathbf{e}_j.$$

The orthogonal tensor \mathbf{Q} belongs to the symmetry group of \mathbf{L} if the following condition is true:

$$(4.3) \quad \mathbf{Q} \star \mathbf{L} = \mathbf{L} \Leftrightarrow L_{mnpq}Q_{im}Q_{jn}Q_{kp}Q_{lq} = L_{ijkl}.$$

Therefore, we have in general 21 scalar equations which impose some constraints on the components of \mathbf{L} for the considered \mathbf{Q} . The classification of the linearly elastic materials according to their symmetry includes the classical eight classes of elastic symmetry [4, 6]. The full anisotropy ($\mathcal{Q}_{\mathbf{L}} = \{\mathbf{1}, -\mathbf{1}\}$) and the full isotropy ($\mathcal{Q}_{\mathbf{L}} = \mathcal{Q}$) are two extreme cases. Symmetry groups for some classes of symmetry are contained within the symmetry group of other class. Corresponding inclusion relations are schematically shown in Fig. 2.

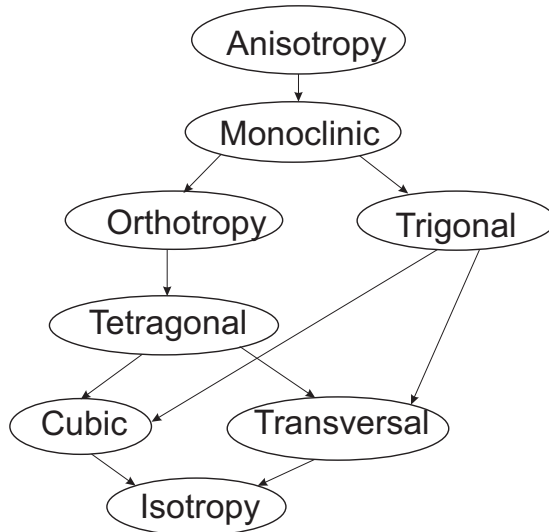


FIG. 2. Scheme of relation between eight classes of elastic symmetry. Each arrow corresponds to the additional symmetry conditions imposed on Hooke's tensor.

Usually, the reduced form of the stiffness (compliance) tensor for the subsequent symmetry groups is derived using the relations (4.3). Then the spectral decomposition of this reduced form is performed to specify the structural indices

valid for the considered symmetry group. Below, we derive the form of a stiffness tensor and the structural indices for the subsequent symmetry groups in a non-standard way. Consider the external symmetry of the eigen-projector of \mathbf{L} . Any orthogonal tensor belonging to the symmetry group of \mathbf{P}_k fulfills the condition

$$(4.4) \quad \bigwedge_{\mathbf{Q} \in \mathcal{Q}_{\mathbf{P}_k}} \mathbf{Q} \star \mathbf{P}_k = \mathbf{P}_k.$$

It can be shown that the symmetry group of the tensor \mathbf{L} , $\mathcal{Q}_{\mathbf{L}}$ is the common set of symmetry groups $\mathcal{Q}_{\mathbf{P}_k}$ of all its projectors, namely

$$(4.5) \quad \mathcal{Q}_{\mathbf{L}} = \mathcal{Q}_{\mathbf{P}_1} \cap \mathcal{Q}_{\mathbf{P}_2} \cap \dots \cap \mathcal{Q}_{\mathbf{P}_\rho}.$$

In the components in the selected basis $\{\mathbf{e}_i\}$, relation (4.4) has the form

$$P_{mnpq}^{(k)} Q_{im} Q_{jn} Q_{kp} Q_{lq} = P_{ijkl}^{(k)}.$$

If the subspace \mathcal{P}_K is one-dimensional then the symmetry condition (4.4), together with (4.5), is equivalent to

$$\bigwedge_{\mathbf{Q} \in \mathcal{Q}_{\mathbf{L}}} \mathbf{Q} \star (\boldsymbol{\omega}_K \otimes \boldsymbol{\omega}_K) = (\mathbf{Q}\boldsymbol{\omega}_K\mathbf{Q}^T) \otimes (\mathbf{Q}\boldsymbol{\omega}_K\mathbf{Q}^T) = \boldsymbol{\omega}_K \otimes \boldsymbol{\omega}_K.$$

Consequently

$$(4.6) \quad \bigwedge_{\mathbf{Q} \in \mathcal{Q}_{\mathbf{L}}} \mathbf{Q}\boldsymbol{\omega}_K\mathbf{Q}^T = \pm\boldsymbol{\omega}_K.$$

In components of $\boldsymbol{\omega}_K$ in the basis $\{\mathbf{e}_i\}$, the above equation is specified as

$$\omega_{mn}^K Q_{im} Q_{jn} = \pm\omega_{ij}^K.$$

If the representation of a IV-th order tensor as a II-nd order tensor in 6-dimensional space is used (see Appendix), then the orthogonal tensor in the 3-dimensional space can be replaced by a corresponding orthogonal tensor \mathbb{Q} in the 6-dimensional space, such that

$$\mathbf{Q} \star \mathbf{L} \Leftrightarrow \mathbb{Q} \hat{\star}^6 \mathbf{L} = L_{KL}(\mathbb{Q}\mathbf{a}_K) \otimes (\mathbb{Q}\mathbf{a}_L)$$

and in components, for $\mathbb{Q} = Q_{KL}\mathbf{a}_K \otimes \mathbf{a}_L$, one has

$$(4.7) \quad L_{KL} = L_{MN}Q_{KM}Q_{LN}.$$

In this paper, using the above conditions imposed on \mathbf{P}_k or $\boldsymbol{\omega}_K$, the specific form of eigen-states and eigen-projectors, two structural indices, as well as the stiffness tensor \mathbf{L} will be derived for all 8 symmetry groups of linear elastic material.

4.2. Fully anisotropic material

The symmetry group of Hooke's tensor is never empty. For **full anisotropy**, that is for totally anisotropic material, a symmetry group is defined as

$$\mathcal{Q}_{\mathbf{L}}^a = \{\mathbf{1}, -\mathbf{1}\}.$$

The symmetry conditions are fulfilled by any normalized set of six mutually orthogonal symmetric II-nd order tensors

$$(4.8) \quad \boldsymbol{\omega}_K \sim \begin{bmatrix} \omega_{11}^K & \omega_{12}^K & \omega_{13}^K \\ \omega_{12}^K & \omega_{22}^K & \omega_{23}^K \\ \omega_{13}^K & \omega_{23}^K & \omega_{33}^K \end{bmatrix}, \quad K = I, \dots, VI.$$

The specific form of them, that is the value of 12 stiffness distributors, depends on the specific properties of the considered anisotropic material which have to be established in experiments. If one of the eigenstates is purely hydrostatic, namely

$$\boldsymbol{\omega} = \pm \frac{1}{\sqrt{3}} \mathbf{1},$$

then material is called volumetrically isotropic [15]. Note that although the number of independent components is then reduced to 16, in general the material may remain fully anisotropic.

Any material, which is not totally anisotropic is called *a symmetric elastic material* [23]. Such material has at least one symmetry plane.

4.3. Material of monoclinic symmetry

For **monoclinic symmetry**, symmetry of a prism with irregular basis, there exists a single symmetry plane (see Fig. 3) and a symmetry group is the following:

$$(4.9) \quad \mathcal{Q}_{\mathbf{L}}^m = \{\mathbf{1}, -\mathbf{1}, \mathbf{I}_{\mathbf{e}_1}\},$$

where $\mathbf{I}_{\mathbf{e}_1}$ denotes the tensor describing the mirror reflection with respect to the plane with unit normal \mathbf{e}_1 . In the basis, in which \mathbf{e}_1 is specified, two angles ϕ_1 and ϕ_2 are specified. Using the symmetry conditions (4.6) one obtains two following matrix equations

$$\begin{bmatrix} -1 & 0 & 0 \\ 0 & 1 & 0 \\ 0 & 0 & 1 \end{bmatrix} \begin{bmatrix} \omega_{11}^K & \omega_{12}^K & \omega_{13}^K \\ \omega_{12}^K & \omega_{22}^K & \omega_{23}^K \\ \omega_{13}^K & \omega_{23}^K & \omega_{33}^K \end{bmatrix} \begin{bmatrix} -1 & 0 & 0 \\ 0 & 1 & 0 \\ 0 & 0 & 1 \end{bmatrix} = \pm \begin{bmatrix} \omega_{11}^K & \omega_{12}^K & \omega_{13}^K \\ \omega_{12}^K & \omega_{22}^K & \omega_{23}^K \\ \omega_{13}^K & \omega_{23}^K & \omega_{33}^K \end{bmatrix}$$

which after performing the multiplications take the form

$$\begin{bmatrix} \omega_{11}^K & -\omega_{12}^K & -\omega_{13}^K \\ -\omega_{12}^K & \omega_{22}^K & \omega_{23}^K \\ -\omega_{13}^K & \omega_{23}^K & \omega_{33}^K \end{bmatrix} = \begin{bmatrix} -\omega_{11}^K & -\omega_{12}^K & -\omega_{13}^K \\ -\omega_{12}^K & -\omega_{22}^K & -\omega_{23}^K \\ -\omega_{13}^K & -\omega_{23}^K & -\omega_{33}^K \end{bmatrix}$$

and

$$\begin{bmatrix} \omega_{11}^K & -\omega_{12}^K & -\omega_{13}^K \\ -\omega_{12}^K & \omega_{22}^K & \omega_{23}^K \\ -\omega_{13}^K & \omega_{23}^K & \omega_{33}^K \end{bmatrix} = \begin{bmatrix} \omega_{11}^K & \omega_{12}^K & \omega_{13}^K \\ \omega_{12}^K & \omega_{22}^K & \omega_{23}^K \\ \omega_{13}^K & \omega_{23}^K & \omega_{33}^K \end{bmatrix}.$$

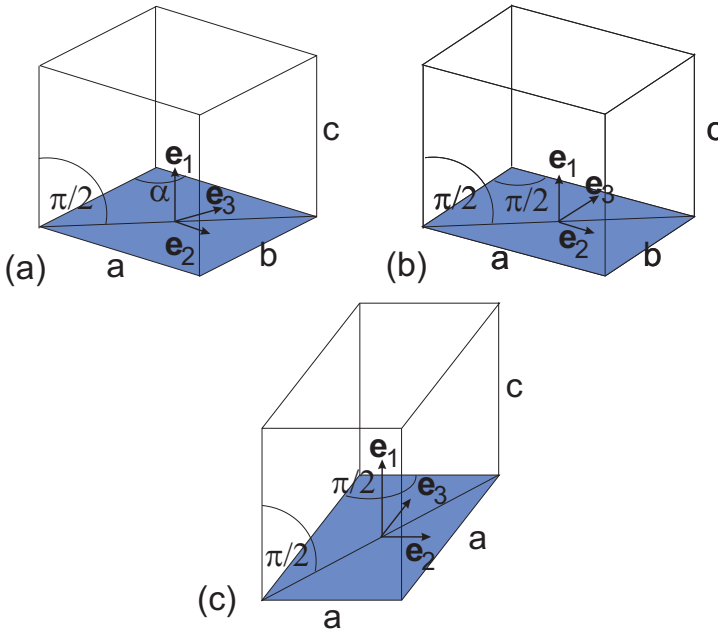


FIG. 3. Schematic representation of monoclinic symmetry (a), orthotropy (b) and tetragonal symmetry (c).

Eigen-states fulfilling the above relations are as follows ($K = III, \dots, VI$):

$$(4.10) \quad \boldsymbol{\omega}_{I,II} \sim \begin{bmatrix} 0 & \omega_{12}^{I,II} & \omega_{13}^{I,II} \\ \omega_{12}^{I,II} & 0 & 0 \\ \omega_{13}^{I,II} & 0 & 0 \end{bmatrix}, \quad \boldsymbol{\omega}_K \sim \begin{bmatrix} \omega_{11}^K & 0 & 0 \\ 0 & \omega_{22}^K & \omega_{23}^K \\ 0 & \omega_{23}^K & \omega_{33}^K \end{bmatrix}.$$

Using orthonormality conditions of eigen-states $\boldsymbol{\omega}_I$ and $\boldsymbol{\omega}_{II}$, the following form of them is obtained

$$(4.11) \quad \boldsymbol{\omega}_I \sim \frac{1}{\sqrt{2}} \begin{bmatrix} 0 & \sin \phi & \cos \phi \\ \sin \phi & 0 & 0 \\ \cos \phi & 0 & 0 \end{bmatrix},$$

$$\boldsymbol{\omega}_{II} \sim \frac{1}{\sqrt{2}} \begin{bmatrix} 0 & \cos \phi & -\sin \phi \\ \cos \phi & 0 & 0 \\ -\sin \phi & 0 & 0 \end{bmatrix}.$$

It can be noted that after changing the basis by proper rotation around \mathbf{e}_1 about $\phi_3 = \phi$ (that way we specify the third Euler angle), one arrives at

$$(4.12) \quad \boldsymbol{\omega}_I \sim \frac{1}{\sqrt{2}} \begin{bmatrix} 0 & 1 & 0 \\ 1 & 0 & 0 \\ 0 & 0 & 0 \end{bmatrix}, \quad \boldsymbol{\omega}_{II} \sim \frac{1}{\sqrt{2}} \begin{bmatrix} 0 & 0 & 1 \\ 0 & 0 & 0 \\ 1 & 0 & 0 \end{bmatrix}.$$

The eigen-states $\boldsymbol{\omega}_I$ and $\boldsymbol{\omega}_{II}$, in the form of pure shears, are identical for any material of monoclinic symmetry, provided a proper frame in the physical space is used. This frame is defined by the unit normal \mathbf{e}_1 to the symmetry plane, being the common direction of shearing for the above pure shears in the sense discussed in [3], and two directions: \mathbf{e}_2 , \mathbf{e}_3 which specify the unit normal to the corresponding shearing planes as they were defined in [3]. The derived form of eigen-states complies with the theorem formulated in [3] according to which for any symmetric material, at least two eigen-states of the stiffness tensor are pure shears. The specific form of remaining eigenstates $\boldsymbol{\omega}_K$, ($K = III, \dots, VI$), defined by 6 stiffness distributors, depends on the properties of the considered material of monoclinic symmetry. Using (1.7) the representation of \mathbf{L} in the poly-basis $\{\mathbf{a}_K\}$ composed of diads of the above selected unit vectors \mathbf{e}_i is derived as

$$(4.13) \quad \mathbf{L} \sim \begin{bmatrix} L_{11} & L_{12} & L_{13} & L_{14} & 0 & 0 \\ L_{12} & L_{22} & L_{23} & L_{24} & 0 & 0 \\ L_{13} & L_{23} & L_{33} & L_{34} & 0 & 0 \\ L_{14} & L_{24} & L_{34} & L_{44} & 0 & 0 \\ 0 & 0 & 0 & 0 & L_{55} = \lambda_{II} & 0 \\ 0 & 0 & 0 & 0 & 0 & L_{66} = \lambda_I \end{bmatrix}$$

therefore it is specified by 12 independent components. The Kelvin moduli $\lambda_{III}, \dots, \lambda_{VI}$ are obtained as eigenvalues of 4×4 upper left sub-matrix of (4.13). An example of material of elastic monoclinic symmetry is the martensite phase, the lower symmetry phase in CuZnAl shape memory alloy.

4.4. Orthotropic material

In the case of **orthotropic** material, that is the material possessing symmetry of a prism with rectangular basis (see Fig. 3), the symmetry group includes the elements

$$(4.14) \quad \mathcal{Q}_{\mathbf{L}}^o = \{\mathbf{1}, -\mathbf{1}, \mathbf{I}_{\mathbf{e}_1}, \mathbf{I}_{\mathbf{e}_2}\}.$$

The symmetry conditions (4.6) can be imposed on the derived form of eigenstates for the material of monoclinic symmetry as far as the symmetry group of the latter material is included in the symmetry group of orthotropic material ($\mathcal{Q}_{\mathbf{L}}^m \subset \mathcal{Q}_{\mathbf{L}}^o$, Fig. 2). Thus, any orthotropic material is the material of monoclinic symmetry. Let us consider two groups of eigenstates obtained for material of monoclinic symmetry. Imposing additional condition (related to the orthogonal tensor $\mathbf{I}_{\mathbf{e}_2}$) on the first group in (4.10), we find

$$\begin{bmatrix} 1 & 0 & 0 \\ 0 & -1 & 0 \\ 0 & 0 & 1 \end{bmatrix} \begin{bmatrix} 0 & \omega_{12}^{I,II} & \omega_{13}^{I,II} \\ \omega_{12}^{I,II} & 0 & 0 \\ \omega_{13}^{I,II} & 0 & 0 \end{bmatrix} \begin{bmatrix} 1 & 0 & 0 \\ 0 & -1 & 0 \\ 0 & 0 & 1 \end{bmatrix} = \pm \begin{bmatrix} 0 & \omega_{12}^{I,II} & \omega_{13}^{I,II} \\ \omega_{12}^{I,II} & 0 & 0 \\ \omega_{13}^{I,II} & 0 & 0 \end{bmatrix}$$

which after multiplications simplifies to the relations

$$\begin{bmatrix} 0 & -\omega_{12}^{I,II} & \omega_{13}^{I,II} \\ -\omega_{12}^{I,II} & 0 & 0 \\ \omega_{13}^{I,II} & 0 & 0 \end{bmatrix} = \begin{bmatrix} 0 & \pm\omega_{12}^{I,II} & \pm\omega_{13}^{I,II} \\ \pm\omega_{12}^{I,II} & 0 & 0 \\ \pm\omega_{13}^{I,II} & 0 & 0 \end{bmatrix}.$$

They are identically true for the eigenstates (4.12), where the direction \mathbf{e}_2 agrees with the unit normal to the shearing plane for one of these eigenstates.

Imposing additional condition on the second group of eigenstates in (4.10), it is obtained

$$\begin{bmatrix} 1 & 0 & 0 \\ 0 & -1 & 0 \\ 0 & 0 & 1 \end{bmatrix} \begin{bmatrix} \omega_{11}^K & 0 & 0 \\ 0 & \omega_{22}^K & \omega_{23}^K \\ 0 & \omega_{23}^K & \omega_{33}^K \end{bmatrix} \begin{bmatrix} 1 & 0 & 0 \\ 0 & -1 & 0 \\ 0 & 0 & 1 \end{bmatrix} = \pm \begin{bmatrix} \omega_{11}^K & 0 & 0 \\ 0 & \omega_{22}^K & \omega_{23}^K \\ 0 & \omega_{23}^K & \omega_{33}^K \end{bmatrix}$$

and after multiplications, the following constraints are found

$$\begin{bmatrix} \omega_{11}^K & 0 & 0 \\ 0 & \omega_{22}^K & -\omega_{23}^K \\ 0 & -\omega_{23}^K & \omega_{33}^K \end{bmatrix} = \begin{bmatrix} \pm\omega_{11}^K & 0 & 0 \\ 0 & \pm\omega_{22}^K & \pm\omega_{23}^K \\ 0 & \pm\omega_{23}^K & \pm\omega_{33}^K \end{bmatrix}$$

which are true for the following forms of $\boldsymbol{\omega}$ ($K = IV, V, VI$)

$$(4.15) \quad \boldsymbol{\omega}_{III} \sim \begin{bmatrix} 0 & 0 & 0 \\ 0 & 0 & \omega_{23}^{III} \\ 0 & \omega_{23}^{III} & 0 \end{bmatrix}, \quad \boldsymbol{\omega}_K \sim \begin{bmatrix} \omega_{11}^K & 0 & 0 \\ 0 & \omega_{22}^K & 0 \\ 0 & 0 & \omega_{33}^K \end{bmatrix}.$$

After normalization we obtain the following eigen-states in the form of pure shears [2] in the basis $\{\mathbf{e}_i\}$ specified by three directions of orthotropy (this way three Euler angles are specified):

$$(4.16) \quad \begin{aligned} \boldsymbol{\omega}_I &\sim \frac{1}{\sqrt{2}} \begin{bmatrix} 0 & 1 & 0 \\ 1 & 0 & 0 \\ 0 & 0 & 0 \end{bmatrix}, \\ \boldsymbol{\omega}_{II} &\sim \frac{1}{\sqrt{2}} \begin{bmatrix} 0 & 0 & 1 \\ 0 & 0 & 0 \\ 1 & 0 & 0 \end{bmatrix}, \\ \boldsymbol{\omega}_{III} &\sim \frac{1}{\sqrt{2}} \begin{bmatrix} 0 & 0 & 0 \\ 0 & 0 & 1 \\ 0 & 1 & 0 \end{bmatrix}, \end{aligned}$$

and three subsequent eigen-states in the diagonal form in this basis, which after utilizing orthonormality conditions we can present in the form [2]

$$\begin{aligned} \boldsymbol{\omega}_{IV} &\sim \begin{bmatrix} \cos \theta_1 & 0 & 0 \\ 0 & \sin \theta_1 \cos \theta_2 & 0 \\ 0 & 0 & \sin \theta_1 \sin \theta_2 \end{bmatrix}, \\ \boldsymbol{\omega}_V &\sim \begin{bmatrix} -\cos \theta_3 \sin \theta_1 & 0 & 0 \\ 0 & \cos \theta_1 \cos \theta_2 \cos \theta_3 + \\ & -\sin \theta_2 \sin \theta_3 & 0 \\ 0 & 0 & \cos \theta_1 \sin \theta_2 \cos \theta_3 + \\ & & + \sin \theta_3 \cos \theta_2 \end{bmatrix}, \\ \boldsymbol{\omega}_{VI} &\sim \begin{bmatrix} \sin \theta_1 \sin \theta_3 & 0 & 0 \\ 0 & -\sin \theta_3 \cos \theta_1 \cos \theta_2 + \\ & -\cos \theta_3 \sin \theta_2 & 0 \\ 0 & 0 & -\sin \theta_3 \cos \theta_1 \sin \theta_2 + \\ & & + \cos \theta_3 \cos \theta_2 \end{bmatrix}. \end{aligned}$$

For any orthotropic material there exist three uniquely defined (within a sign) eigen-states in the form of pure shears, while the form of eigen-states $\boldsymbol{\omega}_{IV,V,VI}$ is specified by three angles $\theta_1, \theta_2, \theta_3$ which themselves are the functions of three stiffness distributors. They depend on the properties of the considered material of orthotropic symmetry. In the paper [15] it was proposed to define these distributors in the following way¹⁾

$$(4.17) \quad \eta_1 = \text{tr} \mathbf{h}_{VI}^2, \quad \eta_2 = \frac{\det \mathbf{h}_{VI}}{(\text{tr} \boldsymbol{\omega}_{VI})^3}, \quad \eta_3 = \frac{\text{tr}(\boldsymbol{\omega}_{VI}^2 \boldsymbol{\omega}_V)}{\text{tr} \boldsymbol{\omega}_V},$$

where \mathbf{h}_K are deviators of $\boldsymbol{\omega}_K$. The above definition must be modified in the case when $\eta_1 = 0$ or two eigenvalues of $\boldsymbol{\omega}_{VI}$ are equal to each other correspondingly in the form

$$(4.18) \quad \eta_3^* = (\det \mathbf{h}_V)^2, \quad \eta_3^{**} = \frac{\det \mathbf{h}_V}{(\text{tr} \boldsymbol{\omega}_V)^3}.$$

The representation of \mathbf{L} in poly-basis $\{\mathbf{a}_K\}$ constructed with use of orthotropy directions $\{\mathbf{e}_k\}$ is

$$(4.19) \quad \mathbf{L} \sim \begin{bmatrix} L_{11} & L_{12} & L_{13} & 0 & 0 & 0 \\ L_{12} & L_{22} & L_{23} & 0 & 0 & 0 \\ L_{13} & L_{23} & L_{33} & 0 & 0 & 0 \\ 0 & 0 & 0 & L_{44} = \lambda_{III} & 0 & 0 \\ 0 & 0 & 0 & 0 & L_{55} = \lambda_{II} & 0 \\ 0 & 0 & 0 & 0 & 0 & L_{66} = \lambda_I \end{bmatrix}$$

therefore it is specified by 9 independent components. The Kelvin moduli $\lambda_{IV}, \dots, \lambda_{VI}$ are obtained as eigenvalues of 3×3 upper left sub-matrix of (4.19). The orthotropic symmetry is characteristic for metal sheets with texture resulting from rolling process.

For the above two classes of symmetry one obtains one-dimensional eigen-subspaces \mathcal{P}_K .

4.5. Material of trigonal symmetry

Material of **trigonal symmetry** (symmetry of a cube uniformly elongated along one of its main diagonals, see Fig. 5, where the diagonal is coaxial with the main symmetry axis \mathbf{e}_1) has the following symmetry group:

¹⁾In [15] it was assumed that Kelvin moduli λ_K are ordered in view of increasing value of the corresponding $(\text{tr} \boldsymbol{\omega}_K)^2$.

$$(4.20) \quad \mathcal{Q}_{\mathbf{L}}^{3t} = \left\{ \mathbf{1}, -\mathbf{1}, \mathbf{R}_{\mathbf{e}_1}^{2\pi/3}, \mathbf{I}_{\mathbf{e}_2} \right\},$$

where $\mathbf{R}_{\mathbf{e}_1}^{2\pi/3}$ denotes the rotation around the axis \mathbf{e}_1 through the angle $2\pi/3$.

It should be noted that the monoclinic symmetry group $\mathcal{Q}_{\mathbf{L}}^m \subset \mathcal{Q}_{\mathbf{L}}^{3t}$ if the direction \mathbf{e}_1 is replaced by \mathbf{e}_2 . For the symmetric direction specified in this way with respect to the basis $\{\mathbf{e}_i\}$, two groups of eigen-states in (4.10) have the representations ($K = III, \dots, VI$)

$$(4.21) \quad \boldsymbol{\omega}_{I,II} \sim \begin{bmatrix} 0 & \omega_{12}^{I,II} & 0 \\ \omega_{12}^{I,II} & 0 & \omega_{23}^{I,II} \\ 0 & \omega_{23}^{I,II} & 0 \end{bmatrix}, \quad \boldsymbol{\omega}_K \sim \begin{bmatrix} \omega_{11}^K & 0 & \omega_{13}^K \\ 0 & \omega_{22}^K & 0 \\ \omega_{13}^K & 0 & \omega_{33}^K \end{bmatrix}.$$

Fulfilling the additional symmetry condition (4.6) related to the orthogonal tensor $\mathbf{R}_{\mathbf{e}_1}^{2\pi/3}$ for the second group of eigen-states (4.21), we derive the constraints

$$\begin{bmatrix} 1 & 0 & 0 \\ 0 & -\frac{1}{2} & -\frac{\sqrt{3}}{2} \\ 0 & \frac{\sqrt{3}}{2} & -\frac{1}{2} \end{bmatrix} \begin{bmatrix} \omega_{11}^K & 0 & \omega_{13}^K \\ 0 & \omega_{22}^K & 0 \\ \omega_{13}^K & 0 & \omega_{33}^K \end{bmatrix} \begin{bmatrix} 1 & 0 & 0 \\ 0 & -\frac{1}{2} & \frac{\sqrt{3}}{2} \\ 0 & -\frac{\sqrt{3}}{2} & -\frac{1}{2} \end{bmatrix} = \pm \begin{bmatrix} \omega_{11}^K & 0 & \omega_{13}^K \\ 0 & \omega_{22}^K & 0 \\ \omega_{13}^K & 0 & \omega_{33}^K \end{bmatrix},$$

which after multiplications take the form

$$\begin{bmatrix} \omega_{11}^K & -\frac{\sqrt{3}}{2}\omega_{13}^K & -\frac{1}{2}\omega_{13}^K \\ -\frac{\sqrt{3}}{2}\omega_{13}^K & \frac{1}{4}(\omega_{22}^K + 3\omega_{33}^K) & \frac{\sqrt{3}}{4}(\omega_{33}^K - \omega_{22}^K) \\ -\frac{1}{2}\omega_{13}^K & \frac{\sqrt{3}}{4}(\omega_{33}^K - \omega_{22}^K) & \frac{1}{4}(3\omega_{22}^K + \omega_{33}^K) \end{bmatrix} = \pm \begin{bmatrix} \omega_{11}^K & 0 & \omega_{13}^K \\ 0 & \omega_{22}^K & 0 \\ \omega_{13}^K & 0 & \omega_{33}^K \end{bmatrix}.$$

The above relations can be fulfilled only by two linearly independent unit eigen-states with the below representation in the basis $\{\mathbf{e}_i\}$ ²⁾

$$(4.22) \quad \boldsymbol{\omega}_{V,VI} \sim \begin{bmatrix} \omega_{11}^{V,VI} & 0 & 0 \\ 0 & \omega_{22}^{V,VI} & 0 \\ 0 & 0 & \omega_{22}^{V,VI} \end{bmatrix}.$$

²⁾As it can be noticed in Fig. 5, the direction \mathbf{e}_2 can be specified with the accuracy to the rotation about $2\pi/3$ around \mathbf{e}_1 .

They define two one-dimensional eigen-subspaces. After normalization and application of orthogonality conditions, they take the form

$$(4.23) \quad \begin{aligned} \boldsymbol{\omega}_V &\sim \frac{1}{\sqrt{2}} \begin{bmatrix} \sqrt{2} \sin \phi & 0 & 0 \\ 0 & -\cos \phi & 0 \\ 0 & 0 & -\cos \phi \end{bmatrix}, \\ \boldsymbol{\omega}_{VI} &\sim \frac{1}{\sqrt{2}} \begin{bmatrix} \sqrt{2} \cos \phi & 0 & 0 \\ 0 & \sin \phi & 0 \\ 0 & 0 & \sin \phi \end{bmatrix}. \end{aligned}$$

In general, the above eigen-states are not pure shears.

Imposing the symmetry condition (4.6) on the first group of eigenstates (4.21) we find only trivial solution $\boldsymbol{\omega} = \mathbf{0}$, which of course is unacceptable. Consequently, the remaining eigen-subspaces must be more than one-dimensional and their form will be found using the symmetry condition (4.4). Any IV-th order tensor orthogonal to the eigen-projectors composed of eigen-states (4.23) has the representation

$$\mathbf{P} \sim \begin{bmatrix} 0 & 0 & 0 & 0 & 0 & 0 \\ 0 & -P_{23} & P_{23} & P_{24} & P_{25} & P_{26} \\ 0 & P_{23} & -P_{23} & -P_{24} & -P_{25} & -P_{26} \\ 0 & P_{24} & -P_{24} & P_{44} & P_{45} & P_{46} \\ 0 & P_{25} & -P_{25} & P_{45} & P_{55} & P_{56} \\ 0 & P_{26} & -P_{26} & P_{46} & P_{56} & P_{66} \end{bmatrix}.$$

The representation of a orthogonal tensor $\mathbf{R}_{\mathbf{e}_1}^{2\pi/3}$ in the six-dimensional space is the following one

$$\mathbf{R}_{\mathbf{e}_1}^{2\pi/3} \sim \begin{bmatrix} 1 & 0 & 0 & 0 & 0 & 0 \\ 0 & \frac{1}{4} & \frac{3}{4} & \frac{\sqrt{6}}{4} & 0 & 0 \\ 0 & \frac{3}{4} & \frac{1}{4} & -\frac{\sqrt{6}}{4} & 0 & 0 \\ 0 & -\frac{\sqrt{6}}{4} & \frac{\sqrt{6}}{4} & -\frac{1}{2} & 0 & 0 \\ 0 & 0 & 0 & 0 & -\frac{1}{2} & \frac{\sqrt{3}}{2} \\ 0 & 0 & 0 & 0 & -\frac{\sqrt{3}}{2} & -\frac{1}{2} \end{bmatrix}.$$

If we perform the rotation operation for the tensor \mathbf{P} using the relation (4.7), then we find the following non-zero components of the rotated tensor $\mathbb{R}_{\mathbf{e}_1}^{2\pi/3\hat{\star}6}\mathbf{P}$:

$$(4.24) \quad \tilde{P}_{22} = \frac{1}{8}(-2P_{23} - 2\sqrt{6}P_{24} + 3P_{44}),$$

$$(4.25) \quad \tilde{P}_{23} = \frac{1}{8}(2P_{23} + 2\sqrt{6}P_{24} - 3P_{44}),$$

$$(4.26) \quad \tilde{P}_{24} = \frac{1}{8}(-2\sqrt{6}P_{23} - 4P_{24} - \sqrt{6}P_{44}),$$

$$(4.27) \quad \tilde{P}_{25} = \frac{1}{8}(2P_{25} - 2\sqrt{3}P_{26} - \sqrt{6}P_{45} + 3\sqrt{2}P_{46}),$$

$$(4.28) \quad \tilde{P}_{26} = \frac{1}{8}(2\sqrt{3}P_{25} + 2P_{26} - 3\sqrt{2}P_{45} - \sqrt{6}P_{46}),$$

$$(4.29) \quad \tilde{P}_{33} = \frac{1}{8}(-2P_{23} - 2\sqrt{6}P_{24} + 3P_{44}),$$

$$(4.30) \quad \tilde{P}_{34} = \frac{1}{8}(2\sqrt{6}P_{23} + 4P_{24} + \sqrt{6}P_{44}),$$

$$(4.31) \quad \tilde{P}_{35} = \frac{1}{8}(-2P_{25} + 2\sqrt{3}P_{26} + \sqrt{6}P_{45} - 3\sqrt{2}P_{46}),$$

$$(4.32) \quad \tilde{P}_{36} = \frac{1}{8}(-2\sqrt{3}P_{25} - 2P_{26} + 3\sqrt{2}P_{45} + \sqrt{6}P_{46}),$$

$$(4.33) \quad \tilde{P}_{44} = \frac{1}{4}(-6P_{23} + 2\sqrt{6}P_{24} + P_{44}),$$

$$(4.34) \quad \tilde{P}_{45} = \frac{1}{4}(\sqrt{6}P_{25} - 3\sqrt{2}P_{26} + P_{45} - \sqrt{3}P_{46}),$$

$$(4.35) \quad \tilde{P}_{46} = \frac{1}{4}(3\sqrt{2}P_{25} + \sqrt{6}P_{26} + \sqrt{3}P_{45} + P_{46}),$$

$$(4.36) \quad \tilde{P}_{55} = \frac{1}{4}(P_{55} - 2\sqrt{3}P_{56} + 3P_{66}),$$

$$(4.37) \quad \tilde{P}_{56} = \frac{1}{4}(\sqrt{3}P_{55} - 2P_{56} - \sqrt{3}P_{66}),$$

$$(4.38) \quad \tilde{P}_{66} = \frac{1}{4}(3P_{55} + 2\sqrt{3}P_{56} + P_{66}).$$

After algebraic manipulations, setting $\hat{P}_{KL} = P_{KL}$, the representations of two projectors in the poly-basis $\{\mathbf{a}_I\}$ are found, namely

$$\mathbf{P}_K \sim \begin{bmatrix} 0 & 0 & 0 & 0 & 0 & 0 \\ 0 & (\omega_{23}^K)^2 & -(\omega_{23}^K)^2 & 0 & \sqrt{2}\omega_{12}^K\omega_{23}^K & 0 \\ 0 & -(\omega_{23}^K)^2 & (\omega_{23}^K)^2 & 0 & -\sqrt{2}\omega_{12}^K\omega_{23}^K & 0 \\ 0 & 0 & 0 & 2(\omega_{23}^K)^2 & 0 & 2\omega_{12}^K\omega_{23}^K \\ 0 & \sqrt{2}\omega_{12}^K\omega_{23}^K & -\sqrt{2}\omega_{12}^K\omega_{23}^K & 0 & 2(\omega_{12}^K)^2 & 0 \\ 0 & 0 & 0 & 2\omega_{12}^K\omega_{23}^K & 0 & 2(\omega_{12}^K)^2 \end{bmatrix}.$$

They project into two two-dimensional subspaces $\mathcal{P}_{I,II}$ and $\mathcal{P}_{III,IV}$ of deviatoric tensors. Using the orthogonality and after normalization of the elements, we arrive at the following representations of these projectors

$$(4.39) \quad \mathbf{P}_{I,II} \sim \frac{1}{2} \begin{bmatrix} 0 & 0 & 0 & 0 & 0 & 0 \\ 0 & (\sin \rho)^2 & -(\sin \rho)^2 & 0 & -\frac{\sqrt{2}}{2} \sin 2\rho & 0 \\ 0 & -(\sin \rho)^2 & (\sin \rho)^2 & 0 & \frac{\sqrt{2}}{2} \sin 2\rho & 0 \\ 0 & 0 & 0 & 2(\sin \rho)^2 & 0 & -\sin 2\rho \\ 0 & -\frac{\sqrt{2}}{2} \sin 2\rho & \frac{\sqrt{2}}{2} \sin 2\rho & 0 & 2(\cos \rho)^2 & 0 \\ 0 & 0 & 0 & -\sin 2\rho & 0 & 2(\cos \rho)^2 \end{bmatrix},$$

$$(4.40) \quad \mathbf{P}_{III,IV} \sim \frac{1}{2} \begin{bmatrix} 0 & 0 & 0 & 0 & 0 & 0 \\ 0 & (\cos \rho)^2 & -(\cos \rho)^2 & 0 & \frac{\sqrt{2}}{2} \sin 2\rho & 0 \\ 0 & -(\cos \rho)^2 & (\cos \rho)^2 & 0 & -\frac{\sqrt{2}}{2} \sin 2\rho & 0 \\ 0 & 0 & 0 & 2(\cos \rho)^2 & 0 & \sin 2\rho \\ 0 & \frac{\sqrt{2}}{2} \sin 2\rho & -\frac{\sqrt{2}}{2} \sin 2\rho & 0 & 2(\sin \rho)^2 & 0 \\ 0 & 0 & 0 & \sin 2\rho & 0 & 2(\sin \rho)^2 \end{bmatrix}.$$

Any second-order tensor belonging to $\mathcal{P}_{I,II}$ and $\mathcal{P}_{III,IV}$, respectively, is deviatoric and has the following representation in the basis $\{\mathbf{e}_i\}$ ($\boldsymbol{\omega}$ any second order tensor):

$$(4.41) \quad \boldsymbol{\omega}_{I,II} = \frac{\mathbf{P}_{I,II} \cdot \boldsymbol{\omega}}{|\mathbf{P}_{I,II} \cdot \boldsymbol{\omega}|} \sim \frac{1}{\sqrt{2}} \begin{bmatrix} 0 & \cos \varphi \cos \rho & \sin \varphi \cos \rho \\ \cos \varphi \cos \rho & -\sin \varphi \sin \rho & -\cos \varphi \sin \rho \\ \sin \varphi \cos \rho & -\cos \varphi \sin \rho & \sin \varphi \sin \rho \end{bmatrix}$$

and

$$(4.42) \quad \boldsymbol{\omega}_{III,IV} = \frac{\mathbf{P}_{III,IV} \cdot \boldsymbol{\omega}}{|\mathbf{P}_{III,IV} \cdot \boldsymbol{\omega}|} \sim \frac{1}{\sqrt{2}} \begin{bmatrix} 0 & \cos \varphi \sin \rho & \sin \varphi \sin \rho \\ \cos \varphi \sin \rho & \sin \varphi \cos \rho & \cos \varphi \cos \rho \\ \sin \varphi \sin \rho & \cos \varphi \cos \rho & -\sin \varphi \cos \rho \end{bmatrix},$$

where $\varphi \in (0, 2\pi)$. The bases in those sub-spaces can be composed of two elements: $\boldsymbol{\omega}_K(\varphi_1)$ and $\boldsymbol{\omega}_K(\varphi_2)$, where $\varphi_2 = \varphi_1 + \pi/2$. The simplest bases in $\mathcal{P}_{I,II}$ and $\mathcal{P}_{III,IV}$ is obtained setting $\phi_1 = 0$ and $\phi_2 = \pi/2$. Note that among infinite number of elements (4.41) and (4.42), one can indicate in both cases three which are pure shears. They are specified by angles φ being the solutions of two trigonometric equations

$$\begin{aligned} \det \boldsymbol{\omega}_{I,II} = 0 &\Leftrightarrow \cos^2 \rho \sin \varphi (\sin \rho - \cos^2 \varphi (3 \sin \rho + \cos \rho)) = 0, \\ \det \boldsymbol{\omega}_{III,IV} = 0 &\Leftrightarrow \sin^2 \rho \sin \varphi (\cos^2 \varphi (3 \cos \rho + \sin \rho) - \cos \rho) = 0. \end{aligned}$$

Therefore, for any elastic material of trigonal symmetry at least six of its eigenstates are the pure shears [3]. Of course, not all of them are pairwise orthogonal as far as some of them correspond to the same eigen-value (the same Kelvin modulus).

The specific form of $\mathbf{P}_{I,II}$ and $\mathbf{P}_{III,IV}$ depends on the angle ρ being the function of one stiffness distributor. The value of this distributor is material characteristic for trigonal symmetry. Similarly, the specific form of eigen-states $\boldsymbol{\omega}_V$ and $\boldsymbol{\omega}_{VI}$ depends on the angle ϕ which is the function of the second stiffness distributor (compare [25]). One can define this distributor as follows:

$$\eta_2 = \frac{\det \mathbf{h}_{VI}}{(\text{tr} \boldsymbol{\omega}_{VI})^3},$$

where \mathbf{h}_{VI} is deviator of $\boldsymbol{\omega}_{VI}$.

The considered **material of trigonal symmetry** is defined by

1. 4 Kelvin moduli: $\lambda_1 = \lambda_{I,II}$, $\lambda_2 = \lambda_{III,IV}$, both of multiplicity 2, and $\lambda_3 = \lambda_V$, $\lambda_4 = \lambda_{VI}$ of multiplicity 1.
2. Two stiffness distributors which specify angles ρ and ϕ .
3. 3 Euler angles which orient symmetry axis \mathbf{e}_1 and the symmetry plane \mathbf{e}_2 with respect to laboratory.

The unique spectral decomposition takes the form

$$(4.43) \quad \mathbf{L} = \lambda_1 \mathbf{P}_1(\rho) + \lambda_2 \mathbf{P}_2(\rho) + \lambda_3 \mathbf{P}_3(\phi) + \lambda_4 \mathbf{P}_4(\phi),$$

where

$$\begin{aligned} \mathbf{P}_1(\rho) &= \mathbf{P}_{I,II}(\rho), & \mathbf{P}_2(\rho) &= \mathbf{P}_{III,IV}(\rho), \\ \mathbf{P}_3(\phi) &= \boldsymbol{\omega}_V(\phi) \otimes \boldsymbol{\omega}_V(\phi), & \mathbf{P}_4(\phi) &= \boldsymbol{\omega}_{VI}(\phi) \otimes \boldsymbol{\omega}_{VI}(\phi). \end{aligned}$$

Using (4.43) the stiffness tensor \mathbf{L} for the material of trigonal symmetry in the poly-basis \mathbf{a}_K composed of diads of the basis \mathbf{e}_i , has the representation

$$(4.44) \quad \mathbf{L} \sim \begin{bmatrix} L_{11} & L_{12} & L_{12} & 0 & 0 & 0 \\ L_{12} & L_{22} & L_{23} & 0 & L_{25} & 0 \\ L_{12} & L_{23} & L_{22} & 0 & -L_{25} & 0 \\ 0 & 0 & 0 & L_{22} - L_{23} & 0 & \sqrt{2}L_{25} \\ 0 & L_{25} & -L_{25} & 0 & L_{55} & 0 \\ 0 & 0 & 0 & \sqrt{2}L_{25} & 0 & L_{55} \end{bmatrix}$$

therefore it is specified by 6 independent components. It can be shown that the Kelvin moduli $\lambda_V = \lambda_3$ and $\lambda_{VI} = \lambda_4$ are obtained as eigenvalues of the following 2×2 matrix

$$(4.45) \quad \frac{1}{3} \begin{bmatrix} L_{11} + 2(2L_{12} + L_{23} + L_{33}) & \sqrt{2}(L_{11} + L_{12} - (L_{22} + L_{23})) \\ \sqrt{2}(L_{11} + L_{12} - (L_{22} + L_{23})) & 2L_{11} - 4L_{12} + L_{23} + L_{22} \end{bmatrix},$$

while the Kelvin $\lambda_{I,II} = \lambda_1$ and $\lambda_{III,IV} = \lambda_2$ of multiplicity 2 can be derived as eigenvalues of the following 2×2 matrix:

$$(4.46) \quad \begin{bmatrix} L_{22} - L_{23} & \sqrt{2}L_{25} \\ \sqrt{2}L_{25} & L_{55} \end{bmatrix}.$$

Single crystal of aluminum oxide Al_2O_3 , ceramic material, has trigonal symmetry.

4.6. Material of tetragonal symmetry

Material of **tetragonal symmetry** (symmetry of a prism of square basis, see Fig. 3) is characterized by the following symmetry group

$$(4.47) \quad \mathcal{Q}_{\mathbf{L}}^{4t} = \{ \mathbf{1}, -\mathbf{1}, \mathbf{I}_{\mathbf{e}_1}, \mathbf{I}_{\mathbf{e}_2}, \mathbf{R}_{\mathbf{e}_1}^{\pi/2} \}.$$

Similarly like in the case of trigonal symmetry it is impossible to fulfill the symmetry conditions (4.6) by 6 mutually orthogonal eigen-states. Using the results for orthotropic material, it can be checked that the additional condition of symmetry imposed by $\mathbf{R}_{\mathbf{e}_1}^{\pi/2}$ is fulfilled³⁾ only by four eigen-tensors. Two of them are pure shears which have the following representations in basis $\{\mathbf{e}_i\}$:

³⁾The eigen-states of the material of tetragonal symmetry can be derived by imposing the additional symmetry condition on the eigen-states of orthotropic material because $\mathcal{Q}_{\mathbf{L}}^o \subset \mathcal{Q}_{\mathbf{L}}^{4t}$, Fig. 2.

$$(4.48) \quad \boldsymbol{\omega}_{III} \sim \frac{1}{\sqrt{2}} \begin{bmatrix} 0 & 0 & 0 \\ 0 & 0 & 1 \\ 0 & 1 & 0 \end{bmatrix}, \quad \boldsymbol{\omega}_{IV} \sim \frac{1}{\sqrt{2}} \begin{bmatrix} 0 & 0 & 0 \\ 0 & 1 & 0 \\ 0 & 0 & -1 \end{bmatrix},$$

while other two eigen-states have the form

$$(4.49) \quad \boldsymbol{\omega}_{V,VI} \sim \begin{bmatrix} \omega_{11}^{V,VI} & 0 & 0 \\ 0 & \omega_{22}^{V,VI} & 0 \\ 0 & 0 & \omega_{22}^{V,VI} \end{bmatrix}.$$

They define four one-dimensional subspaces $\mathcal{P}_K, K = III, IV, V, VI$. Moreover, from the symmetry conditions (4.4) we obtain the following projector $\mathbf{P}_{I,II}$ which projects into two-dimensional subspace $\mathcal{P}_{I,II}$ of pure shears with common shear direction. Its representation in the orthonormal poly-basis $\{\mathbf{a}_I\}$ composed of $\{\mathbf{e}_i \otimes \mathbf{e}_j\}$ (see Appendix) is as follows:

$$(4.50) \quad \mathbf{P}_{I,II} \sim \begin{bmatrix} 0 & 0 & 0 & 0 & 0 & 0 \\ 0 & 0 & 0 & 0 & 0 & 0 \\ 0 & 0 & 0 & 0 & 0 & 0 \\ 0 & 0 & 0 & 0 & 0 & 0 \\ 0 & 0 & 0 & 0 & 1 & 0 \\ 0 & 0 & 0 & 0 & 0 & 1 \end{bmatrix}.$$

Any unit element of this two-dimensional subspace can be written in the form

$$(4.51) \quad \boldsymbol{\omega}_{I,II} \sim \frac{1}{\sqrt{2}} \begin{bmatrix} 0 & \sin \varphi & \cos \varphi \\ \sin \varphi & 0 & 0 \\ \cos \varphi & 0 & 0 \end{bmatrix}, \quad \varphi \in \langle 0, 2\pi \rangle.$$

An orthonormal basis in this subspace is composed of two tensors $\boldsymbol{\omega}_{I,II}(\varphi_1)$ and $\boldsymbol{\omega}_{I,II}(\varphi_2)$, such that $\varphi_2 = \varphi_1 + \pi/2$.

For any material of tetragonal symmetry we have obtained two uniquely specified (within a sign) eigen-states $\boldsymbol{\omega}_{III}$ and $\boldsymbol{\omega}_{IV}$ as well as the uniquely defined projector $\mathbf{P}_{I,II}$. The specific form of $\boldsymbol{\omega}_V$ and $\boldsymbol{\omega}_{VI}$ depends on the value of one stiffness distributor which is the material characteristic for the considered material. Using the result of [15], this distributor can be defined as

$$(4.52) \quad \eta = \eta_2 = \frac{\det \mathbf{h}_{VI}}{(\text{tr} \boldsymbol{\omega}_{VI})^3}.$$

It should be noted that for the material of tetragonal symmetry the direction \mathbf{e}_1 is uniquely defined, while the direction \mathbf{e}_2 can be specified only with accuracy to the angle $\pi/4$.

The considered elastic **material of tetragonal symmetry** is specified by

1. 5 Kelvin moduli: $\lambda_1 = \lambda_{I,II}$ of multiplicity 2, $\lambda_2 = \lambda_{III}$, $\lambda_3 = \lambda_{IV}$, $\lambda_4 = \lambda_V$ and $\lambda_5 = \lambda_{VI}$ of multiplicity 1.
2. One stiffness distributor η which specifies angle ϕ .
3. 3 Euler angles which orient symmetry axis \mathbf{e}_1 and the symmetry plane \mathbf{e}_2 with respect to laboratory.

The unique spectral decomposition takes the form

$$(4.53) \quad \mathbf{L} = \lambda_1 \mathbf{P}_1 + \lambda_2 \mathbf{P}_2 + \lambda_3 \mathbf{P}_3 + \lambda_4 \mathbf{P}_4(\phi) + \lambda_5 \mathbf{P}_5(\phi)$$

where

$$\mathbf{P}_1 = \mathbf{P}_{I,II}, \quad \mathbf{P}_2 = \boldsymbol{\omega}_{III} \otimes \boldsymbol{\omega}_{III}, \quad \mathbf{P}_3 = \boldsymbol{\omega}_{IV} \otimes \boldsymbol{\omega}_{IV}$$

and

$$\mathbf{P}_4(\phi) = \boldsymbol{\omega}_V(\phi) \otimes \boldsymbol{\omega}_V(\phi), \quad \mathbf{P}_5(\phi) = \boldsymbol{\omega}_{VI}(\phi) \otimes \boldsymbol{\omega}_{VI}(\phi).$$

The representation of the stiffness tensor in poly-basis \mathbf{a}_K for the material of tetragonal symmetry has the form similar to orthotropic material with additional relations

$$(4.54) \quad L_{13} = L_{12}, \quad L_{33} = L_{22}, \quad L_{66} = L_{55};$$

therefore, it is specified by 6 independent components. The Kelvin moduli depend on L_{KL} as follows:

$$(4.55) \quad \lambda_{I,II} = \lambda_1 = L_{55}, \quad \lambda_{III} = \lambda_2 = \lambda_{44}, \quad \lambda_{IV} = \lambda_3 = L_{22} - L_{23}$$

and $\lambda_V = \lambda_4$ and $\lambda_{VI} = \lambda_5$ are found as eigenvalues of matrix (4.45). The stiffness distributor η is specified by components of \mathbf{L} as follows

$$(4.56) \quad \eta = \frac{1}{27\sqrt{2}} \frac{\bar{L}_{12}}{\bar{L}_{11} - \lambda_V},$$

where \bar{L}_{KL} denote components of matrix (4.45), while λ_V is taken as a minimum (a maximum) of its eigenvalues if $\bar{L}_{11} > \bar{L}_{22}$ ($\bar{L}_{11} < \bar{L}_{22}$). The latter specification ensures that $(\text{tr} \boldsymbol{\omega}_{VI})^2 > (\text{tr} \boldsymbol{\omega}_V)^2$.

As an example of material of tetragonal symmetry, the γ -TiAl intermetallic is analyzed in Subsec. 4.10. Tetragonal symmetry has also a single crystal of martensitic phase of ferromagnetic shape memory alloy NiMnGa.

4.7. *Transversely isotropic material*

Material of **transversal isotropy** (cylindrical symmetry presented in Fig. 4) has the following symmetry group (note that $\mathcal{Q}_{\mathbf{L}}^{4t} \subset \mathcal{Q}_{\mathbf{L}}^t$):

$$(4.57) \quad \mathcal{Q}_{\mathbf{L}}^t = \left\{ \mathbf{1}, -\mathbf{1}, \mathbf{I}_{\mathbf{e}_1}, \mathbf{I}_{\mathbf{e}_2}, \mathbf{R}_{\mathbf{e}_1}^\phi \right\},$$

where the orthogonal tensor $\mathbf{R}_{\mathbf{e}_1}^\phi$ describes the rotation around the axis \mathbf{e}_1 through any angle ϕ . The symmetry condition (4.6) for this rotation tensor is fulfilled by two eigen-states (4.49) valid for tetragonal symmetry, which describe two one-dimensional subspaces \mathcal{P}_V and \mathcal{P}_{VI} . Furthermore, the symmetry condition (4.4) is fulfilled for projector $\mathcal{P}_{I,II}$ specified by (4.50) and another projector $\mathcal{P}_{III,IV}$, both projecting into two 2-dimensional subspaces of pure shears. The projector $\mathcal{P}_{III,IV}$ has the representation

$$(4.58) \quad \mathbf{P}_{III,IV} \sim \frac{1}{2} \begin{bmatrix} 0 & 0 & 0 & 0 & 0 & 0 \\ 0 & 1 & -1 & 0 & 0 & 0 \\ 0 & -1 & 1 & 0 & 0 & 0 \\ 0 & 0 & 0 & 2 & 0 & 0 \\ 0 & 0 & 0 & 0 & 0 & 0 \\ 0 & 0 & 0 & 0 & 0 & 0 \end{bmatrix}$$

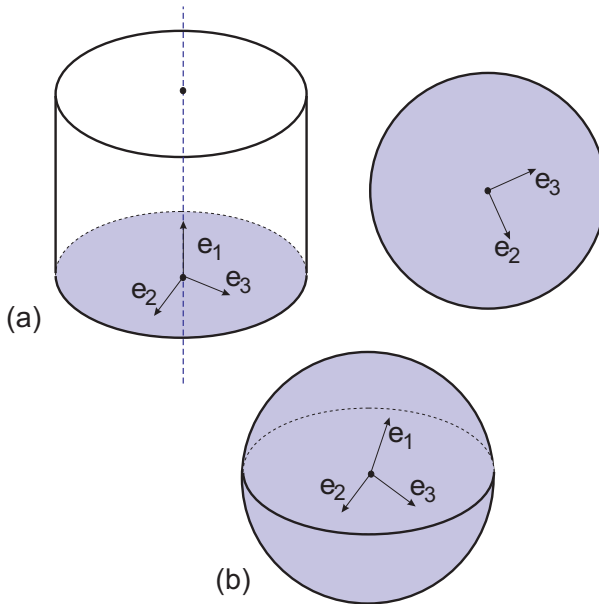


FIG. 4. Schematic representation of transversely isotropic material (a) and isotropic material (b).

written in the poly-basis $\{\mathbf{a}_I\}$. Any unit element of the two-dimensional subspace $\mathcal{P}_{III,IV}$ can be specified in the form

$$(4.59) \quad \boldsymbol{\omega}_{III,IV} \sim \frac{1}{\sqrt{2}} \begin{bmatrix} 0 & 0 & 0 \\ 0 & \cos \psi & \sin \psi \\ 0 & \sin \psi & -\cos \psi \end{bmatrix}, \quad \psi \in \langle 0, 2\pi \rangle.$$

Orthonormal basis in this subspace is composed of two tensors $\boldsymbol{\omega}_{III,IV}(\psi_1)$ and $\boldsymbol{\omega}_{III,IV}(\psi_2)$, such that $\psi_2 = \psi_1 + \pi/2$.

It should be underlined that the representation of the eigen-states $\boldsymbol{\omega}_{V,VI}$ and the projectors $\mathbf{P}_{I,II}$ and $\mathbf{P}_{III,IV}$ is the same in any basis in which the direction \mathbf{e}_1 is coaxial with the material symmetry direction, therefore in order to specify the orientation of material sample with respect to the laboratory it is sufficient to specify two Euler angles ϕ_1 and ϕ_2 .

For any transversely isotropic material one obtains two uniquely specified eigen-projectors $\mathbf{P}_{I,II}$ and $\mathbf{P}_{III,IV}$. The specific form of two eigen-states $\boldsymbol{\omega}_V$ and $\boldsymbol{\omega}_{VI}$, similarly as for the material of tetragonal symmetry depends on the stiffness distributor (4.52), the value of which is the material characteristic for the analyzed material (compare [12]).

Note that we can obtain transversely isotropic material considering also the material of trigonal symmetry if we set the angle $\rho = 0$. In such a case the projector $\mathbf{P}_1 = \mathbf{P}_{I,II}$ project into the space plane deviators (4.59) (they are the pure shears with common shearing plane \mathbf{e}_1) while the projector $\mathbf{P}_2 = \mathbf{P}_{III,IV}$ project into the space of pure shears (4.51) with common shearing direction \mathbf{e}_1 .

The considered **transversely isotropic material** is defined by

1. 4 Kelvin moduli: $\lambda_1 = \lambda_{I,II}$, $\lambda_2 = \lambda_{III,IV}$, both of multiplicity 2, and $\lambda_3 = \lambda_V$, $\lambda_4 = \lambda_{VI}$ of multiplicity 1.
2. One stiffness distributor η which specifies angle ϕ .
3. 2 Euler angles which orient symmetry axis \mathbf{e}_1 with respect to laboratory.

The unique spectral decomposition takes the form

$$(4.60) \quad \mathbf{L} = \lambda_1 \mathbf{P}_1 + \lambda_2 \mathbf{P}_2 + \lambda_3 \mathbf{P}_3(\phi) + \lambda_4 \mathbf{P}_4(\phi)$$

where $\mathbf{P}_1 = \mathbf{P}_1^{\text{trig}}(0)$ and $\mathbf{P}_2 = \mathbf{P}_2^{\text{trig}}(0)$ while

$$\mathbf{P}_3(\phi) = \boldsymbol{\omega}_V(\phi) \otimes \boldsymbol{\omega}_V(\phi), \quad \mathbf{P}_4(\phi) = \boldsymbol{\omega}_{VI}(\phi) \otimes \boldsymbol{\omega}_{VI}(\phi)$$

The representation of the stiffness tensor for the material of transversal isotropy in poly-basis \mathbf{a}_K has the representation similar to orthotropic material with relations (4.54), valid for the tetragonal symmetry and additionally

$$(4.61) \quad L_{44} = L_{22} - L_{12},$$

therefore, it is specified by 5 independent components. Kelvin moduli λ_K and stiffness distributor η are found as for the material of tetragonal symmetry, Eqs. (4.55)–(4.56), where in view of relation (4.61) one has $\lambda_{III} = \lambda_{IV}$.

There are many engineering materials which can be modelled as transversely isotropic. The classical example is the composite with the reinforcement in the form of elongated aligned fibers [5]. Moreover, as it was already signalled in the introduction, all materials for which the single crystal has the hexagonal symmetry, in view of their elastic anisotropy are transversely isotropic. Examples of such metals are analyzed in Subsec. 4.10.

4.8. Material of cubic symmetry

Material of **cubic symmetry** (symmetry of a cube, Fig. 5) has the following symmetry group ($\mathcal{Q}_L^{4t} \subset \mathcal{Q}_L^c$):

$$(4.62) \quad \mathcal{Q}_L^k = \{ \mathbf{1}, -\mathbf{1}, \mathbf{I}_{\mathbf{e}_1}, \mathbf{R}_{\mathbf{e}_1}^{k\pi/2}, \mathbf{R}_{\mathbf{e}_2}^{k\pi/2} \}.$$

The group of trigonal symmetry is also the subset of the cubic symmetry group, however, the symmetry axis is then coaxial with one of the main diagonals of a cube span by the vectors \mathbf{e}_i .

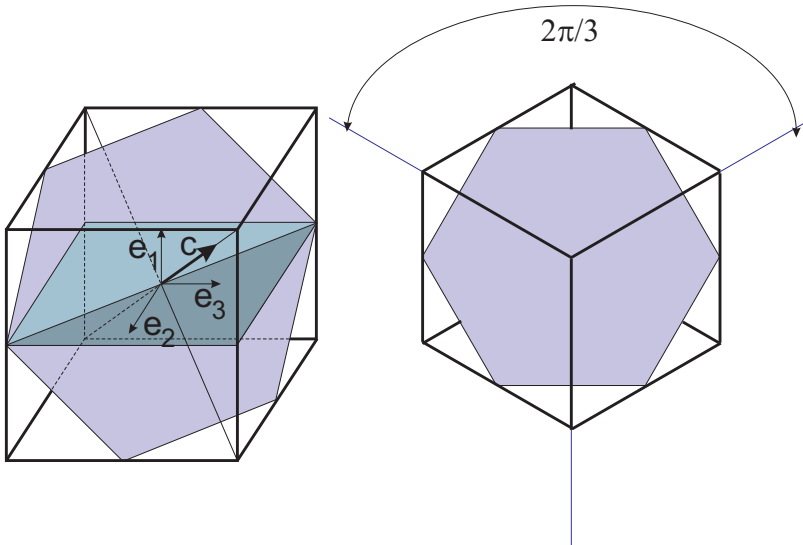


FIG. 5. Schematic representation of a material of cubic symmetry. Note that a crystal elongated along the main diagonal \mathbf{c} would have trigonal symmetry with the main axis of symmetry coaxial with \mathbf{c} .

From the symmetry condition (4.6) one eigen-state is obtained

$$(4.63) \quad \boldsymbol{\omega}_{VI} \sim \frac{1}{\sqrt{3}} \begin{bmatrix} 1 & 0 & 0 \\ 0 & 1 & 0 \\ 0 & 0 & 1 \end{bmatrix},$$

which, as it is easy to note, describes one-dimensional subspace of hydrostatic tensors. From the symmetry conditions (4.4) we obtain two eigen-projectors (compare [19]). A projector $\mathbf{P}_{I,II,III}$ (again in poly-basis $\{\mathbf{a}_I\}$)

$$(4.64) \quad \mathbf{P}_{I,II,III} \sim \begin{bmatrix} 0 & 0 & 0 & 0 & 0 & 0 \\ 0 & 0 & 0 & 0 & 0 & 0 \\ 0 & 0 & 0 & 0 & 0 & 0 \\ 0 & 0 & 0 & 1 & 0 & 0 \\ 0 & 0 & 0 & 0 & 1 & 0 \\ 0 & 0 & 0 & 0 & 0 & 1 \end{bmatrix}$$

projects into the 3-dimensional deviatoric subspace $\mathcal{P}_{I,II,III}$. Any unit element (not necessarily pure shear) of this subspace can be represented as follows:

$$(4.65) \quad \boldsymbol{\omega}_{I,II,III} \sim \frac{1}{\sqrt{2}} \begin{bmatrix} 0 & \sin \varphi \cos \psi & \sin \varphi \sin \psi \\ \sin \varphi \cos \psi & 0 & \cos \varphi \\ \sin \varphi \sin \psi & \cos \varphi & 0 \end{bmatrix},$$

where $\psi \in \langle 0, 2\pi \rangle$ and $\varphi \in \langle 0, \pi \rangle$. The second projector $\mathbf{P}_{IV,V}$ has the form

$$(4.66) \quad \mathbf{P}_{IV,V} \sim \frac{1}{3} \begin{bmatrix} 2 & -1 & -1 & 0 & 0 & 0 \\ -1 & 2 & -1 & 0 & 0 & 0 \\ -1 & -1 & 2 & 0 & 0 & 0 \\ 0 & 0 & 0 & 0 & 0 & 0 \\ 0 & 0 & 0 & 0 & 0 & 0 \\ 0 & 0 & 0 & 0 & 0 & 0 \end{bmatrix}$$

and projects into two-dimensional deviatoric subspace $\mathcal{P}_{IV,V}$. Any unit element of this subspace can be represented as follows:

$$(4.67) \quad \boldsymbol{\omega}_{IV,V} \sim \frac{\sqrt{2}}{\sqrt{3}} \begin{bmatrix} \cos \theta & 0 & 0 \\ 0 & \cos \left(\theta + \frac{2\pi}{3} \right) & 0 \\ 0 & 0 & \cos \left(\theta - \frac{2\pi}{3} \right) \end{bmatrix},$$

where $\theta \in \langle 0, 2\pi \rangle$. Orthonormal basis in this subspace can be composed of any two tensors $\boldsymbol{\omega}_{IV,V}(\theta_1)$ and $\boldsymbol{\omega}_{IV,V}(\theta_2)$ for which $\theta_2 = \theta_1 + \pi/2$.

For any material of cubic symmetry one obtains two uniquely defined projectors $\mathbf{P}_{I,II,III}$ and $\mathbf{P}_{IV,V}$ as well as one uniquely specified (within a sign) eigen-state $\boldsymbol{\omega}_{VI}$. The decomposition of the space \mathcal{S} into three mutually orthogonal eigen-subspaces is identical for any material of cubic symmetry (there are no stiffness distributors). Material of trigonal symmetry reduces to the material of cubic symmetry if we set

$$\phi = \phi^0, \quad \rho = \rho^0, \quad \lambda_1^{trig} = \lambda_3^{trig} = \lambda_1^{cube}$$

and $\tan \phi^0 = \tan \rho^0 = \sqrt{2}$. Note that in this case the stiffness distributor $\eta_2 = 0$.

The considered **material of cubic symmetry** is specified by

1. 3 Kelvin moduli: $\lambda_1 = \lambda_{I,II,III}$ of multiplicity 3, $\lambda_2 = \lambda_{IV,V}$ of multiplicity 2 and $\lambda_3 = \lambda_{VI}$ of multiplicity 1.
2. 0 stiffness distributors.
3. 3 Euler angles which orient symmetry axes \mathbf{e}_i with respect to laboratory.

The unique spectral decomposition takes the form

$$(4.68) \quad \mathbf{L} = \lambda_1 \mathbf{P}_1 + \lambda_2 \mathbf{P}_2 + \lambda_3 \mathbf{P}_3,$$

where

$$\mathbf{P}_1 = \mathbb{I}^S - \mathbb{K}, \quad \mathbf{P}_2 = \mathbb{K} - \mathbb{I}_P, \quad \mathbf{P}_3 = \mathbb{I}_P = \frac{1}{3} \mathbf{1} \otimes \mathbf{1}$$

$$\text{and } \mathbb{K} = \sum_{i=1}^3 \mathbf{e}_i \otimes \mathbf{e}_i \otimes \mathbf{e}_i \otimes \mathbf{e}_i.$$

The representation of the stiffness tensor for the material of cubic symmetry has the form similar to an orthotropic material with additional relations between components, namely

$$(4.69) \quad L_{23} = L_{13} = L_{12}, \quad L_{33} = L_{22} = L_{11}, \quad L_{66} = L_{55} = L_{44},$$

where

$$\lambda_{VI} = \lambda_3 = L_{11} + 2L_{12}, \quad \lambda_{IV,V} = \lambda_2 = L_{11} - L_{12}$$

and

$$\lambda_{I,II,III} = \lambda_1 = L_{44},$$

therefore, it is specified by 3 independent components. Single crystals of Cu or Al are of cubic symmetry. Austenite phase, high-symmetry phase in shape memory alloys, e.g. NiTi, CuZnAl, NiMnGa, usually exhibit cubic symmetry.

4.9. *Isotropic material*

As it was already stated in Subsec. 4.1, the symmetry group of such material is the whole orthogonal group \mathcal{Q} . For **isotropic material** (Fig. 4) fulfillment of condition (4.6) leads to the hydrostatic eigen-state (4.63), while symmetry condition (4.4) leads to the projector being the sum of projectors (4.64) and (4.66) derived for the cubic symmetry, namely

$$(4.70) \quad \mathbf{P}_d = \mathbf{P}_{I,II,III} + \mathbf{P}_{IV,V} = \mathbb{I} - \frac{1}{3} \mathbf{1} \otimes \mathbf{1}.$$

This projector projects the II-nd order tensor into the 5-dimensional subspace of deviators. Its representation in the poly-basis $\{\mathbf{a}_I\}$ composed of diads of basis vectors of any orthonormal basis $\{\mathbf{e}_i\}$ is the same and has the form

$$(4.71) \quad \mathbf{P}_d \sim \frac{1}{3} \begin{bmatrix} 2 & -1 & -1 & 0 & 0 & 0 \\ -1 & 2 & -1 & 0 & 0 & 0 \\ -1 & -1 & 2 & 0 & 0 & 0 \\ 0 & 0 & 0 & 3 & 0 & 0 \\ 0 & 0 & 0 & 0 & 3 & 0 \\ 0 & 0 & 0 & 0 & 0 & 3 \end{bmatrix}.$$

The considered **isotropic material** is specified by

1. 2 Kelvin moduli: $\lambda_1 = \lambda_{I,II,III,IV,V}$ of multiplicity 5 and $\lambda_2 = \lambda_{VI}$ of multiplicity 1.
2. 0 stiffness distributors.
3. 0 Euler angles (they are not needed because all material directions are equivalent).

The unique spectral decomposition takes the form

$$(4.72) \quad \mathbf{L} = \lambda_1 \mathbf{P}_1 + \lambda_2 \mathbf{P}_2,$$

where

$$\mathbf{P}_1 = \mathbf{P}_d = \mathbb{I}^S - \mathbb{I}_P, \quad \mathbf{P}_2 = \mathbb{I}_P = \frac{1}{3} \mathbf{1} \otimes \mathbf{1}.$$

The representation of the stiffness tensor for the isotropic material is obtained from the stiffness tensor for cubic symmetry with additional relation

$$(4.73) \quad L_{44} = L_{11} - L_{12} = \lambda_{I,II,III,IV,V} = \lambda_1;$$

therefore, it is specified by 2 independent components.

In Table 1 I and II structural index is provided for all 8 symmetry groups. In [14] the structural indices have been derived for the volumetrically isotropic materials (that is with the so-called Burzyński constraint) for all elastic symmetry groups. For such materials, the hydrostatic tensor (4.63) is one of the eigen-states. It results in reduction of the number of stiffness distributors. Note that for such materials the elasticity tensor is coaxial with the isotropic elasticity tensor.

Table 1. I and II-structural index for all symmetry classes of linear elastic materials.

| Symmetry group | I structural index | II structural index | Number of parameters |
|--|---|---------------------|----------------------|
| full anisotropy | $\langle 1 + 1 + 1 + 1 + 1 + 1 \rangle$ | $[6 + 12 + 3]$ | 21 |
| monoclinic symmetry (symmetry of a prism with irregular basis) | $\langle (1 + 1 + 1 + 1) + 1 + 1 \rangle$ | $[6 + 6 + 3]$ | 15 |
| orthotropy (symmetry of a prism with a rectangular basis) | $\langle (1 + 1 + 1) + 1 + 1 + 1 \rangle$ | $[6 + 3 + 3]$ | 12 |
| trigonal symmetry (symmetry of an elongated cube) | $\langle (1 + 1) + (2 + 2) \rangle$ | $[4 + 2 + 3]$ | 9 |
| tetragonal symmetry (symmetry of a prism with a square basis) | $\langle (1 + 1) + 1 + 1 + 2 \rangle$ | $[5 + 1 + 3]$ | 9 |
| transversal symmetry (cylindrical) | $\langle (1 + 1) + 2 + 2 \rangle$ | $[4 + 1 + 2]$ | 7 |
| cubic symmetry (symmetry of a cube) | $\langle 1 + 2 + 3 \rangle$ | $[3 + 0 + 3]$ | 6 |
| isotropy | $\langle 1 + 5 \rangle$ | $[2 + 0 + 0]$ | 2 |

4.10. Examples

We apply the derived formulae for assessment of intensity of an elastic anisotropy of single crystals of selected metals and alloys. The intensity of anisotropy is here intuitively meant as a departure of the material behaviour from the isotropic one, i.e. strong variation of elastic properties depending on the direction in which they are measured. More information concerning this issue can be found e.g. in [18, 20, 24]. It should be underlined that in general, the intensity of an anisotropy is not equivalent to the notion of low or high symmetry of material. Material of high symmetry (e.g. cubic) can exhibit strong anisotropy, e.g. strong

variation of directional Young modulus [19] and vice versa: the anisotropy of material of low symmetry can be weak.

In Table 2 the independent components of the elasticity tensor for single crystals of selected materials are collected. The hcp materials (Mg, Zn, Zr, Ti metals and α_2 -Ti₃Al intermetallic) exhibit the hexagonal lattice symmetry, therefore, the stiffness and compliance tensors have the form equivalent to the transversal isotropy case with 5 independent components in anisotropy axes, Subsec. 4.7. In the case of crystal of tetragonal symmetry (γ -TiAl intermetallic) one has 6 independent components, Subsec. 4.6. High symmetry metals such as copper and aluminum are fcc materials of cubic symmetry with three independent components of \mathbf{L} .

Table 2. Elastic constants [GPa] of single crystals for selected metals and alloys of high specific stiffness and some fcc materials (axis 1 is the main symmetry axis).

| Material | L_{2222} | L_{2233} | L_{1122} | L_{1111} | L_{1212} | L_{3232} |
|---|------------|------------|------------|------------|------------|------------|
| Mg [1] | 59.3 | 25.7 | 21.4 | 61.5 | 16.4 | |
| Zn [1] | 163.7 | 36.4 | 53.0 | 63.5 | 38.8 | |
| Zr [30] | 143.5 | 72.5 | 65.4 | 164.9 | 32.1 | |
| Ti [29, 31] | 163.9 | 91.3 | 68.9 | 181.6 | 47.2 | |
| α_2 -Ti ₃ Al [31, 21] | 175 | 88.7 | 62.3 | 220 | 62.6 | |
| γ -TiAl[21] | 183 | 74.1 | 74.4 | 178 | 105 | 78.4 |
| Cu [1] | 171.0 | 122.0 | | | 69.1 | |
| Al [1] | 186 | 157 | | | 42 | |

In Table 3 we provide the invariants resulting from spectral decomposition of the corresponding elasticity tensors for these materials [13] (relation between L_{ijkl} and L_{KLN} components is specified in the Appendix by (A.2)). The following conclusions result from the analysis of this table:

- All analyzed metals and alloys, with exception of Zn, are close to be a volumetrically isotropic materials (ξ is close to zero). Note that Cu and Al, being cubic materials, are volumetrically isotropic exactly.
- In view of above property, the intensity of elastic anisotropy⁴⁾ can be assessed comparing the Kelvin moduli λ_I , λ_{II} , ..., λ_V , or more specifically their properly defined ratios, e.g λ_K/λ_{\max} where $\lambda_{\max} = \max\{\lambda_I, \dots, \lambda_V\}$. For example, one observes that elastic anisotropy of Mg or Al crystals is not strong and it is strong for Zn or Cu. Note that introduction of such indicators of the intensity of the elastic anisotropy generalizes the

⁴⁾Note that if $\xi = 0$ and $\lambda_I = \lambda_{II} = \dots = \lambda_V$, the material is isotropic.

anisotropy factor introduced for cubic crystals by ZENER [32]: $A = (L_{1111} - L_{1122}) / (2L_{1212})$. As it could be easily verified, this factor is the ratio of deviatoric Kelvin moduli of cubic crystal, namely $A = \lambda_2^{\text{cub}} / \lambda_1^{\text{cub}}$.

Table 3. Kelvin moduli λ_K [GPa], a stiffness distributor $\xi^3 = \sqrt{2}\eta$ (Eq. (4.52)) and $\Phi = \arctan(3\xi)$ obtained by spectral decomposition of the local elasticity tensor for single crystals of selected metals and alloys [13].

| Material | λ_{VI} | λ_V | λ_{IV} | λ_{III} | $\lambda_{II} = \lambda_I$ | ξ | Φ [°] |
|--------------------------------|----------------|-------------|----------------|-----------------|----------------------------|---------|------------|
| Mg | 105.7 | 40.8 | 33.6 | | 32.8 | -0.0051 | -0.87 |
| Zn | 233.2 | 30.4 | 127.3 | | 77.6 | -0.0674 | -11.43 |
| Zr | 286.4 | 94.5 | 71.0 | | 64.2 | 0.0117 | 2.01 |
| Ti | 322.6 | 114.2 | 72.6 | | 94.4 | -0.0035 | -0.61 |
| α_2 -Ti ₃ Al | 332.6 | 151.1 | 86.4 | | 125.2 | 0.0161 | 2.77 |
| γ -TiAl | 330.0 | 105.1 | 108.9 | 156.8 | 210 | -0.0033 | -0.56 |
| Cu | 415.0 | 49.0 | | 138.2 | | 0 | 0 |
| Al | 228.9 | 46.5 | | 56.6 | | 0 | 0 |

5. CONCLUSIONS

In the paper, the spectral theorem for the elasticity tensor has been thoroughly discussed. The main aim of the work was the clarification of the issue of invariance of the spectral decomposition. Therefore, the forms of the decomposition for all elastic symmetry groups have been derived in an original way by imposing the symmetry conditions upon the orthogonal projectors, instead of the stiffness tensor itself. Thanks to that, the uniqueness of the orthogonal projectors for the considered Hooke's tensor in contrast to the non-uniqueness of eigen-states has been demonstrated. For completeness of the review, the number of independent eigenvalues (Kelvin moduli) and the corresponding orthogonal projectors have been explicitly outlined for each elastic symmetry class. Finally, the spectral decomposition of the stiffness tensor has been derived for single crystals of the selected metals and alloys.

ACKNOWLEDGMENT

The work was partly supported by the Ministry of Science and Higher Education of Poland in the framework of the research projects N N501 068135 (K. Kowalczyk-Gajewska) and N N501 121536 (J. Ostrowska-Maciejewska).

APPENDIX

The space \mathcal{S} of symmetric second-order tensors possesses all the properties of the six-dimensional Euclidean space with the scalar product defined as follows:

$$\bigwedge_{\mathbf{a}, \mathbf{b} \in \mathcal{S}} \mathbf{a} \cdot \mathbf{b} = \text{tr}(\mathbf{ab}) = a_{ij}b_{ij},$$

where $a_{ij}, b_{ij}, i, j = 1, 2, 3$ are components of tensors \mathbf{a} and \mathbf{b} in some orthonormal basis $\{\mathbf{e}_i\}$ in the three-dimensional physical space. Therefore, any second-order tensor has all the properties of the vector in the six-dimensional Euclidean space.

Due to this property of \mathcal{S} it is possible to select in \mathcal{S} a subset of six mutually orthogonal and normalized tensors $\{\mathbf{a}_K\}, K = I, \dots, VI$ which constitute the basis. One of the possible bases is the following orthonormal subset of basis diads $\{\mathbf{e}_i \otimes \mathbf{e}_j\}$ of the form:

$$\begin{aligned} \mathbf{a}_I &= \mathbf{e}_1 \otimes \mathbf{e}_1 & \mathbf{a}_{IV} &= \frac{1}{\sqrt{2}}(\mathbf{e}_2 \otimes \mathbf{e}_3 + \mathbf{e}_3 \otimes \mathbf{e}_2), \\ \mathbf{a}_{II} &= \mathbf{e}_2 \otimes \mathbf{e}_2, & \mathbf{a}_V &= \frac{1}{\sqrt{2}}(\mathbf{e}_1 \otimes \mathbf{e}_3 + \mathbf{e}_3 \otimes \mathbf{e}_1), \\ \mathbf{a}_{III} &= \mathbf{e}_3 \otimes \mathbf{e}_3, & \mathbf{a}_{VI} &= \frac{1}{\sqrt{2}}(\mathbf{e}_2 \otimes \mathbf{e}_1 + \mathbf{e}_1 \otimes \mathbf{e}_2). \end{aligned}$$

A basis in the six-dimensional space is called a poly-basis. In the above poly-basis, any symmetric tensor of the second order is specified in the following way:

$$\mathbf{a} = a_{ij}\mathbf{e}_i \otimes \mathbf{e}_j = a_K\mathbf{a}_K, \quad K = I, \dots, VI, \quad \text{where} \quad \mathbf{a} \cdot \mathbf{b} = a_Kb_K$$

and relations between representations a_{ij} and a_K are given by

$$(A.1) \quad \begin{aligned} a_I &= a_{11}, & a_{II} &= a_{22}, & a_{III} &= a_{33}, \\ a_{IV} &= \sqrt{2}a_{23}, & a_V &= \sqrt{2}a_{13}, & a_{VI} &= \sqrt{2}a_{12}. \end{aligned}$$

Consequently, the linear projection from the space \mathcal{S} into \mathcal{S} treated as the six-dimensional Euclidean space is described by the second-order tensor belonging to tensorial product $\mathcal{S} \otimes \mathcal{S}$. This reasoning brings us to conclusion that the fourth-order tensor \mathbf{A} that represents this projection in the three-dimensional physical space has all the properties of the second-order tensor in the six-dimensional Euclidean space. Therefore, one can write

$$\mathbf{A} = A_{ijkl}\mathbf{e}_i \otimes \mathbf{e}_j \otimes \mathbf{e}_k \otimes \mathbf{e}_l = A_{KL}\mathbf{a}_K \otimes \mathbf{a}_L.$$

The set of all basis diads $\{\mathbf{a}_I \otimes \mathbf{a}_J\}$ is the basis in the space $\mathcal{S} \otimes \mathcal{S}$. Components A_{KL} depend on components A_{ijkl} of the IV -th order tensor \mathbf{A} in the basis $\{\mathbf{e}_i\}$ in the physical space, in the following way:

$$(A.2) \quad [A_{KL}] = \begin{bmatrix} A_{1111} & A_{1122} & A_{1133} & \sqrt{2}A_{1123} & \sqrt{2}A_{1113} & \sqrt{2}A_{1112} \\ A_{2211} & A_{2222} & A_{2233} & \sqrt{2}A_{2223} & \sqrt{2}A_{2213} & \sqrt{2}A_{2212} \\ A_{3311} & A_{3322} & A_{3333} & \sqrt{2}A_{3323} & \sqrt{2}A_{3313} & \sqrt{2}A_{3312} \\ \sqrt{2}A_{2311} & \sqrt{2}A_{2322} & \sqrt{2}A_{2333} & 2A_{2323} & 2A_{2313} & 2A_{2312} \\ \sqrt{2}A_{1311} & \sqrt{2}A_{1322} & \sqrt{2}A_{1333} & 2A_{1323} & 2A_{1313} & 2A_{1312} \\ \sqrt{2}A_{1211} & \sqrt{2}A_{1222} & \sqrt{2}A_{1233} & 2A_{1223} & 2A_{1213} & 2A_{1212} \end{bmatrix}.$$

The following products can be obtained in two alternative, but fully equivalent ways ($\mathbf{a}, \mathbf{b} \in \mathcal{S}$; $\mathbf{A}, \mathbf{B}, \mathbf{C} \in \mathcal{S} \otimes \mathcal{S}$):

$$\mathbf{a} \cdot \mathbf{b} = a_{ij}b_{ij} = a_K b_K,$$

$$\mathbf{b} = \mathbf{A} \cdot \mathbf{a} \Leftrightarrow b_{ij} = A_{ijkl}a_{kl} \quad \text{or} \quad b_K = A_{KL}a_L,$$

$$\mathbf{D} = \mathbf{A} \circ \mathbf{B} \Leftrightarrow D_{ijkl} = A_{ijmn}B_{mnkl} \quad \text{or} \quad D_{KL} = A_{KM}B_{ML},$$

where a_{ij} , b_{ij} , A_{ijkl} , B_{ijkl} , D_{ijkl} and a_K , b_K , A_{KL} , B_{KL} , D_{KL} are related by Eqs. (A.1) and (A.2).

It should be stressed that, due to the fact that the tensor \mathbf{A} represents linear projection between spaces of the symmetric second-order tensors, one obtains $A_{ijkl} = A_{jikl} = A_{ijlk}$. Note that in the case of the stiffness tensor \mathbf{L} and the compliance tensor \mathbf{M} , additionally one has to do with diagonal symmetry, $A_{KL} = A_{LK}$ ($A_{ijkl} = A_{klij}$).

REFERENCES

1. J. G. BERRYMAN, *Bounds and self-consistent estimates for elastic constants of random polycrystals with hexagonal, trigonal, and tetragonal symmetries*, J. Mech. Phys. Solids, **53**, 2141–2173, 2005.
2. A. BLINOWSKI and J. OSTROWSKA-MACIEJEWSKA, *On the elastic orthotropy*, Arch. Mech., **48**, 1, 129–141, 1996.
3. A. BLINOWSKI and J. RYCHLEWSKI, *Pure shears in the mechanics of materials*, Mathematics and Mechanics of Solids, **4**, 471–503, 1998.
4. P. CHADWICK, M. VIANELLO, and S. C. COWIN, *A new proof that the number of linear elastic symmetries is eight*, J. Mech. Phys. Solids, **49**, 2471–2492, 2001.

5. R. M. CHRISTENSEN, *Mechanics of Composites Materials*, Dover Publications, 1979, 2005.
6. S. C. COWIN and M. M. MEHRABADI, *Anisotropic symmetries of linear elasticity*, Appl. Mech. Rev., **48**, 5, 247–285, 1995.
7. S. C. COWIN and A. M. SADEGH, *Non-interacting modes for stress, strain and energy in hard tissue*, J. Biomechanics, **24**, 859–867, 1991.
8. S. FORTE and M. VIANELLO, *Symmetry classes for elasticity tensors*, J. Elasticity, **43**, 81–108, 1996.
9. R. B. HETNARSKI and J. IGNACZAK, *Mathematical theory of elasticity*, Taylor and Francis, New York, 2004.
10. W. THOMPSON (Lord Kelvin), *Elements of Mathematical Theory of Elasticity*, Chapter XV, On the Six Principal Strains of an Elastic Solid, Phil. Trans. R. Soc. London, **146**, 481–498, 1856.
11. U. F. KOCKS, C. N. TOME, and H.-R. WENK, *Texture and Anisotropy*, Cambridge University Press, II edition, 2000.
12. K. KOWALCZYK and J. OSTROWSKA–MACIEJEWSKA, *Energy-based limit conditions for transversally isotropic solids*, Arch. Mech., **54**, 5–6, 497–523, 2002.
13. K. KOWALCZYK–GAJEWSKA, *Micromechanical modelling of metals and alloys of high specific strength*, IFTR Reports (in preparation), 2010.
14. K. KOWALCZYK–GAJEWSKA and J. OSTROWSKA–MACIEJEWSKA, *The influence of internal restrictions on the elastic properties of anisotropic materials*, Arch. Mech., **56**, 205–232, 2004.
15. K. KOWALCZYK–GAJEWSKA and J. OSTROWSKA–MACIEJEWSKA, *Mechanics of the 21st Century, Proceedings of the 21st International Congress of Theoretical and Applied Mechanics, Warsaw, Poland, 15–21 August 2004*, Chapter “On the invariants of the elasticity tensor for orthotropic materials”, Springer (e-book), 2004.
16. S. G. LEKHNITSKII, *Theory of elasticity of an anisotropic body*, Mir Publishers, 1981.
17. M. M. MEHRABADI and S. C. COWIN, *Eigentensors of linear anisotropic elastic materials*, Quart. J. Mech. Appl. Math., **43**, 15–41, 1990.
18. M. MOAKHER and N. NORRIS, *The closest elastic tensor of arbitrary symmetry to an elasticity tensor of lower symmetry*, J. Elasticity, **85**, 215–263, 2006.
19. J. OSTROWSKA–MACIEJEWSKA and J. RYCHLEWSKI, *Generalized proper states for anisotropic elastic materials*, Arch. Mech., **53**, 4–5, 501–518, 2001.
20. J. PIEKARSKI, K. KOWALCZYK–GAJEWSKA, J. H. WAARSING, and M. MAŹDZIARZ, *Mechanics of the 21st Century, Proceedings of the 21st International Congress of Theoretical and Applied Mechanics, Warsaw, Poland, 15–21 August 2004* Chapter “Approximations of stiffness tensor of bone – determining and accuracy”, Springer (e-book), 2004.
21. A. ROOS, J.-L. CHABOCHE, L. GELEBART, and J. CREPIN, *Multiscale modelling of titanium aluminides*, Int. J. Plasticity, **20**, 811–830, 2004.
22. J. RYCHLEWSKI, “*CEIHNOSSTTUV*”. *Mathematical structure of elastic bodies* [in Russian], Technical Report 217, Inst. Mech. Probl. USSR Acad. Sci., Moskva, 1983.
23. J. RYCHLEWSKI, *Elastic energy decomposition and limit criteria* [in Russian], Advances in Mechanics, **7**, 3, 1984.

24. J. RYCHLEWSKI, *Zur Abschätzung der Anisotropie*, ZAMM, **65**, 256–258, 1985.
25. J. RYCHLEWSKI, *Unconventional approach to linear elasticity*, Arch. Mech., **47**, 2, 149–171, 1995.
26. J. RYCHLEWSKI, *A qualitative approach to Hooke's tensors. Part I*, Arch. Mech., **52**, 737–759, 2000.
27. J. RYCHLEWSKI, *Elastic waves under unusual anisotropy*, J. Mech. Phys. Solids, **49**, 2651–2666, 2001.
28. S. SUTCLIFFE, *Spectral decomposition of the elasticity tensor*, J. Appl. Mech., **59**, 4, 762–773, 1992.
29. K. TANAKA and M. KOIWA, *Single-crystal elastic constants of intermetallic compounds*, Intermetallics, **4**, 29–39, 1996.
30. F. XU, R. A. HOLT, and M. R. DAYMOND, *Modeling lattice strain evolution during uniaxial deformation of textured Zircaloy-2*, Acta Mater., **56**, 3672–3687, 2008.
31. M. H. YOO and C. L. FU, *Physical constants, deformation twinning, and microcracking of titanium aluminides*, Metal. Mater. Trans. A, **29A**, 49–63, 1998.
32. C. ZENER, *Elasticité et Anelasticité des Metaux*, Dunod, Paris, 1955.

Received March 30, 2010; revised version May 13, 2010.

SELECTED PASSAGES FROM WŁODZIMIERZ BURZYŃSKI'S
DOCTORAL DISSERTATION
“STUDY ON MATERIAL EFFORT HYPOTHESES”
PRINTED IN POLISH BY THE
ACADEMY OF TECHNICAL SCIENCES
LWÓW, 1928, 1–192

FRAGMENTY ROZPRAWY DOKTORSKIEJ
WŁODZIMIERZA BURZYŃSKIEGO
“STUDIUM NAD HIPOTEZAMI WYTEŻENIA”
NAKŁADEM AKADEMII NAUK TECHNICZNYCH
LWÓW, 1928, 1–192

WŁODZIMIERZ BURZYŃSKI (1900–1970)

*Translated by Teresa Fraś and Anna Stręk,
scientific editor Ryszard B. Pęcherski*

NOTES FROM THE SCIENTIFIC EDITOR

It seems that the work of Włodzimierz Burzyński was the most extensive research in the field of failure criteria at that time. We are convinced that it would be very useful for the international scientific community to deliver its translation in the whole. We would like to realize this goal in the future. Adapting however to the recent editorial requirements, which delimit the volume of the published text, we have decided to select some passages, which, according to our opinion, contain the most original and less known or even unknown results. At the beginning, the table of contents is presented. The page numbers remain the same as in the original Lwów edition. The list of references given at the end is a collection of the bibliographic footnotes quoted in the original work. It is also worthwhile mentioning that the biographical note of W. Burzyński was published recently in English by Z.S. Olesiak, *Włodzimierz Stanisław Trzywdar Burzyński*, *Engng. Trans.*, 56, 4, 377–382, 2008.

| | |
|---|-----|
| Introduction | 3 |
| I. State of strain | 3 |
| II. State of stress | 15 |
| III. Dependence between the states of strain and stress. Elastic energy. New relations | 25 |
| IV. Material effort | 39 |
| V. Analytical and graphical methods of presentation of material effort. Classification of hypotheses | 48 |
| VI. The hypotheses of limit stresses | 58 |
| A1. The hypothesis of limit tensile stress | 58 |
| A2. The hypothesis of limit normal stress | 59 |
| A3. The hypothesis of constant limit shear | 62 |
| A4. The hypothesis of limit internal friction | 64 |
| A5. The hypothesis of variable limit shear | 68 |
| VII. The hypotheses of limit strains | 74 |
| B1. The hypothesis of limit elongation | 74 |
| B2. The hypothesis of limit longitudinal strain | 77 |
| B3. The hypothesis of limit strain and stress | 84 |
| B4. The hypothesis of limit shear strain | 87 |
| VIII. The hypotheses of limit energies. The author's hypothesis | 96 |
| C1. The hypothesis of constant limit energy of strain | 96 |
| C2. The hypothesis of constant limit energy of volume change and distortion | 100 |
| C3. The hypothesis of limit energy of distortion | 103 |
| C4. The hypothesis of variable limit energy of strain | 106 |
| C5. The hypothesis of variable limit energy of volume change and distortion | 111 |
| IX. Overview of experimental data | 136 |
| X. Discussion on the hypotheses of material effort | 166 |
| Final remarks | 185 |
| Abstract | 189 |

INTRODUCTION

(p. 3)

The main subject of the theory of elasticity is to mathematically determine the state of strain or stress in a solid body being under the conditions determined by the action of a system of external forces, the specific shape of the body and its elastic properties. The solution of this question exhausts the role of the elasticity theory and next the theory of strength of materials comes into play.

Its equally important task is to give the dimensions of the considered body with determined exactness, with respect to the states unwanted regarding the body safety on the one hand and the most advantageous economical conditions on the other hand. This problem, very simple in the case of a uniaxial state of stress, becomes so complicated in a general case that from the beginning of the mentioned theories, special attention had to be paid to this question and an intermediate chapter, being at the same time the final part of the theory of elasticity and the introduction to the strength of materials theory, has been introduced. This new passage deals with material effort and different hypotheses related to this notion. The study of these hypotheses is exactly the subject of the present work.

Material effort is of course closely related with the state of strain, or stress, of the considered body. It is then justified to introduce first the basic relations existing in the mentioned states.

[..., p. 25:] III. DEPENDENCE BETWEEN THE STATES OF STRAIN AND STRESS.
ELASTIC ENERGY. NEW RELATIONS.

[..., p. 27:] The sought function Φ (density of elastic strain energy function – ed. note) can be calculated from the formula:

$$(5) \quad 2\Phi = c_{11}\varepsilon_x^2 + 2c_{12}\varepsilon_x\varepsilon_y + 2c_{13}\varepsilon_x\varepsilon_z + 2c_{14}\varepsilon_x\gamma_x + 2c_{15}\varepsilon_x\gamma_y + 2c_{16}\varepsilon_x\gamma_z \\ + c_{22}\varepsilon_y^2 + 2c_{23}\varepsilon_y\varepsilon_z + 2c_{24}\varepsilon_y\gamma_x + 2c_{25}\varepsilon_y\gamma_y + 2c_{26}\varepsilon_y\gamma_z \\ + c_{33}\varepsilon_z^2 + 2c_{34}\varepsilon_z\gamma_x + 2c_{35}\varepsilon_z\gamma_y + 2c_{36}\varepsilon_z\gamma_z \\ + c_{44}\gamma_x^2 + 2c_{45}\gamma_x\gamma_y + 2c_{46}\gamma_x\gamma_z \\ + c_{55}\gamma_y^2 + 2c_{56}\gamma_y\gamma_z \\ + c_{66}\gamma_z^2$$

(the symbols c_{ik} denote elasticity coefficients and the symbols γ_α denote shear strain in the plane with the normal $\alpha = x, y, z$ – ed. note).

[..., p. 27: The above formula] regards solid bodies which are anisotropic in terms of elasticity. However, in case when certain special properties of the body, simplifying its structure, exist – as it happens e.g. in crystals – the elastic constants become related in a particular way and their number becomes lower¹²⁾.

For example, if there exist in the body three perpendicular planes of structural symmetry and the coordinate axes coincide with these three planes, the function simplifies to the following form with 9 elasticity coefficients:

$$(7) \quad 2\Phi = 2c_{11}\varepsilon_x^2 + 2c_{12}\varepsilon_x\varepsilon_y + 2c_{13}\varepsilon_x\varepsilon_z + c_{22}\varepsilon_y^2 + 2c_{23}\varepsilon_y\varepsilon_z \\ + c_{33}\varepsilon_z^2 + c_{44}\gamma_x^2 + c_{55}\gamma_y^2 + c_{66}\gamma_z^2.$$

The mentioned conditions occur with a very good approximation for a timber cube cut out in the particular way.

For materials in which the elastic properties in the three mentioned perpendicular directions are additionally identical, the function Φ simplifies further to the following form:

$$(8) \quad 2\Phi = c_{11} (\varepsilon_x^2 + \varepsilon_y^2 + \varepsilon_z^2) + 2c_{12} (\varepsilon_x\varepsilon_y + \varepsilon_x\varepsilon_z + \varepsilon_y\varepsilon_z) + c_{44} (\gamma_x^2 + \gamma_y^2 + \gamma_z^2).$$

Further reduction leads to two elastic constants; [...] this last case is possible for an isotropic body.

[..., p. 30:] As it is known, for components of the state of strain or stress it is allowed to apply arbitrary superposition of two (or more) subcomponents, according to the scheme:

$$\varepsilon = \varepsilon' + \varepsilon'', \quad \frac{1}{2}\gamma = \frac{1}{2}\gamma' + \frac{1}{2}\gamma''$$

or relatively:

$$\sigma = \sigma' + \sigma'', \quad \tau = \tau' + \tau''.$$

[...] Let us pose now the question whether it is possible to do such a decomposition for the function Φ in the sense of the equation $\Phi(\varepsilon, \gamma) = \Phi(\varepsilon', \gamma') + \Phi(\varepsilon'', \gamma'')$. In other words, whether it is possible to apply an arbitrary superposition for the function of elastic energy. The answer in a general case, that is for all $c_{ik} \neq 0$ and for arbitrarily taken ε and γ , must be negative, since Φ is a quadratic function. Nevertheless, such a decomposition may turn out to be possible for a particularly assumed decomposition of ε and γ and for a material with certain specific elastic constants c_{ik} . [...]

To all intents and purposes, there are no physical reasons for the strain energy not to be decomposable into a sum of two other energies, that is into: the energy of volume change and the energy of distortion. [...] This assumption is the essence of the whole reasoning – certainly not quite a theoretical one – and leads to five new relations of the following form:

$$(12) \quad \begin{cases} 3 \text{ relations: } \left\{ \begin{array}{l} c_{14} + c_{24} + c_{34} = 0 \\ c_{15} + c_{25} + c_{35} = 0 \\ c_{16} + c_{26} + c_{36} = 0 \end{array} \right. \\ \\ 2 \text{ relations: } \left\{ \begin{array}{l} c_{11} - c_{22} = c_{23} - c_{13} \\ c_{22} - c_{33} = c_{31} - c_{21} \\ c_{33} - c_{11} = c_{12} - c_{32} \end{array} \right. \end{cases}$$

The number of elastic coefficients would be limited in this case to the number of $21 - 5 = 16$. For a body characterized by the Eq. (7), the number of 9 coefficients would be reduced to 7; and for a model described by the Eq. (8), the number of elastic constants remains the same, i.e. 3.

[..., p. 31:] Let us consider what form takes the function Φ , expressed by the Eq. (5), assuming that the relations (12) are true and that the decomposition of the components [..., of the strain state into a deviatoric and a spherical part] holds. For this purpose, let us replace the coefficients c_{14} , c_{25} and c_{36} , appearing [in (5)] in the terms $2c_{14}\varepsilon_x\gamma_x$, $2c_{25}\varepsilon_y\gamma_y$ and $2c_{36}\varepsilon_z\gamma_z$, with three pairs of other coefficients, resulting from the first three relations [in (12)]. Then, the nine mixed terms with could be expressed in the form:

$$-(c_{24}\gamma_x - c_{15}\gamma_y)(\varepsilon_x - \varepsilon_y) - (c_{35}\gamma_y - c_{26}\gamma_z)(\varepsilon_y - \varepsilon_z) - (c_{16}\gamma_z - c_{34}\gamma_x)(\varepsilon_z - \varepsilon_x).$$

Next, let us change the position of the axes of the coordinate system to a certain characteristic orientation – let us call it the basic one [...] – namely, in such a way to have:

$$(13) \quad \begin{aligned} c_{24}\gamma_x - c_{15}\gamma_y &= 0, \\ c_{35}\gamma_y - c_{26}\gamma_z &= 0, \\ c_{16}\gamma_z - c_{34}\gamma_x &= 0. \end{aligned}$$

In such a case [...], the considered terms will disappear and – leaving the names of the coefficients in the new system unchanged without fear of confusion, or denoting additionally:

$$(14) \quad \begin{aligned} P &= c_{44} + 2c_{45}\frac{c_{24}}{c_{15}}, \\ Q &= c_{55} + 2c_{56}\frac{c_{35}}{c_{26}}, \\ R &= c_{66} + 2c_{64}\frac{c_{16}}{c_{34}} \end{aligned}$$

– the last six terms in (5) will transform into:

$$P\gamma_x^2 + Q\gamma_y^2 + R\gamma_z^2.$$

The constants P , Q , R can be called the reduced elastic moduli of distortion (shear), analogously to the shear modulus G , for the reasons which are to be revealed later. Each of the constants contains four elastic coefficients.

Continuing, it remains now to take care of the rest of the terms in Eq. (5), i.e. the six terms depending solely on the components and the six elastic constants, which also require certain transformation. A glance at the unused until now equations in (12) is sufficient to observe their particular property. By rearranging

them and adding the equations: $c_{12} = c_{21}$, $c_{23} = c_{32}$, $c_{13} = c_{31}$ to both sides, we obtain the system:

$$c_{11} + c_{12} + c_{13} = c_{21} + c_{22} + c_{23},$$

$$c_{21} + c_{22} + c_{23} = c_{31} + c_{32} + c_{33},$$

$$c_{31} + c_{32} + c_{33} = c_{11} + c_{12} + c_{13},$$

or in general:

$$(15) \quad c_{i1} + c_{i2} + c_{i3} = c_{1k} + c_{2k} + c_{3k} = 3B, \quad (i, k = 1, 2, 3).$$

From the last relation and the three initial relations it results that the sum of three normal stresses:

$$(16) \quad 3p = \sigma_x + \sigma_y + \sigma_z = \sigma_1 + \sigma_2 + \sigma_3 = 3B(\varepsilon_x + \varepsilon_y + \varepsilon_z) = 3Be$$

is noticeably dependent on the sum of three longitudinal strains along the axes x , y , z ; that is: on volume change and one coefficient of elasticity B . Then [the coefficient B] will be further called modulus of elastic volume change.

Lastly, let us substitute:

$$c_{11} = B + \frac{2}{3}(M + N), \quad c_{22} = \frac{2}{3}(N + L), \quad c_{33} = B + (L + M),$$

therefore:

$$c_{12} = B - \frac{2}{3}N, \quad c_{33} = B - \frac{2}{3}L, \quad c_{32} = B - \frac{2}{3}M$$

and let us insert these values into the six discussed terms of the function Φ (7). Then it will turn out that after the rearrangement, they will assume the following form:

$$B(\varepsilon_x + \varepsilon_y + \varepsilon_z)^2 + \frac{2}{3} [N(\varepsilon_x - \varepsilon_y)^2 + L(\varepsilon_y - \varepsilon_z)^2 + M(\varepsilon_z - \varepsilon_x)^2],$$

where the coefficients

$$(17) \quad L = \frac{2}{3}(B - c_{23}), \quad M = \frac{2}{3}(B - c_{31}), \quad N = \frac{2}{3}(B - c_{12}),$$

can be called the general elastic moduli of distortion.

Finally then, after dividing the Eq. (5) by 2, we obtain:

$$(18) \quad \Phi = \frac{1}{2}B(\varepsilon_x + \varepsilon_y + \varepsilon_z)^2 + \frac{1}{3} [N(\varepsilon_x - \varepsilon_y)^2 + L(\varepsilon_y - \varepsilon_z)^2 + M(\varepsilon_z - \varepsilon_x)^2] \\ + \frac{1}{2}(P\gamma_x^2 + Q\gamma_y^2 + R\gamma_z^2)$$

as a general normal form of elastic strain energy of an anisotropic solid, in the basic orientation determined by the Eqs. (13). The first part of the function denotes the energy of volume change Φ_v and the remaining one – the energy of distortion Φ_f . The total energy then reads:

$$(19) \quad \Phi = \Phi_v + \Phi_f.$$

[..., p. 33:] The use of principal components simplifies (18) to the following special form of strain energy:

$$(20) \quad \Phi = \frac{1}{2}B(\varepsilon_1 + \varepsilon_2 + \varepsilon_3)^2 + \frac{1}{3}[N(\varepsilon_1 - \varepsilon_2)^2 + L(\varepsilon_2 - \varepsilon_3)^2 + M(\varepsilon_3 - \varepsilon_1)^2].$$

[..., p. 34:] It is not difficult to observe that the whole foregoing reasoning can be easily reversed and applied to the states determined by stress components. The respective relations take the form:

$$(25) \quad \begin{aligned} C_{14} + C_{24} + C_{34} &= 0, \\ C_{15} + C_{25} + C_{35} &= 0, \\ C_{16} + C_{26} + C_{36} &= 0, \\ C_{11} - C_{22} &= C_{23} - C_{13}, \\ C_{22} - C_{33} &= C_{31} - C_{21}, \\ C_{33} - C_{11} &= C_{12} - C_{32}. \end{aligned}$$

The generalized elastic constants are expressed by the equations [...]:

$$(26) \quad \begin{aligned} 3B^* &= C_{i1} + C_{i2} + C_{i3} = C_{1k} + C_{2k} + C_{3k}, \\ L^* &= \frac{3}{2}(B^* - C_{23}), & 4P^* &= C_{44} + 2C_{45} \frac{C_{24}}{C_{15}}, \\ M^* &= \frac{3}{2}(B^* - C_{31}), & 4Q^* &= C_{55} + 2C_{56} \frac{C_{35}}{C_{26}}, \\ N^* &= \frac{3}{2}(B^* - C_{12}), & 4R^* &= C_{66} + 2C_{64} \frac{C_{16}}{C_{34}}, \end{aligned}$$

where the additional relation reads:

$$(27) \quad \begin{aligned} e = \varepsilon_x + \varepsilon_y + \varepsilon_z = e_1 + e_2 + e_3 &= 3B^*(\sigma_1 + \sigma_2 + \sigma_3) \\ &= 3B^*(\sigma_x + \sigma_y + \sigma_z) = 9B^*p. \end{aligned}$$

The formulae for elastic energy will take the [following] forms – a general one in the basic system:

$$(28) \quad \Phi = \frac{1}{2}B^*(\sigma_x + \sigma_y + \sigma_z)^2 + \frac{1}{3} [N^*(\sigma_x - \sigma_y)^2 + L^*(\sigma_y - \sigma_z)^2 + M^*(\sigma_z - \sigma_x)^2] \\ + 2(P^*\tau_x^2 + Q^*\tau_y^2 + R^*\tau_z^2)$$

(the symbols τ_α denote the shear stress in the lane with the normal $\alpha = x, y, z$ – ed. note) and a particular one in the principal system:

$$(29) \quad \Phi = \frac{1}{2}B^*(\sigma_1 + \sigma_2 + \sigma_3)^2 \\ + \frac{1}{3} [N^*(\sigma_1 - \sigma_2)^2 + L^*(\sigma_2 - \sigma_3)^2 + M^*(\sigma_3 - \sigma_1)^2].$$

[..., p. 38:] As the conclusion of this chapter there will be given a group of formulae [...], assuming certain special states. These include: the case of uniaxial tension or relative compression and the case of simple torsion [...]. The first one is characterized by the components:

$$\sigma_x = \sigma_0, \quad \sigma_y = \sigma_z = 0, \quad \tau_x = \tau_y = \tau_z = 0$$

and the second one by:

$$\sigma_x = \tau_0, \quad \sigma_y = 0, \quad \sigma_z = -\tau_0, \quad \tau_x = \tau_y = \tau_z = 0,$$

or

$$\sigma_x = \sigma_y = \sigma_z = 0, \quad \tau_x = 0, \quad \tau_y = \tau_0, \quad \tau_z = 0.$$

From the respective relations of the present chapter we obtain for the first case:

$$(49) \quad \Phi_f = \frac{1}{6G}\sigma_0^2, \quad \Phi = \frac{1}{2E}\sigma_0^2, \quad \varepsilon_0 = \frac{1}{E}\sigma_0$$

and similarly for the second case:

$$(50) \quad \Phi_f = \frac{1}{2G}\tau_0^2, \quad \Phi = \frac{1}{2G}\tau_0^2, \quad \gamma_0 = \frac{1}{G}\tau_0.$$

[..., p. 39:] IV. MATERIAL EFFORT

[..., p. 40:] Generally, under the notion *material effort* we understand a physical state of a body, comprehended in the sense of elasticity or plasticity or material strength, generated by a system of stresses, and related with them strains, in the body. This brief qualitative definition will become – I suppose –

completely clear after looking through the discussion in this and next chapters. [...] Generally then, the new notion *material effort* depends on the manner in which external forces act, on the body shape and on individual properties of the body. These notions deserve a few words of explanation.

Under the manner in which external forces act, one should understand not only the distribution of loading but also its variability in time. The recent state of the strength theories does not allow to consider this important factor in calculations, except for a few particular cases.

The body shape is one of the reasons for the dependence of the stress state components on the position of the considered point in the body. It is clear that the uniformity or non-uniformity of the state of stress strongly influences the quality of the physical state of the whole body¹⁵). One has the impression that authors of various hypotheses overlooked this fact; however, the ways of conducting experiments contradict that. Furthermore, it is not known whether the local grouping of stress components leading to the limiting numerical value of material effort accounts for unwanted changes exclusively in this particular point of the body, or influences the physical behaviour of the whole body in general. Similarly, it is unknown whether the experimental observation of the existence of certain planes of unwanted states (planes of shear, *etc.*) is a proof that the corresponding to this planes components [of the state of stress] are the reasons for creation of internal disorders.

These remarks fall out if a uniform state of stress is ascertained in the whole body. For this reason, the results obtained in following chapters should be limited to the case of a *uniform* state of stress or, otherwise, they should be limited exclusively to a point.

[..., p. 41:] Regarding the structure, two kinds of solid bodies are distinguished: crystalline and amorphous ones, depending whether the particles of the body are distributed in space regularly or irregularly. The majority of technical materials (metals) are continuous macroscopic conglomerates of both types of structure. For this reason such bodies behave as isotropic ones, since the anisotropy of particular crystals cannot be shown individually at the macroscopic level. Such bodies are called quasi-isotropic. However, secondary circumstances can trigger, even in such a conglomerate, some remarkable differences in the material behaviour along certain directions – e.g. the influence of rolling [...] *etc.* and the respective differences should be accounted for. There are no such attempts in a general sense; the hypotheses discussed in following chapters assume isotropy of materials without any explanation.

Elastic properties of a body are determined by the so-called elastic moduli or elastic constants, which were discussed in the previous chapter. For a large group of materials these coefficients are constant, so they ascertain that the generalized Hooke's law remains valid. A series of recent precise experi-

ments show irrefutably that the range of solids undergoing the Hooke's law is pretty large (e.g. concrete)¹⁶⁾. The limit of validity of Hooke's law is called *the limit of proportionality*. If additionally, the strains induced within such limits are ideally – at least in the technical meaning – elastic, we obtain a model of a body, to which all equations from the foregoing chapter are applicable. However, these equations are valid only up to the elasticity limit. By the existence of both limits, they ascertain, in general, proximity of these limits. Therefore, confusing both the terms in the vast technical literature does not implicate too serious mistakes. *The proportionality limit* plays the role of a mathematical condition rather than a physical one – whereas it is opposite for *the limit of elasticity*.

Bodies which do not have the limit of proportionality show more or less distinct limits of elasticity; thus the relations of the foregoing chapter have the character of the first approximation only.

[..., p. 42:] Beyond the elastic range, the elasticity coefficients should be considered to be variable or generally, they should not be used in the meaning they were referred to until now. Instead, they should be replaced by certain constants specific not only for the body but also for the considered stress process itself.

To such ranges belongs, first of all, the range of plastic strains, which begins from the so-called *limit of plasticity* [...].

[..., p. 43:] A few words should be said also about the third process connected with a particular body. To the phenomena accompanying permanent strains is related the third stage – belonging, undisputably, to the strength of materials theory – that is the range of material cracking, ending with *the limit of strength* (in a technical sense). Conditions of failure are usually very complicated and, up till now, also not too much theoretically explained²⁰⁾. Uniformity or rather, on the opposite, non-uniformity of the state of stress, which is – as a matter of fact – difficult to be analysed in connection with the shape of a body, plays a considerable role in this region. Disregarding the surface energy^{15,21)} can be a reason of serious errors, even in preliminary calculations. Apart from that, it is not known whether the specific for given materials constants reflect satisfactorily the essence of the phenomenon of failure, as it is assumed by some authors. Qualitative diversity in different strength processes persuaded researchers [...] to divide failure surfaces into two categories, i.e. *the surfaces of shear and tear*²²⁾.

Under the stress properties we understand the behaviour of a body in certain special states; these properties reveal themselves as numerical values of stress in the above-described limit ranges. We know a whole series of such states and, because of obvious benefits and applications in the following chapters, let us set them schematically by means of normal principal stresses, under the assumption $\sigma_1 > \sigma_2 > \sigma_3$, as follows:

- I. Uniaxial tension: $\sigma_1 = k_r, \sigma_2 = 0, \sigma_3 = 0$;
- II. Uniaxial compression: $\sigma_1 = 0, \sigma_2 = 0, \sigma_3 = -k_c$;
- III. Simple torsion (shear): $\sigma_1 = k_s, \sigma_2 = 0, \sigma_3 = -k_s$.

Only few metals are characterized by the equality $k_r = k_c = k$; in principle, these constants are different, namely $k_c > k_r$. The discussed states are accounted as the simplest – the fundamental ones – for the study of material effort.

[..., p. 44:] To the similar, simplest states of stress should be added also the following ones, though more complex indeed, yet in the present state of our knowledge on material effort they can not be omitted. These are in sequence:

- IV. Biaxial uniform tension: $\sigma_1 = k_{rr}, \sigma_2 = k_{rr}, \sigma_3 = 0$;
- V. Biaxial uniform compression: $\sigma_1 = 0, \sigma_2 = -k_{cc}, \sigma_3 = -k_{cc}$;
- VI. Triaxial uniform tension: $\sigma_1 = k_{rrr}, \sigma_2 = k_{rrr}, \sigma_3 = k_{rrr}$;
- VII. Triaxial uniform compression: $\sigma_1 = -k_{ccc}, \sigma_2 = -k_{ccc}, \sigma_3 = -k_{ccc}$.

Any other experimental states can be of course put between the ones given above. The aforementioned values k refer to the states lying on the elasticity limit (or proportionality limit), the limit of plasticity and the strength limit. [...]

[..., p. 48:] V. ANALYTICAL AND GRAPHICAL METHODS OF PRESENTATION OF MATERIAL EFFORT. CLASSIFICATION OF HYPOTHESES.

[..., p. 51:] In the present work, the following classification is assumed as the best illustration of the contents of the [material effort] hypotheses²⁹⁾ and at the same time, as it partly corresponds to chronological relations of these theories.

- A. *The hypotheses of limit stresses.*
- B. *The hypotheses of limit strains.*
- C. *The hypotheses of limit energies. [...]*

[..., p. 96:] VIII. THE HYPOTHESES OF LIMIT ENERGIES.
THE AUTHOR'S HYPOTHESIS.

C1. THE HYPOTHESIS OF CONSTANT LIMIT ENERGY OF STRAIN

The mentioned in the title hypothesis is known since the times of BELTRAMI⁵⁴⁾, who for the first time suggested the use of strain energy for calculation of material effort. Independently of BELTRAMI⁵⁴⁾, HUBER⁵⁶⁾ stated an identical theory; already then, however, emphasizing certain additional thought resulting in the change of the contents of (C1) into (C2), which will be discussed in the

next paragraph. Finally, in recent time HAIGH³²⁾, an Englishman, repeated the suggestion of Beltrami, not having known – like Huber – Beltrami’s publication.

[..., p. 97: Formula of the hypothesis reads:]

$$(C1_0) \quad \boxed{\sigma_x^2 + \sigma_y^2 + \sigma_z^2 - 2\mu(\sigma_x\sigma_y + \sigma_y\sigma_z + \sigma_z\sigma_x) + 2(1+\mu)(\tau_x^2 + \tau_y^2 + \tau_z^2) = k^2},$$

where: $k = k_c = k_r$.

With the use of the principal components [of stress], the hypothesis takes a shorter form [...]:

$$(C1) \quad \boxed{\sigma_1^2 + \sigma_2^2 + \sigma_3^2 - 2\mu(\sigma_1\sigma_2 + \sigma_2\sigma_3 + \sigma_3\sigma_1) = k^2}.$$

[..., p. 99:] The above equation represents a rotationally symmetric ellipsoid of the axis oriented at equal angles to the axes of the system $\sigma_1, \sigma_2, \sigma_3$, with lengths of the half-axes:

$$b_1 = b_3 = \frac{k}{\sqrt{1+\mu}},$$

$$b_2 = \frac{k}{\sqrt{1-2\mu}}.$$

[..., p. 100:] C2. THE HYPOTHESIS OF CONSTANT LIMIT ENERGY
OF VOLUME CHANGE AND DISTORTION

As it was mentioned before, independently of Beltrami, Huber brought forward a similar proposition. He used his hypothesis for limit states of strength supposing however, that the theory would be valid also for elastic ranges. Basing on certain facts related experimentally to exceeding the strength limit, he observed that in the case of the states with three negative normal components [of stress], one should consider rather the energy of distortion Φ_f than the total Φ as a measure of material effort.

About his final, mathematically precisely stated position [on this matter] we learn from the letter to FÖPPL⁸⁾ and the following statement contained there: “Material effort is measured by the sum of these parts of density of strain energy, which result from the distortion and increase of volume”. The measure of material effort is then $\Phi = \Phi_v + \Phi_f$ if the above assumption is fulfilled, i.e. when $e > 0$ or $\sigma_x + \sigma_y + \sigma_z > 0$; in the opposite case, i.e. when $e < 0$ or $\sigma_x + \sigma_y + \sigma_z < 0$, the assessment of material effort is given by Φ_f exclusively. In this way, a discontinuous hypothesis is created; the states I, IV, and VI belong to the first group of phenomena, while the states II, V and VII belong to the latter one; the state III is proved in both ranges.

This last state fits best to express the Huber hypothesis; comparing then respectively the complete or partial formula (37) with the pertinent ones (49) and (50), from the Chapter III we obtain:

$$\frac{1}{2(1+\mu)}(\sigma_x^2 + \sigma_y^2 + \sigma_z^2) - \frac{\mu}{1+\mu}(\sigma_x\sigma_y + \sigma_y\sigma_z + \sigma_z\sigma_x) + (\tau_x^2 + \tau_y^2 + \tau_z^2) = k_s^2$$

(C2₀) for: $\sigma_x + \sigma_y + \sigma_z \geq 0$, furthermore:

$$\frac{1}{3}(\sigma_x^2 + \sigma_y^2 + \sigma_z^2 - \sigma_x\sigma_y - \sigma_y\sigma_z - \sigma_z\sigma_x) + (\tau_x^2 + \tau_y^2 + \tau_z^2) = k_s^2$$

for: $\sigma_x + \sigma_y + \sigma_z \leq 0$,

as a mathematical formula of Huber's hypothesis in a general case. The particular form [for principal stress components] reads of course:

$$\frac{1}{2(1+\mu)}(\sigma_1^2 + \sigma_2^2 + \sigma_3^2) - \frac{\mu}{1+\mu}(\sigma_1\sigma_2 + \sigma_2\sigma_3 + \sigma_3\sigma_1) = k_s^2$$

for: $\sigma_1 + \sigma_2 + \sigma_3 \geq 0$, and

(C2)

$$\frac{1}{3}(\sigma_1^2 + \sigma_2^2 + \sigma_3^2 - \sigma_1\sigma_2 - \sigma_2\sigma_3 - \sigma_3\sigma_1) = k_s^2,$$

for: $\sigma_1 + \sigma_2 + \sigma_3 \leq 0$.

[..., p. 103:] C3. THE HYPOTHESIS OF LIMIT ENERGY OF DISTORTION

The decomposition of elastic energy into two characteristic parts, applied for the first time for the assessment of material effort by Huber, has earned in the process of time a well-deserved experimental and theoretical confirmation and created the foundation of unusually fine and mathematically simple hypothesis (C3).

According to this new theory, the measure of material effort is exclusively the energy of distortion Φ_f . The hypothesis was for the first time proposed, it seems, by MISES⁵⁹). Having drawn the attention to the fact that the spatial picture of the hypothesis (A3) [related with the criterion of Tresca] in the orthogonal system of axes [of the principal shear stresses] $\tau_I, \tau_{II}, \tau_{III}$ shows a cube of the edge k , Mises expressed a conviction, that this rather should be the sphere:

$$\tau_I^2 + \tau_{II}^2 + \tau_{III}^2 = \frac{k^2}{2}.$$

The second author who raised the mathematical formula (C3) to the rank of the fundamental equation of the theory of plasticity was HENCKY^{19),60)}.

[..., p. 104:] The mathematical form of the hypothesis (C3) [...] in a general case reads:

$$\sigma_x^2 + \sigma_y^2 + \sigma_z^2 - \sigma_x\sigma_y - \sigma_y\sigma_z - \sigma_z\sigma_x + 3(\tau_x^2 + \tau_y^2 + \tau_z^2) = k^2$$

or in particular [for principal stresses]:

$$\sigma_1^2 + \sigma_2^2 + \sigma_3^2 - \sigma_1\sigma_2 - \sigma_2\sigma_3 - \sigma_3\sigma_1 = k^2.$$

[..., p. 106:] C4. THE HYPOTHESIS OF VARIABLE LIMIT ENERGY OF STRAIN

In such a way one could name the hypothesis which was – as it appears – presented during one of Mises's lectures in 1925 and published by SCHLEICHER⁵⁰⁾ in 1925/1926.

According to Schleicher's theory, the "equivalent" stress, expressed by the left-hand side of (C1) – let us denote it shortly: $\sigma_{vf} = \sqrt{2E\bar{\Phi}}$ – is in the limit state a variable value depending on the state of stress, that is on:

$$p = \frac{\sigma_x + \sigma_y + \sigma_z}{3} = \frac{\sigma_1 + \sigma_2 + \sigma_3}{3}.$$

In other words, [the equation] $\sigma_{vf} = f(p)$ is a mathematical form of the hypothesis of variable limit energy.

Schleicher relates his theory to elastic and plastic states and recommends to seek for the shape of the function f experimentally, similarly as it was advised by Mohr in the case of the shape of envelope.

[..., p. 107] It is possible to approximate the experimental curve, according to Schleicher, by means of

$$(C4^*) \quad \text{a parabola} \quad \sigma_{vf}^2 = s^2 - 3mp,$$

$$(C4^{**}) \quad \text{or a line} \quad \sigma_{vf} = t - 3mp.$$

In the first case it is: $s^2 = k_c k_r$, $m = k_c - k_r$, and in the second one:

$$t = \frac{2k_c k_r}{k_c + k_r}$$

and the already known

$$n = \frac{k_c - k_r}{k_c + k_r};$$

in other words, the hypothesis is dependent on two parameters k_c and k_r . [...]

Expressing p and σ_{vf} by means of the components of stress, we get (from (C4*) and (C4**)) the following relations:

$$(C4') \quad \sigma_x^2 + \sigma_y^2 + \sigma_z^2 - 2\mu(\sigma_x\sigma_y + \sigma_z\sigma_y + \sigma_x\sigma_z) + 2(1 + \mu)(\tau_x^2 + \tau_y^2 + \tau_z^2) \\ + (k_c - k_r)(\sigma_x + \sigma_y + \sigma_z) = k_c k_r$$

and

$$(C4'') \quad \sigma_x^2 + \sigma_y^2 + \sigma_z^2 - 2\mu''(\sigma_x\sigma_y + \sigma_z\sigma_y + \sigma_x\sigma_z) + 2(1 + \mu'')(\tau_x^2 + \tau_y^2 + \tau_z^2) \\ + (k_c - k_r)(\sigma_x + \sigma_y + \sigma_z) = k_c k_r,$$

or with use of principal stresses:

$$(C4_1) \quad \sigma_1^2 + \sigma_2^2 + \sigma_3^2 - 2\mu(\sigma_1\sigma_2 + \sigma_2\sigma_3 + \sigma_1\sigma_3) \\ + (k_c - k_r)(\sigma_1 + \sigma_2 + \sigma_3) = k_c k_r$$

as well as:

$$(C4_2) \quad \sigma_1^2 + \sigma_2^2 + \sigma_3^2 - 2\mu''(\sigma_1\sigma_2 + \sigma_2\sigma_3 + \sigma_1\sigma_3) \\ + (k_c - k_r)(\sigma_1 + \sigma_2 + \sigma_3) = k_c k_r,$$

whereas:

$$\mu'' = \frac{\mu + n^2}{1 - n^2} = \frac{\mu(k_c + k_r)^2 + (k_c - k_r)^2}{4k_c k_r}.$$

For $k_c = k_r$, the Schleicher hypothesis expressed either by (C4') and (C4'') or by (C4₁) and (C4₂), transforms in the hypothesis of Beltrami.

[..., p. 111:] C5. THE HYPOTHESIS OF VARIABLE LIMIT ENERGY
OF VOLUME CHANGE AND DISTORTION

The review of enormous theoretical material, which was presented in the previous chapters, together with an equally extensive set of experiments, allows judging discerningly the merits and drawbacks of the discussed hypotheses. This assessment leads to the rejection of the theories A and B and compels to accept the theories C, which are more consistent mathematically and therefore more flexible for experiments.

Individual properties of the studied bodies suggest that basing the theories on one or two experimental data does not in general render faithfully the phenomenon of material effort and demands to introduce more parameters into account, as it was suggested by Schleicher. Controlling the phenomena by the modulus of elasticity causes many problems and the only rarely returns reliable services.

For this reason I have tried to state a hypothesis as general as (C4) which would be, however, free of these additions which seemed for me inadequate in the study of material effort. The starting point is the attitude similar to what Huber stated in (C2); however, much more general and continuous. It is the following conviction: *The measure of local material effort in elastic and plastic ranges is the sum of density of quasi-energy of distortion and a certain part – dependent on the state of stress and individual properties of a body – of the density of the pseudo-energy of volume change.*

By adding “quasi” – or “pseudo” – we try to emphasize that the analytic expressions used in continuation, quoted in the third chapter, do not mean – for a certain group of bodies or relatively in certain experimental fields – elastic energy in the sense discussed in this chapter.

The mathematical formula for the hypothesis is the equation:

$$\Phi_f + \eta\Phi_v = K.$$

Expansions of the functions Φ_f and Φ_v are very well known to us. Determination of constant K does not present difficulties; it is the value of the left-hand side of the equation, determined for one of the basic states, the simplest ones, that is: I, II or III. The remaining to be discussed η is – as it results from the assumption – a function of individual material properties as parameters and of the state of stress as an independent variable. The individual properties should be expressed also by the moduli of the simplest states. To the latter one should apply several magnitudes created from the components of state of stress; because of the proved minor significance of the component τ , one should express the independent variable of the function η by the component σ . From possible expressions, due to the mathematical character of the energies Φ_f and Φ_v , there suggests itself the invariant which does not privilege any of the three components, namely

$$p = \frac{\sigma_x + \sigma_y + \sigma_z}{3} = \frac{\sigma_1 + \sigma_2 + \sigma_3}{3}.$$

In general then, we assume that: $\eta \equiv \eta(p)$. Considering series of correct experiments seems to suggest generally that the influence of Φ_v decreases with the algebraic increase of the mean stress p ; this leads to a very well applicable function:

$$\eta = \omega + \frac{\delta}{3p}.$$

The written [above] type [of function] does not always stand in ideal agreement with experimental facts, but increasing of the number of the introduced parameters K , ω , δ leads to a very complicated hypothesis, so this was abandoned and the sometimes unavoidable shortcomings [of the expression] were compensated in continuation in a more – as it will appear – appropriate manner.

On this occasion, it should be remarked that the role of experiment is not to determine directly the constants K , ω , δ , as it would seem at the first moment, but three other data which will be discussed now.

Anticipating what will follow, let us put here:

$$\frac{1-2\mu}{1+\mu} \omega = \frac{1-2\nu}{1+\nu}, \quad 12GK = \frac{2k_c k_r}{1+\nu}, \quad \frac{1-2\mu}{1+\mu} \delta = \frac{2(k_c - k_r)}{1+\nu}.$$

Moreover, let us substitute for shortening: $12G\Phi_f = \sigma_f^2$. And [now] let us insert the complete set of the mentioned transformations into the main equation. After a simple transformation we obtain:

$$\frac{1+\nu}{3} \sigma_f^2 + 3(1-2\nu)p^2 + 3(k_c - k_r)p - k_c k_r = 0.$$

The introduction of the parameters k_r and k_c into the last equation is justified, since it is easy to demonstrate that it is identically fulfilled for the states I and II. By assuming, additionally, the state III, we obtain the relation:

$$\nu = \frac{k_c k_r}{2k_s^2} - 1.$$

From the last reasoning it follows that the hypothesis (C5) is a theory based on the three constants: k_r , k_c , k_s or relatively: k_r , k_c , ν . Let us hold the last group for later consideration because of vital mathematical benefits which will appear in the course of time. The coefficient ν – as it will also appear – very strongly determines individual properties of an examined body in the range of its brittle or – opposite – plastic behaviour. It could be advantageous to call it the “*plasticity coefficient*”, because it turns out that for tough and brittle materials there is: $\nu < \frac{1}{2}$, for tough and plastic materials there is: $\nu = \frac{1}{2}$, and for soft (plastic) bodies: $\nu > \frac{1}{2}$. There is no way to the state the limits within which ν ranges; the possible excess over $\frac{1}{2}$ grows not so high, the matter of decreasing the value presents itself similarly. There arises a supposition that the interval where ν ranges fits between 0 and 1. With the course of the discussion it will turn out that in the main we need to do this kind of assumption out of necessity. After the above remarks, there arises the question whether the coefficient ν , or another approximate one, could be – by instance – used for determining the extent of [a magnitude] quite close to plasticity, i.e. hardness, with mathematical description of which theoretical researchers have been bothering for so many years.

Returning, however, to the recently written equation, let us transform it into the following formula:

$$(C5') \quad \frac{1 + \nu}{3} \sigma_f^2 + 3(1 - 2\nu)(p + \sigma')^2 = k'^2$$

where:

$$\sigma' = \frac{k_c - k_r}{2(1 - 2\nu)},$$

$$k'^2 = k_c k_r + \frac{3}{4} \frac{(k_c - k_r)^2}{1 - 2\nu} = \frac{3k_s^2(k_c + k_r)^2 - 4k_c^2 k_r^2}{4(3k_s^2 - k_c k_r)} = -k_1^2.$$

In the system of axes (p, σ_f) , the equation $(C5')$ represents – similarly to the system of the axes (p, σ_{vf}) by Schleicher – curves of the second degree, the type of which should be now considered.

Of course there occur to mind the [three] cases: $\nu > \frac{1}{2}$; $\nu = \frac{1}{2}$; $\nu < \frac{1}{2}$. Due to the dependent on that algebraic value of k'^2 or k_1^2 , one detail should be emphasized here. Namely, from some later discussion it will follow that within the sphere of experimental facts there should be: $k_s \geq \frac{2}{\sqrt{3}} \frac{k_c k_r}{k_c + k_r}$. The lower limit of this inequality seems to be quite convincing, since it is enough to assume: $k_c = k_r = k$ to obtain: $k_s = \frac{k}{\sqrt{3}}$, that is the relation well known to us from $(C3)$ and currently strongly emphasized in a series of publications. While for: $k_r \neq k_c$ $\left[\varkappa = \frac{k_c}{k_r} \neq 1 \right]$ this inequality would indicate that for technically possible materials in the group of $\nu > \frac{1}{2}$, there has to be $\nu < 3.5$ ($\varkappa \cong 8$). However, one can be assured that ν will not reach such a value, because: as k_c increases in comparison to k_r , at the same time k_s begins to significantly more strongly exceed the given [above] limit $\frac{2}{\sqrt{3}} \frac{k_c k_r}{k_c + k_r}$, which results in the fact that ν considerably lowers its limiting value. In any case, a bound on k_s is followed by a bound on ν ; in the especially important case $k_r = k_c$, that is: $\varkappa = 1$, we obtain – as it was mentioned – $k_s \geq \frac{k}{\sqrt{3}}$ and consequently: $\nu \leq \frac{1}{2}$. After such bounds on the magnitude k_s , we can start the promised discussion.

And so, in the case when $\nu < \frac{1}{2}$, which means $k_s > \sqrt{\frac{k_c k_r}{3}}$, there is: $1 - 2\nu > 0$ and moreover $k'^2 > 0$, and the equation $(C5')$ represents in the mentioned system [of coordinate axes] an ellipse, or relatively a circle, whose centres lie on the negative direction of p (Fig. 64) – or in the special case: $k_r = k_c$ i.e. $\varkappa = 1$ – they coincide with the origin of the coordinate system (Fig. 65).

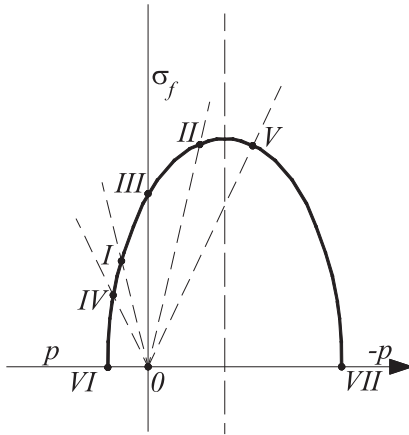


Fig. 64.

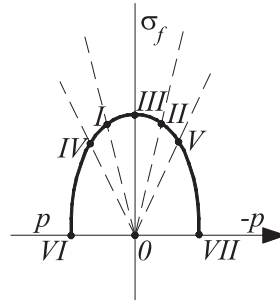


Fig. 65.

In the case of $\nu = \frac{1}{2}$, the equation (C5') turns into a parabola of the second degree for $\chi > 1$ (Fig. 66), or into two lines parallel to the axis p for $\chi = 1$ (Fig. 67).

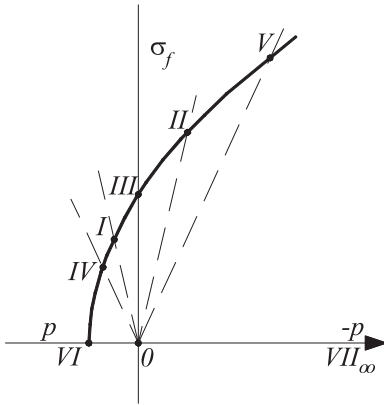


Fig. 66.

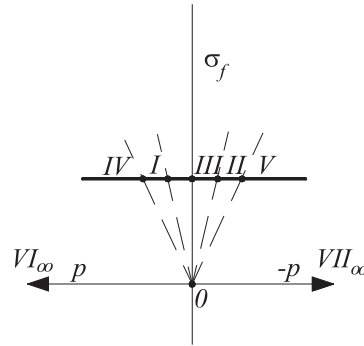


Fig. 67.

In the case of $\nu > \frac{1}{2}$, that is $\frac{2}{\sqrt{3}} \frac{k_c k_r}{k_c + k_r} < k_s < \sqrt{\frac{k_c k_r}{3}}$, there is [both] $1 - 2\nu > 0$ as well as $k_1'^2 > 0$ (which means also that $k_1^2 > 0$) and the equation (C5') represents a hyperbola, whose one branch only, of course, comes into play (Fig. 68). In the case when: $k_s = \frac{2}{\sqrt{3}} \frac{k_c k_r}{k_c + k_r}$ the hyperbola degenerates into two crossing lines [only one of lines is depicted due to the symmetry] (Fig. 69). Because of the already mentioned bound on the lower limit of k_s , the case of a hyperbola rotated by the angle $\frac{\pi}{2}$ from the formerly discussed position is excluded.

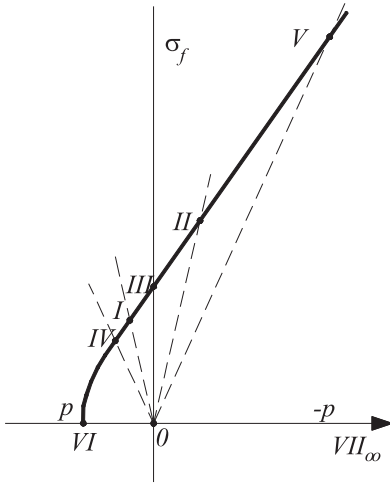


Fig. 68.

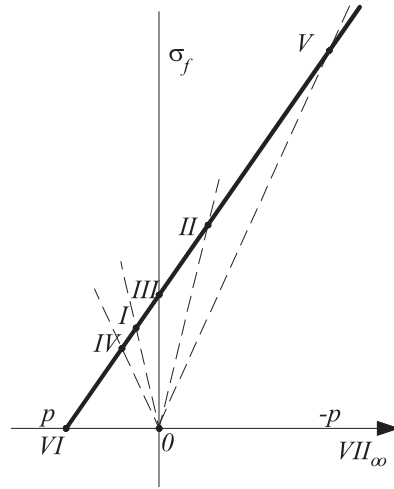


Fig. 69.

In the enclosed schemes are shown only halves of the considered curves relevant for $\sigma_f > 0$. Besides, there are added lines for the states I and II, III, IV and V, VI, and VII, similarly as it was performed in the discussed Schleicher's theory. The equations for these lines read: $\sigma_f = \pm 3\sqrt{2}p$, $p = 0$, $\sigma_f = \pm \frac{3}{2}\sqrt{2}p$ and finally, for the last two ones: $\sigma_f = 0$. Positions of intersections of those lines with the referred curves characterize very well the category of the investigated material.

The given discussion, together with the set graphs allows – under the assumption of the truthfulness of the theory (C5) – judging certain phenomena, and especially it graphically explains changes of the limit value of quasi-energy of distortion in the critical range. Uniformity of this study demands, however, to expand the formula (C5') into the types used in the present work. With this aim let us expand σ_f according to (C3₀), with p – as above; then we obtain directly:

$$(C5_0) \quad \boxed{\sigma_x^2 + \sigma_y^2 + \sigma_z^2 - 2\nu(\sigma_x\sigma_y + \sigma_y\sigma_z + \sigma_z\sigma_x) + 2(1 + \nu)(\tau_x^2 + \tau_y^2 + \tau_z^2) + (k_c - k_r)(\sigma_x + \sigma_y + \sigma_z) = k_c k_r}$$

or in a simpler form:

$$(C5) \quad \boxed{\sigma_1^2 + \sigma_2^2 + \sigma_3^2 - 2\nu(\sigma_1\sigma_2 + \sigma_2\sigma_3 + \sigma_3\sigma_1) + (k_c - k_r)(\sigma_1 + \sigma_2 + \sigma_3) = k_c k_r.}$$

At first sight, the new hypothesis – apart from the change of the notation μ or μ'' into ν – does not differ from Schleicher's theory and therefore from the equations (C4') and (C4'') or relatively (C4₁) and (C4₂); however, exactly this

subtle difference in notation constitutes the fundamental superiority of (C5) over (C4). Since while μ or μ'' are elastic constants in direct or relatively – let us say – reduced meaning, ν does not have – with advantage to the hypothesis – this property at all.

It could seem that the discussed superiority is ostensible as Schleicher's theory employs only two constants in the quoted equations and the hypothesis (C5) uses three of them. However, it should be reminded that Schleicher doubts the possibility of sufficient representation of the material effort phenomenon by two parameters and, as I mentioned, by examining some experiments, he assumed four of those parameters using independently both equations quoted in the section (C5) for one research series. Finally, regardless of the number of these coefficients, the hypothesis (C4) cannot free itself from the disturbing influence of the constant μ , the lack of which is particularly advantageous in (C5).

That there is some distinguishing generality in employing [the plasticity coefficient] ν into the range of the theory (C5), can be proved by the following facts. For $\nu < \frac{1}{2}$ the hypothesis can transform in a special case into Schleicher's theory; namely, if there is: $\nu = \mu$ or $\nu = \mu''$. Similarly for $\nu = \mu$ and $\varkappa = 1$, the theory (C5) transforms directly into Beltrami's hypothesis (C1), or partly into Huber's theory (C2). In the case of $\nu = \frac{1}{2}$ we create a new eventuality: namely for $\varkappa = 1$ the theory (C5) becomes identical to (C3). For $\nu > \frac{1}{2}$ and in both previous cases, the hypothesis contains a whole series of eventualities, which are not considered in other theories.

[. . . , p. 127:] There arises the question if and how the current formula takes into account the influences of – often inevitable – anisotropy of material. Comparison of the expressions for Φ_v and Φ_f for isotropic and anisotropic bodies in the Eqs. (28) and (31), or relatively (29) and (32), in the Chapter III indicates a distinct difference only in the expressions for Φ_f . Therefore one should suppose that also in the discussed hypothesis, this elusive anisotropy must become visible through an analogous change.

The use of the word “elusive” is deeply grounded. Indisputably, creation of hypotheses of material effort for anisotropic bodies is the distant future. Although, even today it can be supposed that the measure of material effort of some bodies, indicating certain simplified properties in three directions, can be pretty well [expressed by] the energy Φ_f – as it was ascertained in the theory (C3) regarding certain isotropic materials. However, the currently discussed task consists in catching the influences of slight anisotropy, [being] difficult to state in terms of quantity but to some extent visible in terms of quality.

For this purpose, the best suitable will be certainly the general [form of the] function Φ_f (Chapter III). However, [it should be] appropriately simplified,

since introducing it in the complete form with six elasticity constants would give as a result a hypothesis with eight constants. So, in the first place, not being interested in introducing approximate relations between groups L^* , M^* , N^* and P^* , Q^* , R^* at the cost of losing the energy-based character of the functions, let us rather at the start give up on expressing the theory in the basic system – as it was called in the Chapter III – and let us refer it from now on to the system of principal directions. In this manner we obtain a hypothesis of five constants instead of three, as it was until now.

However, even this number could turn out to be too large for the approximate assessment of the symptoms of anisotropy and – even though such a kind of increase would introduce into the account two new mutually supplementing parameters k_{rr} and k_{cc} – one should rather give up on this symmetry and try to continue the reduction of the number of constants down to four. Successful solution of this question presents itself obvious after the provided till now direct reasoning. Let us assume, beforehand, that the general type of the equation linking the variables p and σ_f – presented in the beginning of this section – will not receive any external change after the present remarks.

This equation is obtained analogically as previously. Namely, let us substitute into the main equation: $\Phi_f + \eta\Phi_v = K$ the complete expressions for Φ_f , Φ_v from the formula (29) in the Sec. III. Let us multiply both sides of the equation by $\frac{3M^*}{L^*N^*}$ and put for reduction the replacements:

$$\frac{1 - 2\nu^*}{1 + \nu^*} = \frac{3B^*M^*}{2L^*N^*}\omega, \quad \frac{3(k_c - k_r)}{1 + \nu^*} = \frac{3B^*M^*}{2L^*N^*}\delta, \quad \frac{3k_c k_r}{1 + \nu^*} = \frac{3KM^*}{L^*N^*}$$

and furthermore:

$$\frac{M^{*2}}{L^*N^*} = 2\lambda.$$

By multiplying both sides of the equation transformed in such a way by $\frac{1 + \nu^*}{3}$, we will obtain:

$$\frac{1 + \nu^*}{3}\sigma_f^{*2} + 3(1 - 2\nu^*)p^2 + 3(k_c - k_r)p - k_c k_r = 0,$$

where:

$$\sigma_f^{*2} = \frac{M^*}{N^*}(\sigma_2 - \sigma_3)^2 + 2\lambda(\sigma_3 - \sigma_1)^2 + \frac{M^*}{N^*}(\sigma_1 - \sigma_2)^2 \quad \text{and} \quad p = \frac{\sigma_1 + \sigma_2 + \sigma_3}{3}$$

are variables of the function written above. Instead of the variable p it would be more rational to use in this case a slightly different one, namely:

$$p^* = \frac{\lambda\sigma_1 + (1 - \lambda)\sigma_2 + \lambda\sigma_3}{1 + \lambda}.$$

The reasons for such a remark, significantly changing the energy-based sense of the hypothesis, will appear in the Chapter X.

The obtained equation ostensibly does not differ in its structure from the previous one. [Nevertheless,] the essential difference lies, first of all, in the plasticity coefficient ν^* , whose numerical value can be now quite seriously modified by the anisotropy. Besides, the difference can possibly be in p^* but mainly in σ_f^{*2} , which is currently remarkably different from σ_f^2 involving – at least for this moment – three parameters. These last ones – needless to say – are not treated as representations of the ratio of elasticity constants but as coefficients particularly connected with the experimental essence of material effort. It seems, apparently, that σ_f^{*2} involves three such parameters, but assuming such a special structure of the equation entails certain consequences. We find about them by assuming States I and II; there occur from that the following results:

$$\frac{M^*}{L^*} = \frac{M^*}{N^*} = 2(1 - \lambda),$$

in which case, finally, [the following]:

$$\sigma_f^{*2} = 2(1 - \lambda)(\sigma_2 - \sigma_3)^2 + 2\lambda(\sigma_3 - \sigma_1)^2 + 2(1 - \lambda)(\sigma_1 - \sigma_2)^2$$

is a function of one parameter λ only, and the whole hypothesis will now belong to the category of theories of the four constants k_r , k_c , ν , and λ , or other four if convenience would demand to introduce them.

For $\lambda = \frac{1}{2}$ there is $\sigma_f^{*2} = \sigma_f^2$ and $p^* = p$ and the hypothesis as a whole transforms into the previous, comprehensively discussed one. If one assumes that accidental influences of anisotropy are quite strongly limited, it seems reasonable to expect that the interval within which λ varies is quite modest, and so that it ranges e.g. from 0 to 1. The significance of the parameter λ will come out from the assumption of the State III for the previously written equation; namely, after the auxiliary substitution:

$$\varphi = \sqrt{\frac{2(1 + \lambda)}{3}}$$

we will obtain the relation:

$$\nu^* = \frac{1}{\varphi^2} \frac{k_c k_r}{2k_s^2} - 1,$$

very strongly reminding the previous formula expressing ν .

The “coefficient of anisotropy” φ modifies then quite significantly the “plasticity coefficient” ν to the value ν^* . The last one then will not be contained within the limits from 0 to 1, but within a little more extended ones. If we assume the conditions $0 \leq \lambda \leq 1$ and $0 \leq \nu \leq 1$, the interval of changes of ν^* will

be described by the inequality $-\frac{1}{4} \leq \nu \leq 2$; similarly, the coefficient φ will be limited within the interval $\sqrt{\frac{2}{3}} \leq \varphi \leq \frac{2}{\sqrt{3}}$. However – similarly as it was previously considered – going up or down from the value $\nu^* = \frac{1}{2}$ will be distinctively reflected in the contents of the theory.

The mutual dependence of the discussed coefficients is described by the expression:

$$\nu = \frac{2\lambda(1 + \nu^*) - (1 - 2\nu^*)}{3}.$$

The difference: $\delta^* = \nu^* - \nu = \frac{1 + \nu^*}{3}(1 - 2\lambda)$ can be $\delta^* > 0$ or $\delta^* = 0$ or $\delta^* < 0$, depending on $\lambda > \frac{1}{2}$ or $\lambda = \frac{1}{2}$ or $\lambda < \frac{1}{2}$. Now, the use of the parameter δ^* instead of the parameter $\lambda = \frac{1 + \nu^* - 3\delta^*}{2(1 + \nu^*)}$ can turn out to be more advantageous. For the assumptions made, the parameter δ^* is described by the interval: $-\frac{1 + \nu^*}{3} \leq \delta^* \leq \frac{1 + \nu^*}{3}$.

Nevertheless, first let us notice also what follows: the previously written equation can be transformed, analogously to the initial reasoning, into the following form:

$$(C5)^* \quad \frac{1 + \nu^*}{3} \sigma_f^{*2} + 3(1 - 2\nu^*)(p + \sigma'^*)^2 = k'^{*2},$$

where:

$$\sigma'^* = \frac{k_c - k_r}{2(1 + \nu^*)},$$

$$k'^{*2} = k_c k_r + \frac{3}{4} \frac{(k_c - k_r)^2}{1 - 2\nu^*} = \frac{3\varphi^2 k_s^2 (k_c + k_r)^2 - 4k_c^2 k_r^2}{4(3\varphi^2 k_s^2 - k_c k_r)} = -k_1'^{*2}.$$

In the system (p, σ_f^*) or (p^*, σ_f^*) the Eq. (C5)'* represents figures analogous to the ones given before – of course with certain subtle differences, the presence of which is obvious for $\lambda \neq \frac{1}{2}$ that is $\varphi \neq 1$ or $\nu^* \neq \nu$ i.e. $\delta^* \neq 0$. These differences mean that everywhere instead of k_s we will write φk_s , and instead of ν we will insert ν^* and finally, we will replace σ_f for σ_f^* .

The present discussion has only a sketchy character; for this reason we omit discussion of these new details. Let us notice, however, that the current and continued mathematical argument is in the present conditions valid only with the assumption of inequality $\sigma_1 > \sigma_2 > \sigma_3$ or relatively $\sigma_1 < \sigma_2 < \sigma_3$, without which we managed in the previous part of the section (C5).

By expanding the last equation we come to the fundamental formula of the author's hypothesis for quasi-isotropic bodies, as below:

$$(C5)^* \quad \boxed{\sigma_1^2 + (1 + 2\delta^*)\sigma_2^2 + \sigma_3^2 - 2(\nu^* + \delta^*) \left(\sigma_2\sigma_3 + \frac{\nu^* - \delta^*}{\nu^* + \delta^*} \sigma_3\sigma_1 + \sigma_1\sigma_2 \right) + (k_c - k_r)(\sigma_1 + \sigma_2 + \sigma_3) = k_c k_r.}$$

The equation (C5)* represents – with omission of certain slight changes which would result from the introduction of p^* – the final form of the improved hypothesis, and so we should devote next a few comments to it. With the assumption that $\nu^* = \nu$, which means $\delta^* = 0$, [the formula] (C5)* transforms, of course, into (C5), i.e. into the form involving – depending on the values of ν and \varkappa – various special cases, [including] among others all hypotheses of the group C, which were already extensively commented. [...]

As for the special cases of the formula (C5)*, these arise, before all, in the case of $\nu^* = \frac{1}{2}$; then the hypothesis transforms into the equation:

$$(1 - \lambda)(\sigma_2 - \sigma_3)^2 + \lambda(\sigma_3 - \sigma_1)^2 + (1 - \lambda)(\sigma_1 - \sigma_2)^2 + (k_c - k_r)(\sigma_1 + \sigma_2 + \sigma_3) = k_c k_r.$$

The assumption $\lambda = 0$ leads now to one special form, unknown to us until now. The assumption $\lambda = \frac{1}{2}$ gives one of the forms of (C5) already discussed for $\nu = \frac{1}{2}$. Finally, putting $\lambda = 1$, we obtain an equation which for plane states (i.e. for $\sigma_2 = 0$) becomes identical to the corresponding one in Mohr's [theory] (A5). If for an arbitrary λ we assume $k_c = k_r = k$, we will obtain the correct theory (C3), namely:

$$(1 - \lambda)(\sigma_2 - \sigma_3)^2 + \lambda(\sigma_3 - \sigma_1)^2 + (1 - \lambda)(\sigma_1 - \sigma_2)^2 = k^2.$$

The simplicity of the last equation, hiding in itself the theories (C3) and (A3), deserves special emphasizes and attention; let us devote some time to it at the end of this section.

Coming back to the general form (C5)*, let us try to show it graphically. For this purpose, let us – similarly to previous considerations – ascertain that the discussed equation can be transformed to the form:

$$(C5')^* \quad \sigma_1'^{*2} + (1 + 2\delta^*)\sigma_2'^{*2} + \sigma_3'^{*2} - 2(\nu^* + \delta^*) \cdot \left(\sigma_2'^* \sigma_3'^* + \frac{\nu^* - \delta^*}{\nu^* + \delta^*} \sigma_3'^* \sigma_1'^* + \sigma_1'^* \sigma_2'^* \right) = k'^{*2} = -k_1'^{*2},$$

where: $\sigma_i'^* = \sigma_i + \sigma'^*$ and the meanings of the expressions $\sigma_i'^*$ and $k_i'^*2 = -k_1'^*2$ remain unchanged. The equation (C5)* is valid for arbitrary \varkappa and $\nu^* \neq \frac{1}{2}$. In the case of $\nu^* = \frac{1}{2}$ and $\varkappa > 1$, the transformation leads to the function:

$$(C5'')^* \quad \sigma_1''*2 + (1 + 2\delta^*)\sigma_2''*2 + \sigma_3''*2 - 2(1 + 2\delta^*)\sigma_2''*\sigma_3''* - 2(1 - 2\delta^*)\sigma_3''*\sigma_1''* \\ - (1 + 2\delta^*)\sigma_1''*\sigma_2''* + (k_c - k_r)(\sigma_1''* + \sigma_2''* + \sigma_3''*) = 0,$$

where: $\sigma_i''* = \sigma_i + \sigma''*$ and $\sigma''* = -\frac{k_c k_r}{3(k_c - k_r)}$.

Finally, for $\nu^* = \frac{1}{2}$ and $\varkappa = 1$ the hypothesis will be expressed by the equation just written above, which – because of the currently reduced relation: $\lambda = \frac{1}{2} - \delta^*$ – will assume after rearrangement the form:

$$(C5''')^* \quad \sigma_1^2 + (1 + 2\delta^*)\sigma_2^2 + \sigma_3^2 - 2(1 + 2\delta^*)\sigma_2\sigma_3 \\ - 2(1 - 2\delta^*)\sigma_3\sigma_1 - (1 + 2\delta^*)\sigma_1\sigma_3 = k^2.$$

Introduction of the parameter a into the equations (C5')*, (C5'')* and (C5''')* leads to the types similar to (C5₁), (C5₂), (C5'₁) and (C5''₂). Their discussion leads to appropriate determination of the intervals in which Mohr's circles have, or relatively do not have, envelopes and for the first ones leads to the shapes of the envelopes, picture of which is slightly different from the previous graphs. For this reason we omit the respective illustration devoting more attention to Haigh's limit surfaces.

The last one, in the case of $\nu^* < \frac{1}{2}$, is a triaxial ellipsoid with the lengths of the half-axes:

$$b_1^* = \frac{k'^*}{\sqrt{1 + \nu^* + 3\delta^*}}, \quad b_2^* = \frac{k'^*}{\sqrt{1 - 2\nu^*}}, \quad b_3^* = \frac{k'^*}{\sqrt{1 + \nu^* - \delta^*}},$$

[the ellipsoid] is shifted to the centre: $\sigma_1 = \sigma_2 = \sigma_3 = -\sigma'^*$. In the case of $\nu^* = \frac{1}{2}$, $\varkappa > 1$, we obtain an elliptical paraboloid with a vertex in the point: $\sigma_1 = \sigma_2 = \sigma_3 = -\sigma''*$ and the parameters:

$$q_1^* = \frac{k_c - k_r}{1 + 2\delta^*} \frac{1}{\sqrt{3}}, \quad q_3^* = \frac{k_c - k_r}{3 - 2\delta^*} \sqrt{3}.$$

Under the conditions: $\nu^* = \frac{1}{2}$ and $\varkappa = 1$ the critical surface is an elliptical cylinder with the semi-axes:

$$b_1^* = \frac{k_1^*}{\sqrt{1 + \nu^* + 3\delta^*}}, \quad b_2^* = \frac{k_1^*}{\sqrt{2\nu^* - 1}}, \quad b_3^* = \frac{k_1^*}{\sqrt{1 + \nu^* - \delta^*}}.$$

This cylinder can degenerate into two parallel planes for $\delta^* = -\frac{1}{2}$ or relatively $\lambda = 1$ (or even transform into a hyperboloid cylinder for $\lambda > 1$). Finally, the assumption $\nu^* > \frac{1}{2}$ hides in itself a two-shell triaxial hyperboloid with the centre: $\sigma_1 = \sigma_2 = \sigma_3 = -\sigma'^*$ and the semi-axes:

$$b_1^* = \frac{k_1^*}{\sqrt{\nu^* + 1 + 3\delta^*}}, \quad b_2^* = \frac{k_1^*}{\sqrt{2\nu^* - 1}}, \quad b_3^* = \frac{k_1^*}{\sqrt{\nu^* + 1 - \delta^*}}.$$

Here belongs also the special case determined by the assumption:

$$k_s = \frac{1}{\varphi} \frac{2}{\sqrt{3}} \frac{k_c k_r}{k_c + k_r},$$

leading to an elliptical cone as the searched surface.

The contour of a plane state is shown regardless of $\nu^* < \frac{1}{2}$, $\nu^* = \frac{1}{2}$, $\nu^* > \frac{1}{2}$ by the equation:

$$\sigma_{1^*}^2 + \sigma_{3^*}^2 - 2(\nu^* - \delta^*)\sigma_{1^*}\sigma_{3^*} = k_*^2,$$

where:

$$\sigma_{i^*} = \sigma_i + \sigma_*, \quad \sigma_* = \sigma'^* \frac{1 - 2\nu^*}{1 - 2\nu^* + \delta^*} = \frac{kc - kr}{2(1 - \nu^* + \delta^*)},$$

$$k_*^2 = k'^* - \sigma'^* 2 \frac{(1 + \nu^* + 3\delta^*)(1 - 2\nu^*)}{1 - \nu^* + \delta^*} = kc kr + \frac{kc - kr}{2(1 - \nu^* + \delta^*)}.$$

Taking into account the initial assumption: $\nu^* - \delta^* = \nu$ and resulting from this the following: $1 - \nu^* + \delta^* = 1 - \nu$, we recognize in the last equation the contour known to us from the basic hypothesis (C5). It is an ellipse with the semi-axes:

$$\frac{k^*}{\sqrt{1 + \nu^* - \delta^*}} \quad \text{and} \quad \frac{k^*}{\sqrt{1 + \nu^* + \delta^*}},$$

properly translated and rotated or relatively two parallel lines.

[..., p. 136:] IX. OVERVIEW OF EXPERIMENTAL DATA

[..., p. 160:] It is possible to show that the function [defining a measure of material effort, which is] created from the components of the state of stress and possessing an assumed characteristic property, can only be the expression build from the differences between those [stress] components, that is in general:

$$f_1(\sigma_2 - \sigma_3) + f_2(\sigma_3 - \sigma_1) + f_3(\sigma_1 - \sigma_2) = K.$$

If we keep the restriction to a homogeneous form of the second degree, we will obtain from the above the equation:

$$L^*(\sigma_2 - \sigma_3)^2 + M^*(\sigma_2 - \sigma_3)^2 + N^*(\sigma_2 - \sigma_3)^2 = 3\Phi_f,$$

i.e. the formula already known to us from the Chapters III and VIII.

Finally, the demand upon the invariance of this form [with respect to arbitrary rotation] leads to the equation:

$$(\sigma_2 - \sigma_3)^2 + (\sigma_2 - \sigma_3)^2 + (\sigma_2 - \sigma_3)^2 = 2k^2,$$

i.e. directly to the hypothesis (C3); additionally, for $L^* = N^* = 0$, we obtain the hypothesis (A3). [...]

[... , p. 188:] *Lwów, in December 1927.*

[REFERENCES]

- 1) M.T. Huber, Criteria of constancy of equilibrium (in Polish), the Academy of Technical Sciences, Lwów, 1926.
- 2) H.V. Helmholtz, Dynamik kontinuierlich verbreiteter Massen, Leipzig, 1902.
- 3) A.E.H. Love, Treatise on the theory of elasticity; in German translation of A. Timpe, Lehrbuch der Elastizität, Leipzig u. Berlin, 1907.
- 4) W. Voigt, Elementare Mechanik, Leipzig, 1901.
- 5) W. Voigt, Göttingen Nachrichten, 1900.
- 6) H. Lorenz, Technische Elastizitätslehre, München u. Berlin, 1913.
- 7) E. Winkler, Die Lehre von Elastizität und Festigkeit, Praga, 1867.
- 8) A. Föppl u. L. Föppl, Drang und Zwang, I Bd., München u. Berlin, 1920.
- 9) K. Culmann, Graphische Statik, Zürich, 1866.
- 10) O. Mohr, Über die Darstellung des Spannungszustandes und des Deformationszustandes eines Körperelementes, Zivilingenieur, 1882.
- 11) O. Mohr, Technische Mechanik, Berlin, 1906.
- 12) W. Voigt, Annal. Phys. Chem. (Wiedemann), Bde. 31, 1887; 34 u. 35 1888, 38, 1889.
- 13) Todhunter and Pearson, History of the Theory of Elasticity, Vol. 1, Cambridge, 1886.
- 14) M. Born, Probleme der Atomdynamik, Berlin, 1926.
- 15) W. Voigt, Annalen der Physik, Leipzig, 1901.
- 16) R. Knoop, Feinmessung für Druck u. Zug an Betonbalken mit Mikrokomparator, Dissertation, Braunschweig, 1926.
- 17) W. Voigt, Annalen Phys. Chem., Bd. 52, Leipzig, 1894.
- 18) W. Voigt, Berliner Berichte, 1901.
- 19) H. Hencky, Zur Theorie plastischer Deformationen und der hierdurch im Material hergerufenen Nachspannungen, ZAMM, 1924.
- 20) A.A. Griffith, The Theory of Rupture, Proceedings of the First International Congress of Applied Mechanics, Delft, 1925.

- 21) O.L. Von der Festigkeitsfrage, Zft. öster. Ing.-u. Arch. Ver. Wien, 1901.
- 22) Th. V. Kármán, Festigkeitversuche unter allseitigem Druck, Z.v.V.D.I., 1911.
- 23) C. Bach, Elastizität u. Festigkeit, Berlin, 1905.
- 24) O. Mohr, Welche Umstände bedingen die Elastizitätsgrenze u. den Bruch eines Materials, Z.d.V.D.I., 1900.
- 25) A. Föppl, Vorlesungen über technische Mechanik, V. Bd, Leipzig, 1907.
- 26) M. Roš and A. Eichinger, Versuche zur Klärung der Frage der Bruchgefahr, Zurich, 1926.
- 27) H. Mierzejewski, Foundations of Mechanics of Plastic Bodies (in Polish), Warszawa, 1927.
- 28) B. de Saint Venant, Journal de Mathetics, 308, 373, 1871.
- 29) K.v. Sanden, Die Energiegrenze der Elastizität nach Huber u. Haig him Vergleich zu den alteren Dehnungs- u. Schubspannungs- Theorien, Zft. Werft u. Rederei, H. 8, 1921.
- 30) M. Mesnager, Deformation et rupture de solides, Revue de metallurgie, Nr. 6 and 7, 1922.
- 31) A. Föppl, Mitteilungen aus dem mech.-techn. Laboratorium der k. techn. Hochschule in München, 1896.
- 32) B.T. Haigh, The strain-energy function and the elastic limit, Engineering, Vol. CIX, 1920.
- 33) G.D. Sandel, Festigkeitsbedingungen, Leipzig, 1925.
- 34) E. Pascal, Repetitorium der Hoheren Mathematik I. 1, Leipzig u. Berlin, 1910.
- 35) Galileo Galilei, Discorsi e dimonstrazione matematiche, Leyden, 1638.
- 36) G.W. Leibniz, Demonstrationes novae de resistentia solidarum, Acta Erudit., 1684.
- 37) B. Navier, De la résistance des corps solides, 1826, 3. éd. par Barré de St. Venant (1864), Historique Nr. XLIV.
- 38) Lamé et Clapeyron, Memoire sur l'équilibre interieur des corps solides homogenes, Mem. Par divers savants, t. 4, Paris, 1833.
- 39) W.J.M. Rankine, Applied Mechanics, London, 1856.
- 40) A. Clebsch, Theorie der Elastizität fester Körper, Leipzig, 1862.
- 41) C.A. Coulomb, Essai sur une application des règles de Maximis et Minimis à quelque problèmes . . . , Mem. par divers savants, Paris, 1776.
- 42) H. Tresca, Memoire sur l'eculement des corps solides. Memoires par divers savants, Paris, tt. XVIII, 1868 and XX, 1872.
- 43) G.H. Darwin, On the stresses produced in the interior of the Earth by the weigth of Continente and Mountains, Phil Trans. Roy. Soc., Vol. 173, 1882.
- 44) J. Guest, Strength of ductile materials under combined stress, Phil. Mag., Vol. 50, 1900.
- 45) Ch. Duguet, Limite d'elasticite et resistance a la rupture. Statique generale, 1885.
- 46) J. Perry, Applied Mechanics, London, 1907 or in German: Angewandte Mechanik, Leipzig u. Berlin, 1908.P. Roth, Die Festigkeitstheorien und die von ihnen abhängigen Formeln, Zft. F. Math. U. Phys., Leipzig, 1902.
- 47) P. Roth, Die Festigkeitstheorien u. die von ihnen abhängigen Formeln des Maschinenbaues, Zft. f. Math. u.Phys., Leipzig, 1902.
- 48) B. de Saint Venant, Leçons de Navier, Historique Abrégé, 1837.
- 49) F. Grashof, Elastizitäts u. Festigkeit, Berlin, 1878.
- 50) F. Schleicher, Der Spannungszustand an der Fliessgrenze, ZAMM, Bd. 6, 1926.

- 51) J. Becker, The Strength and Stiffness of Steel under Biaxial Loading, Univ. of Illinois Bull., 13, 1916.
- 52) H.M. Westergaard, On the Resistance of Ductile Materials to Combined Stresses in two or three directions perpendicular to one another, J. Franklin Inst., 189, 627, 1920.
- 53) G.D. Sandel, Über die Festigkeitsbedingungen, Dissertation, T.H. Stuttgart, 1919.
- 54) E. Beltrami, Sulle condizioni di resistenza dei corpi elastici, Opere matematiche, Rend. Ist. Lomb. ser. Vol. LXXXI, 1885.
- 55) M.T. Huber, About the foundations of the strength theory (in Polish), Prace mat.-fiz., T. XV, Warszawa, 1904.
- 56) M.T. Huber, Właściwa praca odkształcenia jako miara wyężenia materiału, Czasopismo Techniczne, Lwów, 1904 (see also the recent edition of the English translation in the centennial of original Polish publication: Specific work of strain as a measure of material effort, Arch. Mech., 56, 173-190, 2004).
- 57) Girtler, Über das Potential der Spannkkräfte in elastischen Körpern als Mass der Bruchgefahr, Sitzungsberichte der Wiener Akad. Bd. CXVI, 1907.
- 58) H. Wehage, Die zulässige Anstrengung eines Materials bei Belastung nach mehreren Richtungen, Z.d.V.D.I., 1905.
- 59) R. v. Mises, Mechanik der festen Körper im plastisch-deformablen Zustand, Göttingen Nachrichten, Math. phys. Klasse, Z. 4 (1), 582–592, 1913.
- 60) H. Hencky, Über langsame stationäre Strömungen in plastischen Massen mit Rücksicht auf die Vorgänge beim Walzen, Pressen und Ziehen von Metallen, ZAMM, Bd. 5, 1925.
- 61) P.W. Bridgman, The compressibility of thirty metals, Proc. Amer. Acad., Vol. 58, Nr. 5, 1923.
- 62) P. Ludwik, Elemente der technologische Mechanik, Berlin, 1909.
- 63) J. Barba, Etude sur la resistance des materiaux, experiences a la traction, Paris, 1880.
- 64) Grübler, Versuche über die Festigkeit an Schleifsteinen, V. d. J., 1899.
- 65) A. Föppl, Vorlesungen über technischen Mechanik, B.G. Teubner-Verlag, Leipzig, 1920.
- 66) Coker, Engineering, 1912.
- 67) J. Bauschinger, Civilingenieur, Leipzig, 1879.
- 68) J. Bauschinger, Zft. f. Baumaterialkunde, 1879.
- 69) A. Föppl, Mitteilungen aus dem mech.-techn. Laboratorium der k. techn. Hochschule in München, H. 27, 1900.
- 70) A. Pomp, Mitteil. D. K.-W.-Inst. F. Eisenforsch., Die Ermittlung der Formänderungsfestigkeit von Metallen durch den Stauchversuch, Düsseldorf, Bd. 9, 1927.
- 71) E. Siebel, Grundlagen zur Berechnung des Kraft.- und Arbeitsbedarfes beim Schmieden und Walzen, Dissertation, Berlin, 1923.
- 72) R. Scheu, Vergleichende Zug-Druck-Dreh- und Walzenversuche, Stahl. U. Eisen, bd. 45, 1925.
- 73) Th. V. Kármán, Festigkeitsversuche unter allseitigem Druck, Z. d. V. D.I., 1911.
- 74) A. Náday, Der bildsame Zustand der Werkstoffe, Berlin, 1927.
- 75) J. Bauschinger, Mitteil. A. d. mechan.-techn. Labor., München, H. 3, 1874.
- 76) E.L. Hancock, Philosophical Magazine, T. 12, 1906.
- 77) W. Scoble, Philosophical Magazine, T. 12, 1906.
- 78) W. Mason, Institution of mechanical engineers, Proceedings, 1909.
- 79) W. Wehage, Mitteilungen der techn. Versuchsanstalten zu Berlin, 1888.

- 81) H. Bonte, V. D. I., Bd. 64, Nr. 51.
- 82) W. Voigt, Wiedemanns Annalen d. Phys., Bd. 53, 1894; Bd. 67, 1899.
- 83) Th. V. Kármán, Festigkeitsversuche unter allseitigen Druck., Mitteil über Forschungsarbeiten V. D. J. H., 118, 1912.
- 84) R. Böcker, Die Mechanik der bleibenden Formänderung in kristallinisch aufgebauten Körpern, Forschungsarbeiten, H. 176/176, Berlin, 1915.
- 85) J. Meyer, Zur Kenntniss des negative Druckes in Flüssigkeiten, Abhandl. d. deutsch. Runsen-Ges., T. III, Nr. 1, Halle, 1911.
- 86) Z. Fuchs, Phenomen of negative pressure in fluids (in Polish), Czasop. Techn., Lwów, 1925.
- 87) A. Joffe u. M. Levitsky, über die Kohäsionsfestigkeit von Steinsalz, Zeit.f. Phys., 35, Nr. 6, 1926.
- 88) P.W. Bridgman, Proc. An. Acad., Vol. 61, 1926.
- 89) C.A.M. Smith, Institution of mechanical engineers, Proceedings, 1910.
- 90) Cook u. Robertson, Engineering, 1911.
- 91) R. Boker, Versuche, die Grenzkurve der Umschlingungsversuche und der Druckversuche zur Deckung zu bringen, Dissertation, Aachen, 1914.
- 92) W. Lode, Versuche über den Einfluss der mittleren Hauptspannung auf die Fließgrenze, Zft. F. Ang. Math. u. Mech., Bd. 5, 1925.
- 93) Dingers Journal, 1860.
- 94) A. Martens- E. Heyn, handbuch der Materialkunde, Berlin, 1912.
- 95) L. Hartmann, Distribution des deformations dans les métaux soumis a des efforts, Paris, 1896.

Received June 17, 2010.

ENGINEERING TRANSACTIONS Appears since 1952

Copyright ©2009 by Institute of Fundamental Technological Research,
Polish Academy of Sciences, Warsaw, Poland

Aims and Scope

ENGINEERING TRANSACTIONS promotes research and practise in engineering science and provides a forum for interdisciplinary publications combining mechanics with material science, electronics (mechanotronics), medical science and biotechnologies (biomechanics), environmental science, photonics, information technologies and other engineering applications. The Journal publishes original papers covering a broad area of research activities including experimental and hybrid techniques as well as analytical and numerical approaches. Engineering Transactions is a quarterly issued journal for researchers in academic and industrial communities.

INTERNATIONAL COMMITTEE

S. A. ASTAPCIK (*Byelorussia*)

G. DOBMANN (*Germany*)

JI-HUAN HE (*China*)

M. N. ICHCHOU (*France*)

W. JÜPTNER (*Germany*)

A. N. KOUNADIS (*Greece*)

P. KUJALA (*Finland*)

J. LIN (*U.K.*)

G. PLUVINAGE (*France*)

V. V. SKOROKHOD (*Ukraine*)

P. C. B. TSAY (*Taiwan*)

Z. WESOŁOWSKI (*Poland*)

EDITORIAL COMMITTEE

L. DIETRICH – **Editor**

B. GAMBIN

K. KOWALCZYK-GAJEWSKA

Z. KOWALEWSKI

B. LEMPKOWSKI – secretary

J. HOLNICKI-SZULC

R. PEÇHERSKI

Address of the Editorial Office:
Engineering Transactions
Institute of Fundamental Technological Research
Pawińskiego 5B,
PL 02-106 Warsaw, Poland

Phone: (48-22) 826 60 22, Fax: (48-22) 826 98 15, E-mail: publikac@ippt.gov.pl

Abstracted/indexed in:

Applied Mechanics Reviews, Current Mathematical Publications, Inspec, Mathematical Reviews, MathSci, Zentralblatt für Mathematik.

<http://et.ippt.gov.pl/>

SUBSCRIPTIONS

Address of the Editorial Office: Engineering Transactions

Institute of Fundamental Technological Research

Pawińskiego 5B, PL 02-106 Warsaw, Poland

Tel.: (48-22) 826 60 22, Fax: (48-22) 826 98 15, E-mail: publikac@ippt.gov.pl

Subscription orders for all journals edited by IPPT (Institute of Fundamental Technical Research) may be sent directly to the Publisher: Institute of Fundamental Technological Research

e-mail: subscribe@ippt.gov.pl

Please transfer the subscription fee to our bank account: Payee: IPPT PAN,

Bank: Pekao S.A. IV O/Warszawa,

Account number 0512401053111100004426875.

All journals edited by IPPT are available also through:

- Foreign Trade Enterprise ARS POLONA ul. Obrońców 25,
03-933 Warszawa, Poland, Tel. (48-22) 509 86 38, 509 86 37
e-mail: arspolona@arspolona.com.pl
- RUCH S.A. ul. Jana Kazimierza 31/33,
01-248 Warszawa, Poland,
Tel. (48-22) 532 88 16, Fax (48-22) 532 87 31
e-mail: prenumerata@okdp.ruch.com.pl
- International Publishing Service Sp. z o.o ul. Noakowskiego 10 lok. 38
00-664 Warszawa, Poland, Tel./fax: (48-22) 625 16 53, 625 49 55
e-mail: books@ips.com.pl

Warunki prenumeraty

Prenumeratę na wszystkie czasopisma wydawane przez IPPT PAN przyjmuje Dział Wydawnictw IPPT. Bieżące numery można nabywać, a także zaprenumerować roczne wydanie Engineering Transactions, bezpośrednio w IPPT PAN, ul. Pawińskiego 5B, 02-106 Warszawa

Tel.: (48-22) 826 60 22; Fax: (48-22) 826 98 15

e-mail: subscribe@ippt.gov.pl

Czasopisma można zamówić (przesyłka za zaliczeniem pocztowym) w Warszawskiej Drukarni Naukowej PAN, ul. Śniadeckich 8, 00-656 Warszawa

Tel./Fax (48-22) 628 87 77; (48-22) 628 76 14, e-mail: dystrybucja@wdnpan.pl

Wpłaty na prenumeratę przyjmują także regionalne Działy Sprzedaży Prasy RUCH S.A.

Infolinia: 804 200 600. Zamówienia można przysłać pocztą elektroniczną ze strony

www.prenumerata.ruch.com.pl

Arkuszy wydawniczych 7.25; Arkuszy drukarskich 5.75

Papier offset. kl. III 70 g. B1

Skład w systemie L^AT_EX K. Jezierska

Druk i oprawa: Drukarnia Braci Grodzickich, Piaseczno ul. Geodetów 47A
